Structural Continuity Effects in Steel Frames under Fire Conditions

By
Ha Hoang

A Thesis
Submitted to the Faculty
of the

WORCESTER POLYTECHNIC INSTITUTE

in partial fulfillment of requirements for the
Degree of Master of Science
in
Civil Engineering

May, 2010

APPROVED:

Professor Leonard D. Albano, Major Advisor
Civil and Environmental Engineering

Professor Robert W. Fitzgerald, Co-Advisor
Civil and Environmental Engineering

Professor Tahar El-Korchi, Head of Department
Civil and Environmental Engineering

Abstract

Fire has always been one of the most serious threats of collapse to structural building frames. The September 11 incident has stimulated significant interests in analyzing and understanding the behavior of the structures under fire events. The strength of the material decreases due to the elevated temperature caused by fire, and this reduction in strength leads to the failure of the member. Frames that do not have sufficient ductility can suffer progressive collapse of the entire structure if one member fails during a fire event. Such collapse could result in loss of human life and serious economic consequences.

The motivation for this thesis is to provide an understanding of the continuity effects in steel frames under fire conditions. The continuity effects of the structure can provide additional strength to the system to sustain the loads under fire event. Different scenarios of the frame and beam structures which include changes to member sizes, fire locations, and bay size, are investigated with the assistance of SAP2000 and ANSYS. These programs can provide the collapse analysis for each scenario at different temperature. The continuity effect was investigated from the strength point of view of the structure.

Ultimately, the thesis presents a design tool for aiding member design under fire conditions. The design tool consists of different graphs that maybe use to determine the collapse load capacity of a continuous structure at elevated temperature based on the analysis of a simpler, determinate structure.

Acknowledgement

I would like to express special thanks to my advisor, Professor Leonard D. Albano, for his guidance, encouragement, time and efforts in helping me complete this thesis. I have known Professor Albano since my undergraduate years at WPI. He has been both a mentor and a friend to me. Without his counsel, this project would not been completed.

I would like to thank Professor Robert W. Fitzgerald for his input and advice in developing the thesis focus area. His input helped me narrow down my research topic.

I would like to thank Douglas Heath for helping me to model in ANSYS. He saved me a lot of time in understanding how ANSYS works.

I would like to thank my family and friends for their endless support especially my parents who are in Vietnam. They constantly encourage me even though they are half-way around the world. Lastly, I want to thank my girlfriend who always stays by my side and gives me countless suggestions.

Contents

List of Figures

Lists of Tables

List of Equations

1. Introduction

Fire has always been a serious threat to every aspects of human life. It can cause the loss of human life and bring significant economic consequences. From 1999 to 2008, there were more than 500,000 structural fires in the United States annually. Every year, during those fire incidents, there were approximately 3000 fatalities and 15,000 injuries. The United States loses more than 10 billion USD annually because of structural fires (United States Fire Administration, 2010). In addition, during the September 11 incident, there were 2,451 civilian deaths and 800 civilian injuries. The total loss for this incident was $33.5 billion (United States Fire Administration, 2010). This incident has stimulated interest in researching the behavior of building structures during fire events. Because the loss of life is always more important than economic damage, the ultimate goal of structure design for fire conditions is to prevent collapse when the structure is subjected to high temperature.

During a fire event, the strength of construction materials decrease as the temperature rises. Under initial loading, the reduction in material strength could lead to failure of a member. For the continuous structure, the load carrying capacity relies on plastic behavior and the load redistribution within the frames. Therefore, if frames don't have enough redundancy and ductility, the failure of a single member could lead to progressive collapse of the entire structure.

Predicting the frame behavior during fire events is very challenging. Traditionally, the design for fires of the structure is still based on the behavior of a single element in the fire resistance test (Lamont, 2001). It doesn't capture the true behavior of the whole frame. There are interactions between elements of the frame that make the structure behavior complicated to predict.

The motivation for this thesis is to understand the continuity effects of steel frame under fire conditions. All members of the frame will act together to carry additional loads after the initial yielding has occur. This additional load carrying capacity is beneficial to the structure during extreme events.

There have been many tests on how the determinate structure behavior during fire conditions; however, due to the limit in resources, there are not too many full scale tests for indeterminate structures such as high redundant frames. Moreover, in reality, the behavior of a determinate structure cannot resemble the behavior of an indeterminate frame structure. With the assistance of finite elements programs such as SAP2000 and ANSYS, the continuity effect was investigated from the strength point of view of the structure. The thesis also presents a design aiding tools for structure engineer to predict the capacity of the frame under elevated temperature. These tools address the structural fire performance of the complex structure by using a much simpler structure such as simply supported beam. It's definitely a benefit for fire structure engineer since they can have a handle on what the collapse loads of a frame at elevated temperature is.

2. Background

Structural fire has always been a serious threat to the safety of individuals and the collapse of the structure. In this chapter, some statistics of fire incidents in world, especially in the United States, are presented to show the importance of the needs for researching performance of the structural frames under fire conditions.

According to United States Fire Administration (USFA), the threat posed by fire is severe: thousands of Americans die each year, over ten thousands of people are injured and the properties loss go over billions of dollars. The USFA also stated that 87% of civilian fire deaths and 90% of civilian injuries were caused by structure fires in 2008 alone.

Table 1: Structure fires in the United States (1999-2008) (United States Fire Administration, 2010)

Structure Fires

Year	Fires	Deaths	Injuries	Direct Dollar Loss In Millions
1999	523,000	3,040	18,525	$8,490
2000	505,500	3,535	19,600	$8,501
2001[1]	521,500	3,220	17,225	$8,874
2002	519,000	2,775	15,600	$8,742
2003[2]	519,500	3,385	15,600	$8,678
2004	526,000	3,305	15,525	$8,314
2005	511,000	3,105	15,325	$9,193
2006	524,000	2,705	14,350	$9,636
2007	530,500	3,000	15,350	$10,638
2008	515,000	2,900	14,960	$12,361

[1] In 2001, there were an additional 2,451 civilian deaths and 800 civilian injuries that occurred as a result of the events of September 11, 2001. The total property loss due to September 11, 2001 was $33,440,000,000.

[2] In 2003, the estimate for fire deaths includes 100 fire deaths in the Station Nightclub Fire in Rhode Island, and 31 deaths in two nursing home fires in Connecticut and Tennessee.

Source: National Fire Protection Association Fire Loss in the U.S. 2008.

Table 1 shows that the number of fires in incidents in the United States from 1999-2008 approximately stay the same at more than 500,000. Even with established building code provisions for fire safety, the number of structural fires in the United States in the last 10 years still doesn't show any signs of declining trend. However, in order to create the awareness of the importance of the damage due to fire, there were numerous reports of structure fires in the past.

Based on the information from National Fire Incident Reporting System (NFIRS) and National Fire Protection Association (NFPA) survey, John R. Hall, Jr. has developed a report on "high rise building fire". He divided the high-rise buildings into four different categories which are:

- Apartment
- Hotels
- Facilities that care for sick - hospitals, clinic, and doctor's office
- Offices

In 2003-2006, with four of these categories combined, average of 9,600 fires in high-rise buildings were reported per year, and resulted in 29 civilian deaths, 320 civilian injuries, and $44 million in direct property damage annually. The detailed information of the structure fires in high rise building is presented in Table 1. The statistics that are presented in Table 2 show that the fire problem declined from 1985 to 1998. The trends in civilian deaths show a decrease, but an increase in number of civilian injuries in the 1990's. The report also shows that most of the fires that are reported to U.S. Fire Department occurred in the one to six story building. Overall, in 2003-2006, there were only 2.7% of the structural fires occurred in high-rise building. The locations of the fire origin are also mentioned in this report. They are broken down to four sub-categories for each of the building types above. Figure 1 shows that for hotels and apartments building types, most of the fire occurred on second floor to sixth floor. However, for facilities that care for sick and office, it usually happened on the grade to first floor.

Table 2: High-Rise Building Fire Experience Selected Property Classes, by Year 1985-98 (From Hall, 2009)

E. Four Property Use Groups Combined

Year	Fires	Civilian Deaths	Civilian Injuries	Direct Property Damage (in Millions) As Reported	2006 Dollars
1985	17,200	66	670	$25	$48
1986	15,100	38	550	$41	$76
1987	13,000	52	640	$36	$64
1988	14,600	94	780	$104	$177
1989	14,800	111	800	$58	$94
1990	13,300	84	620	$47	$73
1991	13,100	23	750	$150	$222
1992	13,600	35	830	$83	$119
1993	12,400	43	700	$60	$84
1994	11,400	57	950	$60	$82
1995	10,000	55	690	$44	$59
1996	12,100	64	790	$69	$88
1997	11,400	33	560	$43	$54
1998	10,000	37	680	$42	$52
2003-2006 average	9,600 (3,200)	29 (29)	320 (250)	$44 ($44)	$46 ($45)

Note: Figures in parentheses exclude fires reported as confined fires – confined to fuel burner or boiler, cooking vessel, chimney or flue, trash, incinerator, or commercial compactor. These are fires reported to U.S. municipal fire departments and so exclude fires reported only to Federal or state agencies or industrial fire brigades. Estimates include proportional share of fires with unknown building height (until 1998) or number of stories above ground coded as unknown, blank or zero (from 1999 on). Fires are rounded to the nearest hundred, civilian deaths to the nearest one, civilian injuries are rounded to the nearest ten, and direct property damage to the nearest million dollars. Property damage has been adjusted for inflation, using the Consumer Price Index, to 2006 dollars.

Property damage figures for apartments in 1991 are inflated by problems in handling the Oakland wildfire in the estimates. Property damage figures for office buildings are underestimated in several years due to problems in handling some large-loss fires, such as the $325 million One Meridian Plaza fire in Pennsylvania in 1991 and the $230 million World Trade Center incident in 1993, whose more than 1,000 injuries also are not properly reflected in national estimates. The events of September 11, 2001, are not reflected in these figures.

Source: NFIRS and NFPA survey.

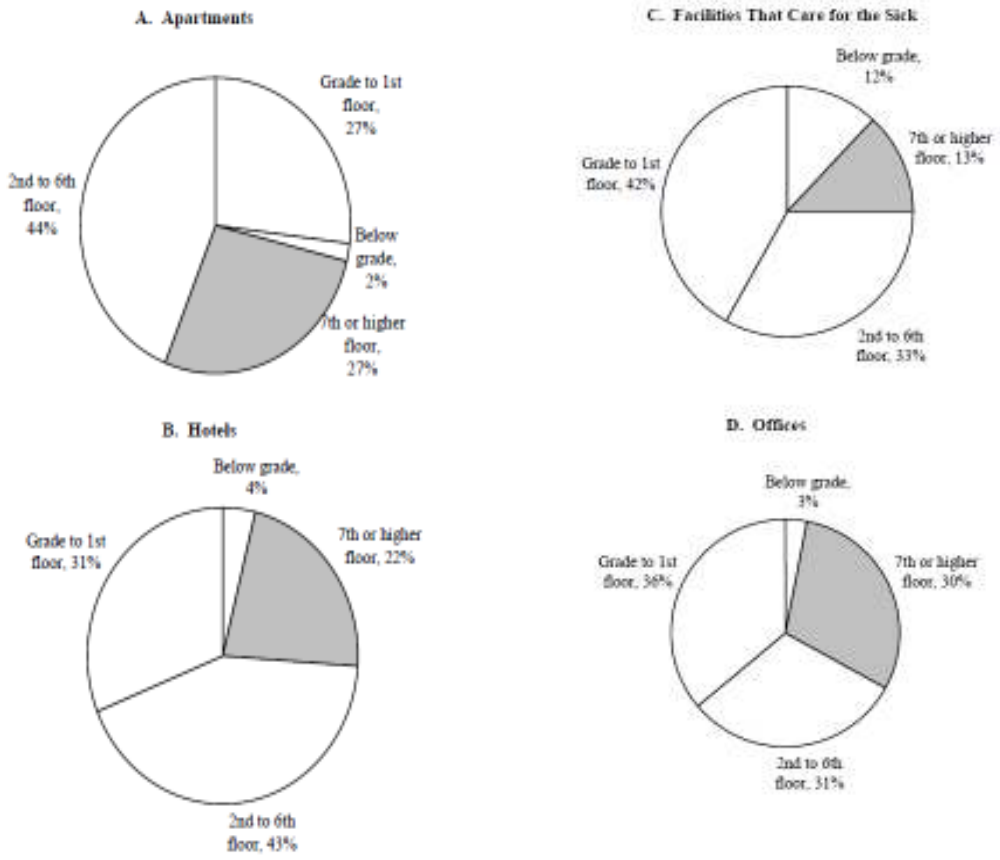

Figure 1:High-Rise Building Fires, by Level of Fire Origin Percentage of 2003-2006 Structure Fires Reported to U.S. Fire Departments (From Hall, 2009)

Note: These are fires reported to U.S. municipal fire departments and so exclude fires reported only to Federal or state agencies or industrial fire brigades. "High-rise" means seven or more stories in height. Includes proportional share of fires with level of fire origin or height of building unknown. There are six types of confined fires – confined to fuel burner or boiler, chimney or flue, cooking vessel, trash, incinerator or commercial compactor. Fires coded as confined do not require reporting of most details, including building height.

Source: NFIRS and NFPA survey.

The results of this report are very important because they show that the research for fire prevention is needed not only for high-rise buildings but also for low-rise buildings. Even though the numbers of structural fires show a decreasing trend for the time period, there were still a substantial amount of fires annually.

After the 9/11 tragedy, National Institute of Standards and Technology (NIST) conducted a survey of "historical information on fire occurrences in multi-story buildings, which results in full or

partial structure collapse" (NIST, 2008). The reported is called "Analysis of Needs and Existing Capabilities for Full-Scale Fire Resistance Testing". It's prepared for the U.S. Department of Commerce to request for the additional unique testing facilities so that they can perform full-scale testing of different structures and materials under fires. Part one of the report is the historical research on significant fire incidents. The report includes a total of 22 incidents from 1970 to 2002, with 15 from the U.S. and 2 from Canada. These 22 incidents were selected based on fire-induced collapse. They were broken down into various categories such as building materials, building story height, and occupancy.

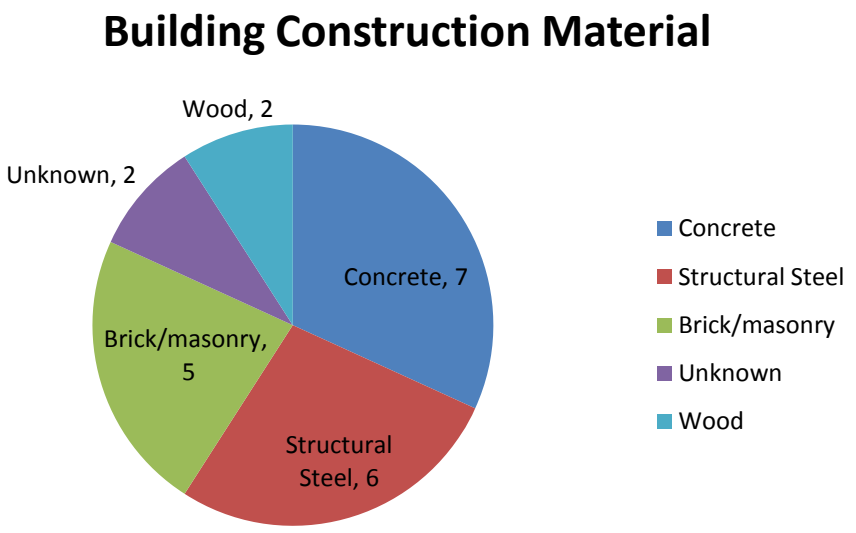

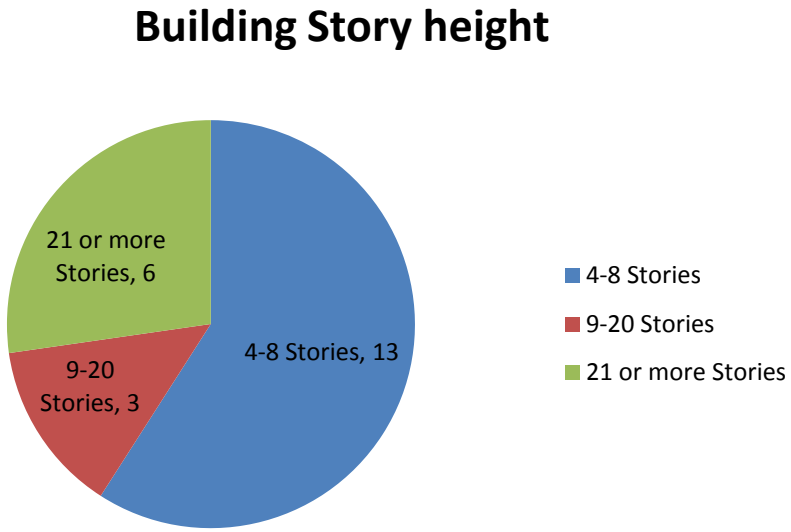

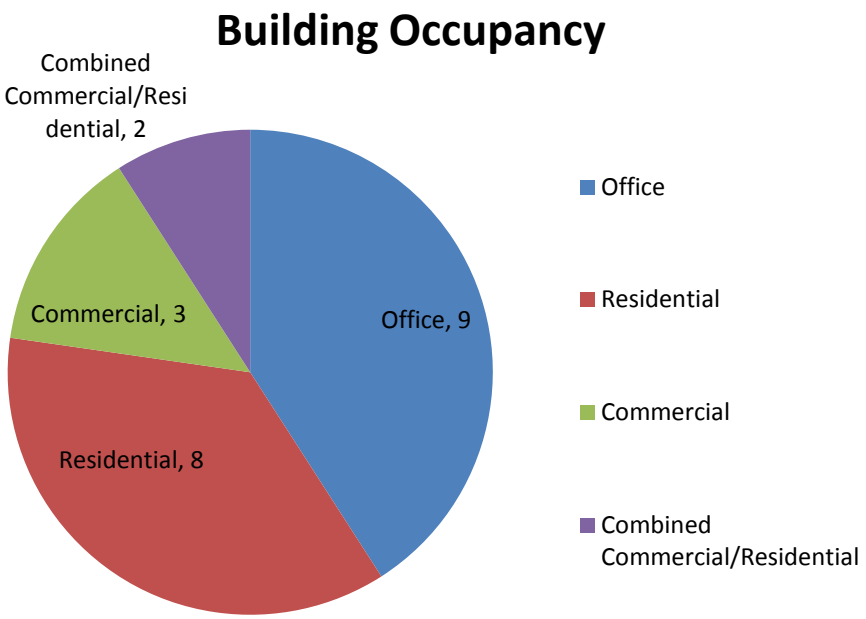

Figure 2: Different Category of 22 incidents from 1970 to 2002

Source: (NIST, 2008)

The data in Figure 2 demonstrated that buildings of all types of construction and occupancy all around the world are at risk due to fire-induced collapse. However, 17 out of 22 cases are office and residential buildings. The performance of these building types and their typical constructions need to be studied to reduce the number of structural collapse for those building types. Structural frame is a very complicated system especially under extreme event such as fires. More and more investigations are being conducted to predict the behavior of these complicated systems.

3. Literature Review

In order to understand and model the behavior of structural frames under fire conditions, some key points and analysis methods needed to be studied. This chapter introduces the key points, technical terms, and analysis methods that were used in this thesis to try to capture the performance of structural steel frames. In addition, this chapter also talks about the ideas, work, finding from previous research relating to this subject. This thesis has adapted some ideas of others to develop useful results for structural engineers.

3.1.Structural Redundancy

Understanding the behavior and plastic collapse of structural frames at elevated temperature is the objective of the thesis. Structural redundancy is an important concept in collapse analysis. Initially, it's described as the degree of indeterminacy of a system. It's also referred to as the "additional support reactions that are not needed to keep the structure in stable equilibrium" (Hibbeler, 2005).It means that if the structure has a high redundancy, it has more strength to prevent collapse. The indeterminate structure has the capability to transfer the load through many different load paths. The loads can be transferred to stiffer parts of the structure to help the structure to survive when one or more elements fail (Lamont, 2001).

The redundancy of the structure is also related to the number of plastic hinges of the structural system that are necessary for structural collapse (Ghaffarzadeh & Ghalghachi, 2009) The concept of redundancy of the structure is widely used in seismic-design because of its positive effects on structural resistance for earthquake. This concept can also be applied to the investigations of structural behavior under fire conditions.

3.2.Plastic Theory of Structures

Theories and methods for plastic analysis of structures were introduced back in the 1950s and are widely accepted. Also, it is recognized that the ultimate limit state for steel structure is plastic collapse

(Neal, 1977). The objective of plastic analysis is to predict the critical loads at which the structure will fail. At the limit state, the structural behavior goes beyond the elastic limit into the plastic range where plastic hinges start to form. The yield stress in the plastic range is fairly constant as Figure 3 illustrates, which indicate that the element doesn't not have any more capacity to carry additional load.

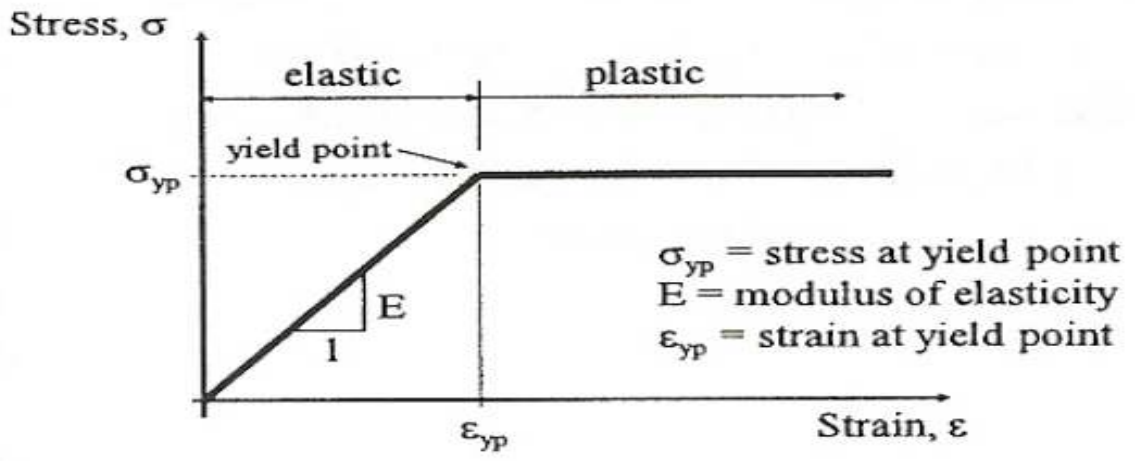

Figure 3: Ideal Stress-Strain Diagram of Steel

A plastic hinge is defined as a hinge that can allow rotation when the bending moment at the hinge location reaches the plastic moment capacity M_p. As the loading increases, the moment at different points along the member also increase; however, when the moments reach the plastic moment M_p, the plastic hinge is formed at that location. As the applied load continues increasing, the hinge doesn't have any more capacity to resist rotation, and much like a hinge, the member is free to rotate at that location. The plastic moment can be calculated by multiplying the yield stress with the plastic section modulus for the member cross section. In order to have the plastic hinges formed, the structural members must have sufficient lateral bracing to prevent lateral buckling and must be compact sections which means they have a "sufficiently stocky profile so that they are capable of developing fully plastic stress distributions before they buckle" (McCormac, 2008).

When an indeterminate structural frame is subjected to steady increasing load, the formation of the first hinge doesn't cause the structure collapse. The structure still can carry load even though its

behavior is in the plastic range. As the applied load is increased, more hinges form until there are sufficient number of hinges to create a collapse mechanisms. The number of plastic hinges depends on the redundancy of the structure. If the structure has the degree of redundancy *r*, the maximum number of plastic hinges, *n*, is equal to *r* +1 (Horne, 1979). Figure 4 shows some examples of different degree of structural redundancy and the corresponding collapse mechanism to number of plastic hinges. Case (a), (b), and (d) in Figure 4 are only showing the degree of redundancy for the study of bending.

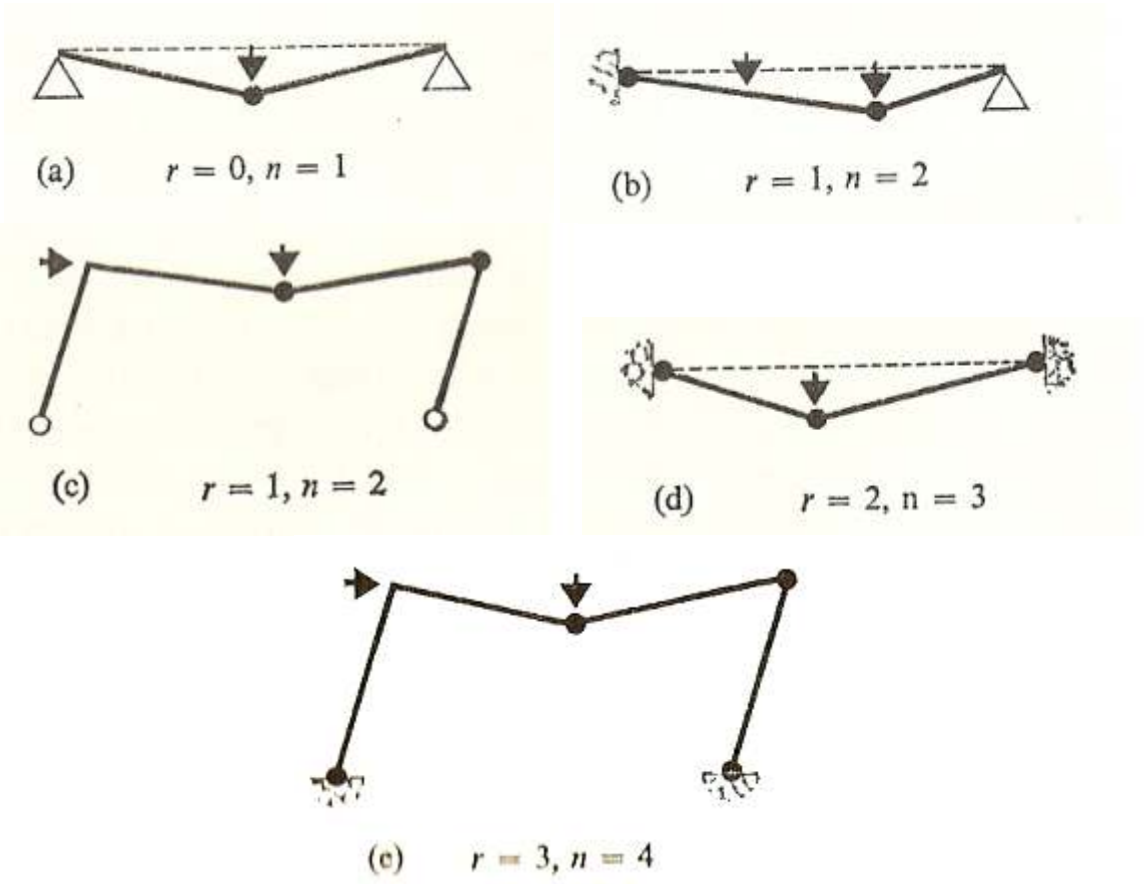

Figure 4: Number of Plastic Hinge example (Horne, 1979)

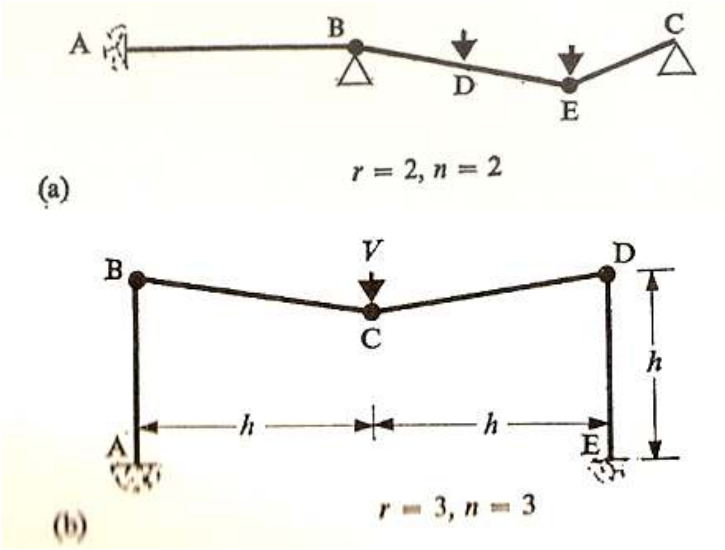

Figure 5: Collapse - Beam Mechanism (Horne, 1979)

A collapsed structure is defined when all the plastic hinges are fully developed or a beam mechanism is presented. Figure 5 illustrates the beam mechanism of the structure, which consists of three hinges along the beam span. The number of plastic hinges in both Figure 5(a) and Figure 5(b) are equal to the degree of redundancy of the structure. In order to find the collapse limit load of an indeterminate structure, a steadily increasing load must be applied to the structure until all the plastic hinges are formed or a beam mechanism is presented.

3.3.Material Properties of Steel at Elevated Temperature

Steel starts to lose strength as the temperature increases. As the temperature reach 550°C, steel loses 40% of its room temperature strength. (Lamont, 2001) and also 40% of its modulus of elasticity. The *SFPE Handbook of Fire Protection Engineering* (Society of Fire Protection Engineers, 1988) has equations that express the yield strength and modulus of elasticity of steel depends solely on temperature, and these are presented in Table 3. These equations are based on the yield strength and modulus of elasticity at the room temperature. At room temperature, the yield strength of A992 steel F_{y0} is 50ksi and the modulus of elasticity E_0 is 29,000 ksi. Figure 6 and Figure 7 illustrate the reduction in yield strength

and modulus of elasticity of A992 steel. One of the notable observations is that the slopes of these two curves are getting steeper as the temperature goes beyond 500°C.

Table 3: Yield strength and modulus of elasticity equations at elevated temperature (Society of Fire Protection Engineers, 1988)

	$0°C \leq T \leq 600°C$	$600°C < T \leq 1000°C$
Yield Strength	$F_{yT} = \left(1.0 + \frac{T}{900 \ln\left(\frac{T}{1750}\right)}\right) F_{y0}$	$F_{yT} = \left(\frac{340 - 0.34T}{T - 240}\right) F_{y0}$
Modulus of Elasticity	$E_T = \left(1.0 + \frac{T}{2000 \ln\left(\frac{T}{1100}\right)}\right) E_0$	$E_T = \left(\frac{690 - 0.69T}{T - 53.5}\right) E_0$

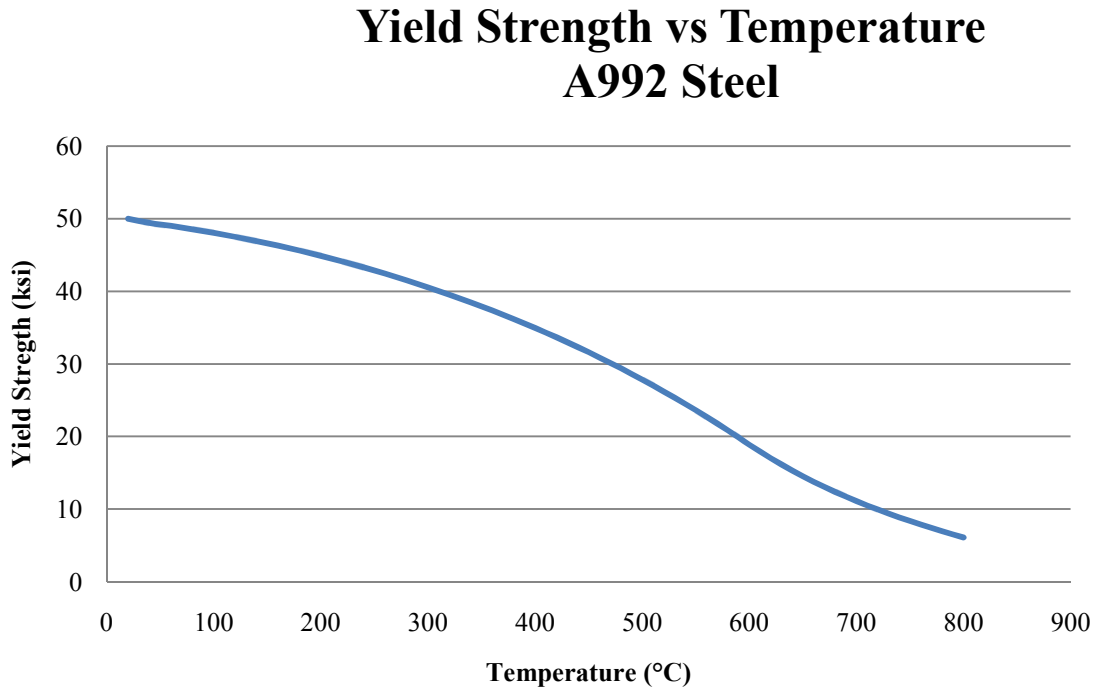

Figure 6: Yield Strength of Steel Vs Temperature

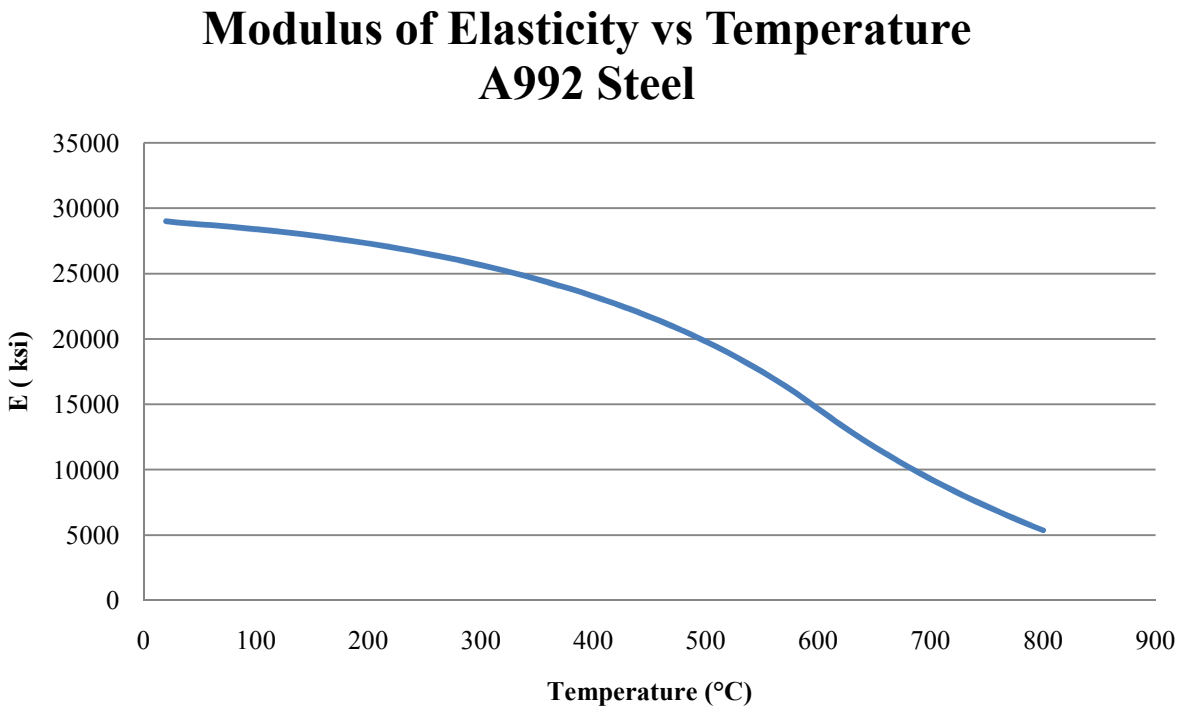

Figure 7: Modulus of Elasticity of Steel Vs Temperature

3.4.Findings from Previous Research

Traditionally, structural design for fire has been based solely on single element behavior in the fire resistance tests. There are a number of research studies focused on individual parts of the structure such as beam, column, slab and connection. However, it is evidenced that the failure of a single determinate element under fire testing has little resemblance to the failure of a similar element that is part of a highly redundant structure. Unfortunately, research studies of an entire structure is still limited since the frame experiments are quite expensive. Nevertheless, some physical tests have been conducted around the world.

In Japan in the 1980s, Nakamura did a full-scale of six story steel frame (Grant & Pagni, 1986). He investigated different fire locations within the building. Both the girders and the columns were unprotected steel. He found that the local buckling of a column influenced the whole structure. Thus, the fire protection of column is very important for structural fire safety (Grant & Pagni, 1986). The BHP Research Laboratories Australia and Stuttgart-Vaihingen University Germany conducted some large scale

tests in the 1990s. However, the test frame sizes in both cases were fairly small. The results showed the beneficial inherent resistance of steel framed building subjected to fire (Bailey, 1997).

In 1990, an accidental fire occurred in a partially complete 14-story office building in the Broadgate development in London. Because the structure was still in the construction phase, the steel frame was only partially protected. However, despite being subjected to very high temperature and experiencing considerable deflections in composite slabs, the structure did not collapse (British Steel plc, 1999). This accident initiated construction of an 8-story composite steel frame at the Building Research Establishment's (BRE's) test facility in Cardington, United Kingdom. The building simulated a real commercial office in UK. It was designed according to the British Standards and checked for compliance with the *Eurocode*. The experimental studies included a series of seven large-scale fire tests in which the fires were started at different locations. The beam system of this experimental building had no fire protection while the columns were fully protected to their full height (Lamont et al, 2006). Despite the fact that the building was subjected to a number of full-scale fire tests, the building still continued to carry loads without failure. The results of these tests showed that structural behavior in fire should be investigated as a complete entity and not as a collection of isolated members.

Due to limited resources, further analyses of frames have concentrated on developing numerical method such as the finite element software programs. For instance, Colin Bailey (1997) used two software programs, INSTAF and NARR2, to investigate the structural behavior of the Cardington fire test models. The physical data was benchmarked and compared to the computer simulation to show the analysis ability of these two programs. Y.C. Wang (1994) also has two papers describing about the development and verification of a finite element program at BRE to study the structural response of steel frames at elevated temperature. In his papers, he explained the procedure of developing the finite element program including different equations and analysis methods (Lamont, 2001).

3.5.Design Methods for Fire

In Europe, fire design for steel structures is provided in *Eurocode 3 part 1.2*. It provides design rules that are required to avoid premature structural collapse. Generally, the *Eurocode* uses the partial safety factors to modify loads and material strengths or capture the uncertainty phenomenon. The *Eurocode 3* also presents three level of calculations for the fire design of steel structure: tabular method, simple calculation, and advanced calculation. The tabular method involves referencing data from design tables based on different parameter such as loading and geometry. It is used mostly for common design. The simple calculation techniques are based on the plastic analysis theory taking into account the reduction in material strength as the temperature rises. Last, the advanced calculation methods are analyses that need to be performed by computer programs which generally are not used in routine design.

In 2005, the *AISC Specification for Structural Steel Buildings* specifies that the member of the structure need to be designed taking the fire effects in consideration. The *Appendix 4: Structural Design for Fire Conditions* of the specification presents the load combination to determine the required strength of the structure due to design-basic fire. Similar to *Eurocode 3,* the *Specification* also introduces two analysis methods: simple methods and advanced methods. The simple methods relate to the lumped heat transfer analysis to find the temperature within the member due to design fire. The advanced methods are the analyses that can be done by computer programs.

3.6.Adaptation Factors

Use of adaptation factors was introduced in *Eurocode 3* for structural steel design under fire conditions as a part of the procedures for simple calculations. It provides a simple means to estimate the moment capacity of a member that is subjected to a temperature gradient. The idea of using adaptation factor is to capture the complexity and uncertainty of the member's behavior at elevated temperature. The adaptation factors that are presented in Table 4 are k_1 and k_2.

The design moment resistant $M_{fi,t,Rd}$ can be calculated by Equation 1. The k_i value can be determined from Table 4 for different temperature distributions.

$$M_{fi,t,Rd} = M_{fi,\theta,Rd} / \kappa_1 \kappa_2$$

Equation 1: Design Moment Resistant for non-uniform temperature distribution

$M_{fi,t,Rd}$ is the design moment resistance of the cross-section for a non-uniform temperature

$M_{fi,\theta,Rd}$ is the design moment resistance of the cross-section for a uniform temperature

k_1 is an adaptation factor for non-uniform temperature across the cross-section

k_2 is an adaptation factor for non-uniform temperature along the beam

Table 4: Adaptation Factors from *Eurocode 3 part 1.2(Eurocode 3)*

Reference in ENV 1993-1-2	Description	Symbol	Condition	Value	
				ENV value	Value for UK use
4.2.3.3(8)	The adaptation factor for non-uniform temperature distribution across a cross-section	k_1	For a beam exposed on all four sides	1.0	1.0
4.2.3.3(8)	The adaptation factor for non-uniform temperature distribution across a cross-section	k_1	For a beam exposed on three sides with a composite or concrete slab on side 4	0.7	0.7
4.2.3.3(9)	The adaptation factor for non-uniform temperature distribution along a beam	k_2	At the supports of a statically indeterminate beam	0.85	0.85
			In all other cases	1.0	1.0

Because the United Kingdom uses different unit than other countries that have adopted the *Eurocode*, in all *Eurocode*, the ENV values are modified for UK use; however, in the case of the adaptation factor, the k_i values are the same both within and outside of the UK. Table 4 illustrates that the maximum value of K factor is 1.0. The smaller the K value, the bigger the required moment resistance for design.

Pettersson and Witteven also introduced an adaptation factor method in their research paper on fire resistance of steel structures (Petterssona & Witteveen, 1980). In their report, the factor *f* was used to account for discrepancy between the experimental results and analytical approach.

$$f = f_m f_i f_{Tc} f_{Ta}$$

$$k = \frac{1}{f}$$

Equation 2: Pettersson and Witteven Adaptation Factor

where

f_m is a correction factor accounting for material properties at elevated temperature

f_i is a correction factor accounting for imperfection

f_{Tc} is a correction factor accounting for non-uniform temperature distribution in the cross section of the member

f_{Ta} is a correction factor accounting for non-uniform temperature distribution along the member

Source: (Wong, 2006)

The *k* value from Pettersson and Witteven is the similar to the k_i value from *Eurocode 3*. However, the *f* value from Pettersson and Witteven captures both non-uniform temperature across the cross section of the member and along its length. The *k* value from Pettersson and Witteven varies from 0.8 to 1.0 for a statically determinate beam and from 0.4 to 1.0 for statically indeterminate beam.

Other researchers have also developed similar ideas to adaptation factors such as M.B. Wong (Wong, 2000) and the *Swedish Design Manual* (1976).

3.7.Multiplier α by M.B. Wong

M.B. Wong in his paper, *"Elastic and plastic methods for numerical modeling of steel structures subject to fire"*(2002), established a method based on plastic analysis and the virtual work method to predict the failure temperature of the structure. He introduced the multiplier α to capture the change in collapse mode as the temperature of the frame increased (Wong, 2000). The initial temperature needed to

be assumed in order to calculate the multiplier. After several assumptions of temperature and virtual work calculations, the multiplier α was defined. The multiplier α changed as the geometry and section properties changed. By multiplying α with the initial temperature, the critical temperature of the structure is calculated. The task of doing this method is tedious when it comes to a large number of elements in the frame. In his paper, a couple of examples are shown to illustrate how to use α.

3.8. Swedish Design Manual

In the 1970s, the *Swedish Design Manual* introduced one of the most innovative design guides for fire safety design. Pettersson and his collaborators developed a series of calculation methods for steel members under fire conditions. Similar to the adaptation factor from *Eurocode 3*, the design presents a temperature-dependent coefficient β. The coefficient is used to predict the critical load as a function of yield stress, section modulus, and length of the beam. The critical deflection y_{cr} of the beam was defined by the following equation

$$y_{cr} = \frac{L^2}{800d}$$

Equation 3: Critical Deflection at mid span (*Swedish Design Manual*)

where
y_{cr} = Critical deflection at mid span

L = Length of the beam

d = Depth of the beam

Based on this deflection criterion, the critical load that causes the mid span deflection to exceed y_{cr} can be calculated by Equation 4

$$P_{cr} = \beta \frac{C\sigma_s W}{L}$$

Equation 4: Critical Load (*Swedish Design Manual*)

where

P_{cr} = Critical load

C = Constant dependent on the loading

W = Elastic Section Modulus (S_x for AISC)

σ_a = Yield Stress at normal temperature (F_y for AISC)

Source: (Pettersson, Magnusson, & Thor, 1976)

These equations were applied to series of model which included different loading patterns, and boundary conditions. The results were plotted versus steel temperature. Figure 8 is one example in the series of graphs that are presented in the *Manual*. Based on the plot, the coefficient β can be determined at the temperature of interest. In Figure 8, which refers to a uniformly loaded simple beam, the constant dependent on the loading is equal to 8. By using equation 8, the critical load at temperature can be calculated. The *Swedish Design Manual* provides a simple and useful tool to predict the collapse load, and this thesis also contributed to developing a similar tool for designers.

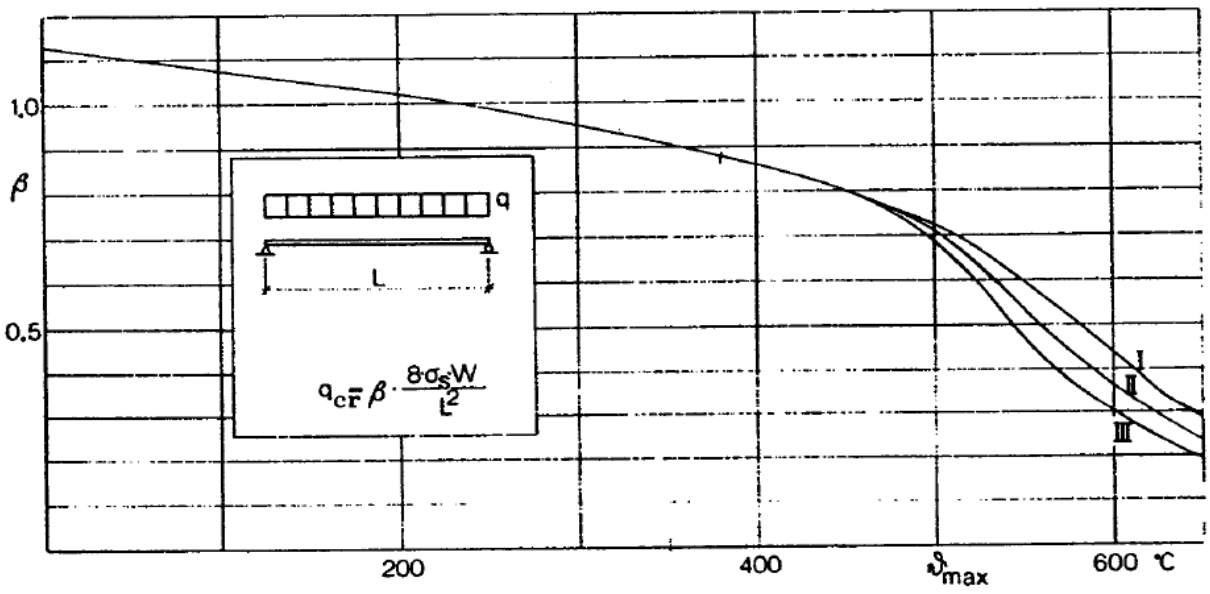

Figure 8: Coefficient *β* for simple supported beam with distributed load

4. Scope of Work

The primary objective of this thesis was to understand the continuity effects in structural frames under fire conditions. In addition, this thesis also introduced a simple tool that can help structural engineers predict strength of steel structures based on analysis of a simpler model. All other phenomena of structural behavior under fire conditions such as thermal expansion, large deflection, and creep were not considered. Continuity effects in structural frames were studied by using plastic limit analysis to determine mathematically the collapse loads and mechanisms for various temperature distributions. Because hand calculation for plastic limit analysis for an indeterminate structure is very tedious, two finite elements software programs SAP2000 (Computers and Structures Inc., 2009) and ANSYS (ANSYS Inc., 2009) were used. These two programs have their advantages and disadvantages for collapse analysis. Therefore, they were used simultaneously to serve different tasks of this thesis. More information about these two programs is presented in Appendix A

Figure 9 shows the different study areas that this thesis investigated. The work was divided into five major activities. The first activity was the investigation of the moment redistribution effects at elevated temperature. The activity was an initiated determination of whether the reduction in yield strength and modulus of elasticity of the A992 steel could lead to redistribution of moment within the frames. The second activity was the validation of the ability of SAP2000 and ANSYS to do collapse analysis. The third activity was to establish and analyze a base model for structural continuity investigations. The analysis was carried out by using finite element programs SAP2000 and ANSYS. The fourth activity was to conduct parametric investigation of the base model. Much like the third activity, SAP2000 and ANSYS were used to investigate the collapse loads and mechanism of these models. The last activity was to create the design aid tools to predict in approximate manner the structural behavior under fire conditions The tool was based on the data collected in second activity.

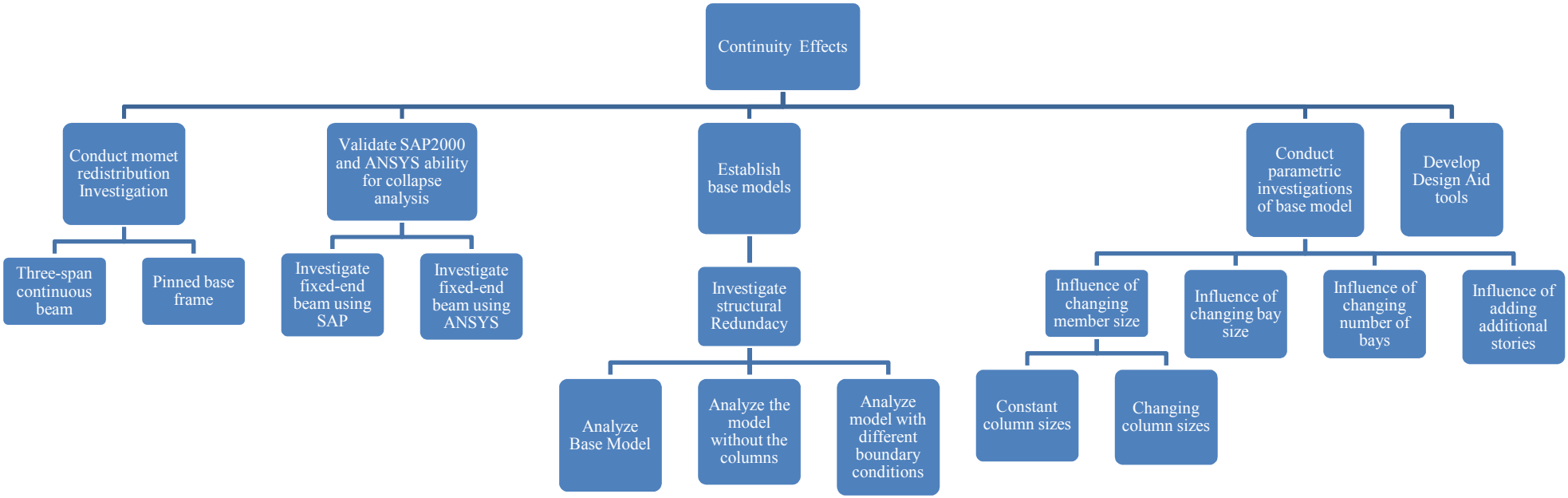

Figure 9: Methodology Chart

4.1.Activity 1: Conduct Moment Redistribution Investigation

Consistent with the moment distribution method, the moment within the frame was distributed based on the modulus of elasticity, moment of inertia and the length of each element. At the elevated temperature, the stiffness of the heated member changed. Thus, it was expected that its end moment would be redistributed. In order to investigate this phenomenon, a three-span continuous beam and pinned-base frame models were established.

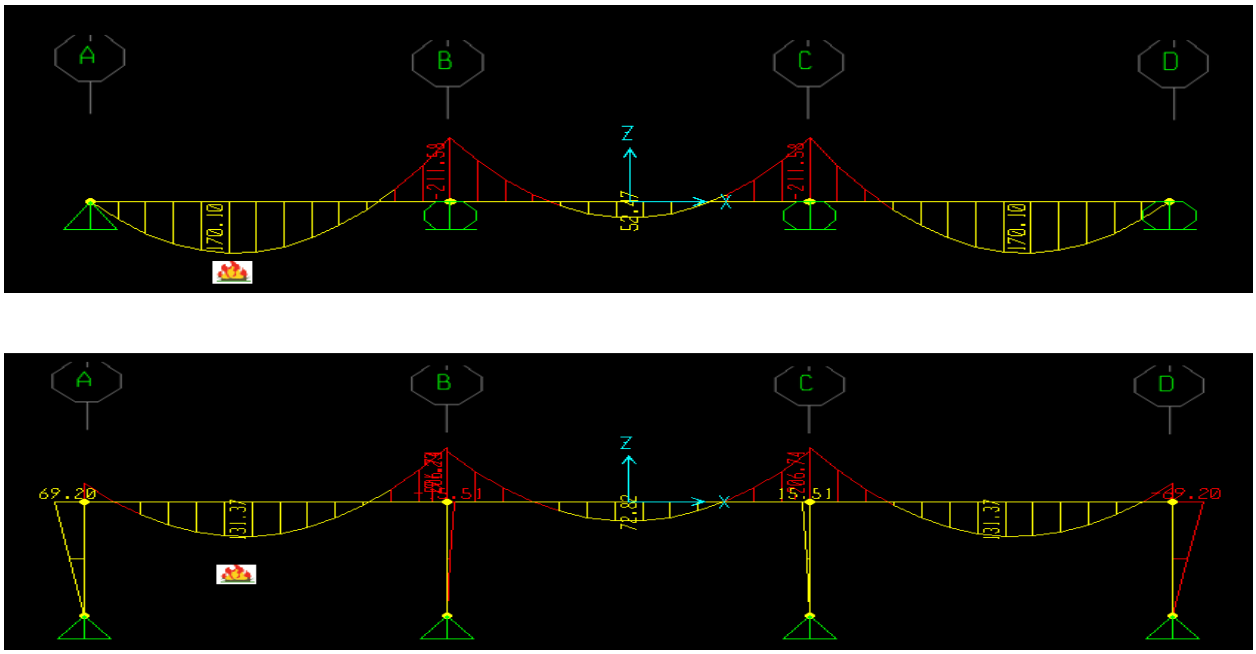

Figure 10: Models for moment redistribution investigation

In both models, the girder was assumed to be W18x50 and subjected to total of dead load and live load of 3.4 kips/ft. In the frame model, the column size was W12x22 and assumed to have fire proofing material so that the fire only affect the girder. The column size W12x22 was determined based on the axial load and bending moment due to office loadings. The fire was assumed to be in the exterior bay of the structure. These two models were investigated not only by looking at the moment diagram but also at support reactions at the column bases.

4.3.Activity 2: Validate SAP2000 and ANSYS for Plastic Limit Method.

In order to validate the ability of SAP2000 and ANSYS to determine the plastic limit loads, a simple model was established. If the results complied, it would prove that SAP2000 and ANSYS have ability to do collapse analysis and would be valid to use for the planned investigations of collapse loads and mechanism. The fixed-end beam model was loaded uniformly *w* along its entire length. The beam size was assumed to be W12x53, and the length *L* of the beam was 10 feet. A schematic diagram is shown in Figure 11

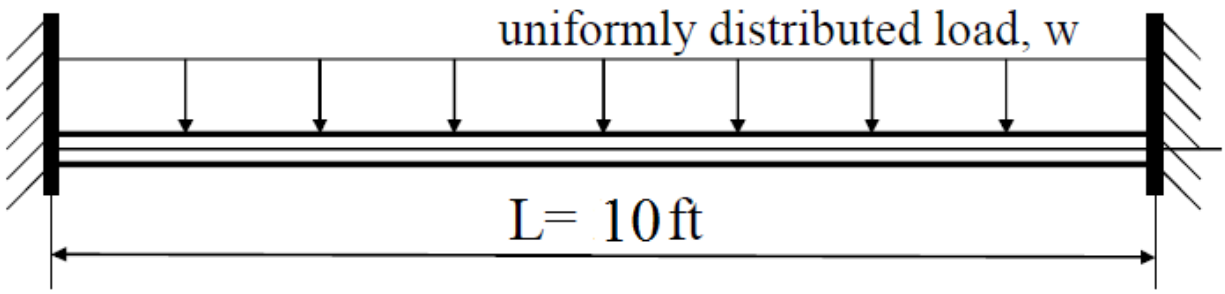

Figure 11: Fixed - End Beam Model

This structure is statically indeterminate to the third degree. However, this beam only has two redundancies for the study of bending. Therefore, the structure would require the formation of 3 plastic hinges for collapse. When subjected to steadily increasing loads, the first and second hinges would occur simultaneously at both ends of the beam when $w = \frac{12M_p}{L^2}$ and the third hinge would form at mid-span of the beam when $w = \frac{16M_p}{L^2}$. M_p is the plastic moment capacity of the beam which is equal to F_y*Z (F_y is the yield strength of the material and Z is plastic section modulus of the member). For the W12x53 member at the normal temperature, the first and second hinges formed at w =3.25 kips/in and collapsed at w = 4.33kips/in. The structure was modeled in SAP2000 and ANSYS to establish whether or not their results complied with the hand calculation.

4.4.Activity 3: Establish and Analyze the Base Model

The main purpose of this activity was to understand the collapse load pattern and collapse mechanism of the established base model at different temperature exposures. This section also investigated the structural redundancy effects of the base model. In order to investigate the continuity effects of the steel structure, a typical office frame was designed. The typical office bay size is 25 ft by 25 ft (Moore, 2003). The layout of the frame is presented in Figure 12. The frame of interest is marked with the red marker. The frame has 3 bays and each one spans 25 ft. The spacing between frames in this layout is also 25 ft. The frame is designed for office gravity loads which include dead load and office live load. The frame has 4 pinned-ended columns as it is shown in Figure 13 which is the side view of the frame. This base model is only one story steel frame with no fire protection. The members for this structural frame were designed based on the information that is presented in Table 5. It was referenced form the work of Amanda Moore, an WPI student, about "*Development of a Process to Define Design Fires for Structural Design of Buildings for Fire*" (Moore, 2003).

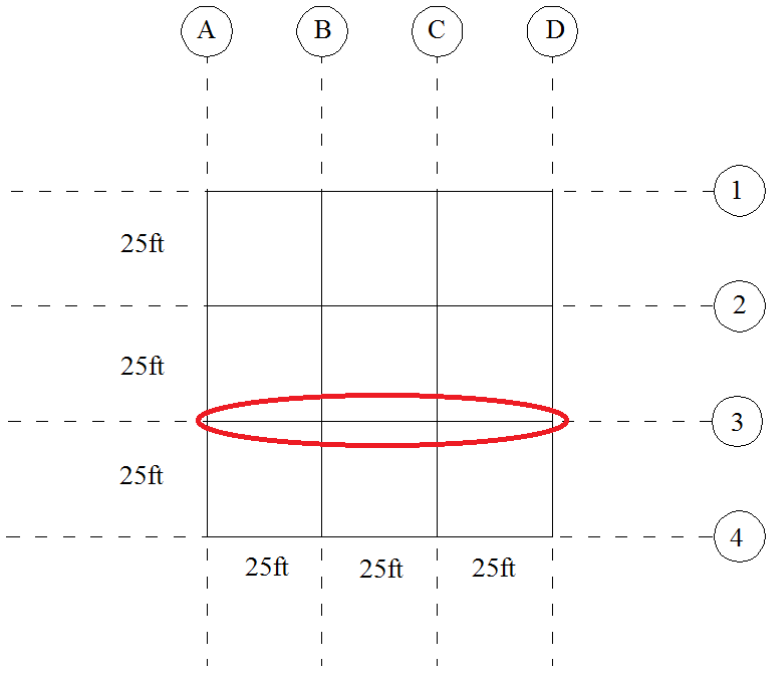

Figure 12: Plan View of office building model

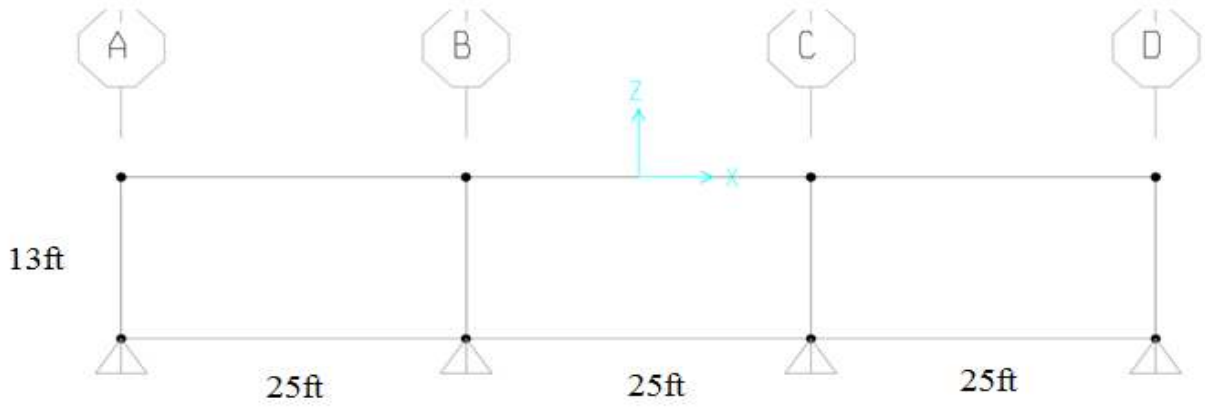

Figure 13: Side View of office building Model

Table 5: Base Model Design Criteria

Occupancy Type	Office
Frame Spacing	25 ft
Number of Bay	3
Slab thickness	4.5 in
Office Live Load	50 psf
Partition	15 psf
MEP	5 psf
Beam Construction Type	Non-Composite

After the base model was established, the structure was analyzed at elevated temperatures. The fire was assumed to be in the exterior compartment of the structure for the first scenario. In the second scenario, fire was assumed to be in the interior compartment of the structure and lastly, fire was in both an exterior and the interior compartment. The fire scenarios are presented in Figure 14. For each scenario, the fire was assumed to be in a particular compartment, and the girder was the only part of the structure that was affected by the fire. By looking at different fire locations, the critical location resulting in the lowest collapse load for fire could be identified.

By using ANSYS and SAP2000, the maximum load capacities of the frame at different temperature exposures were calculated. The structure was investigated at different discrete temperatures and different fire locations. The temperature was assumed to be uniform within the affected girders, and there were seven temperature value considered: 20°C, 100°C, 200°C, 300°C, 400°C, 500°C, and 600°C. The yield strength and the modulus of elasticity of steel at these temperatures, which is presented in Table 6 were input into SAP2000 and ANSYS for the collapse analysis.

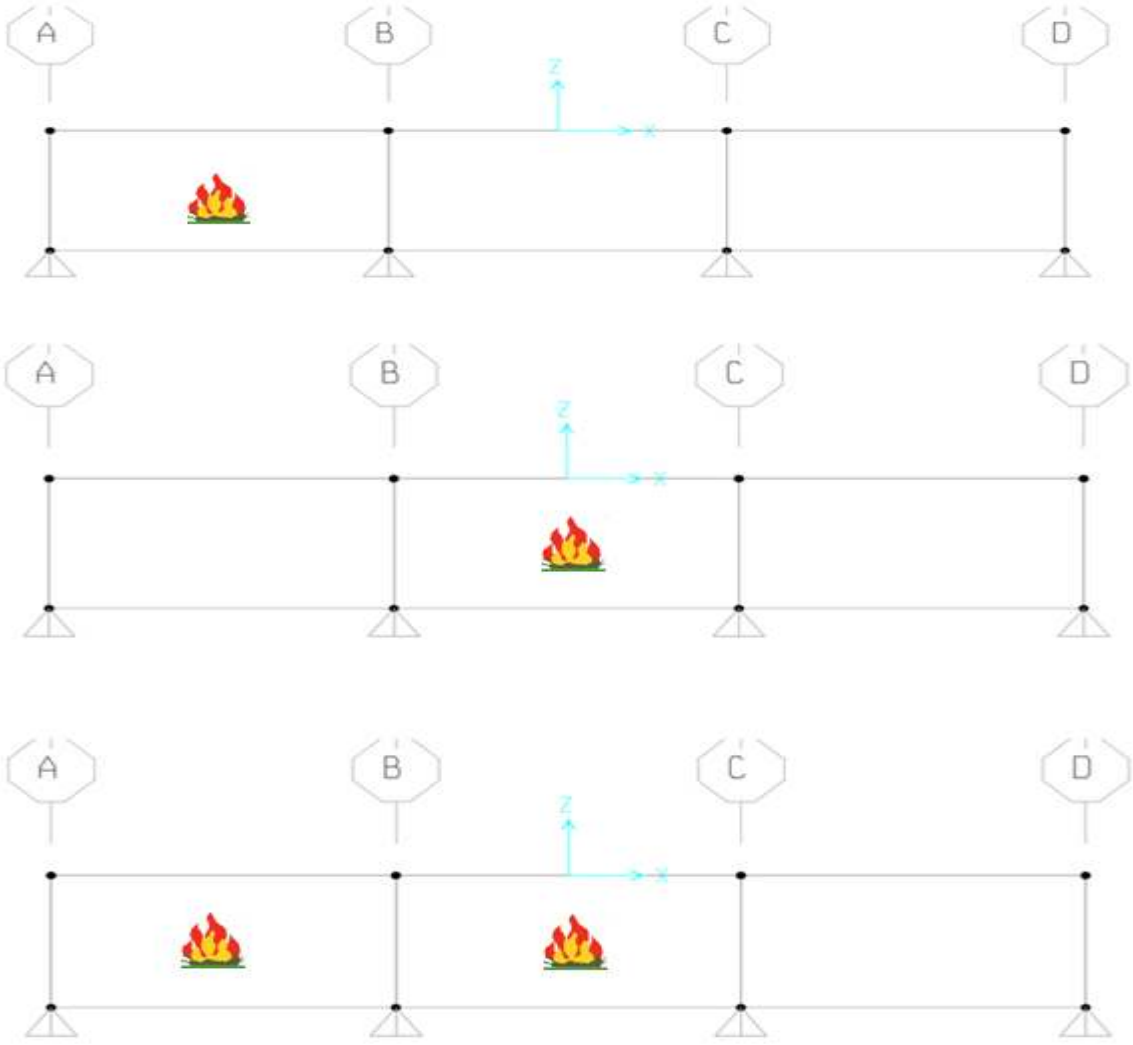

Figure 14: Fire Location Scenarios

Table 6: Yield Strength and Modulus of Elasticity of A992 Steel at elevated Temperature

T (°C)	Et (ksi)	Fyt (ksi)
20	29000	50
100	28395.3	48.06
200	27298.87	44.88
300	25652	40.55
400	23266.51	34.94
500	19804.83	27.83
600	14646.78	18.86

4.4.1. Investigate Effects of Structural Redundancy

In order to investigate the effects of redundancy of the base model, in the first scenario, the columns were removed. Once all the columns were removed, the frame became a three span continuous beam as it's shown in Figure 15. By removing the columns, the structure had fewer redundancies. The collapse load limit for this scenario was expected to be much less than the base case. The second scenario is to change the boundary condition of the base case from pinned-end columns to fixed-end columns to increase the number of redundancies, which is shown in Figure 16. The fire that was applied for these models was in the same compartment as the base case which is shown in Figure 14. By looking at the load carrying capacity of three different cases, the performance of the structural frame based on the redundancy can be evaluated.

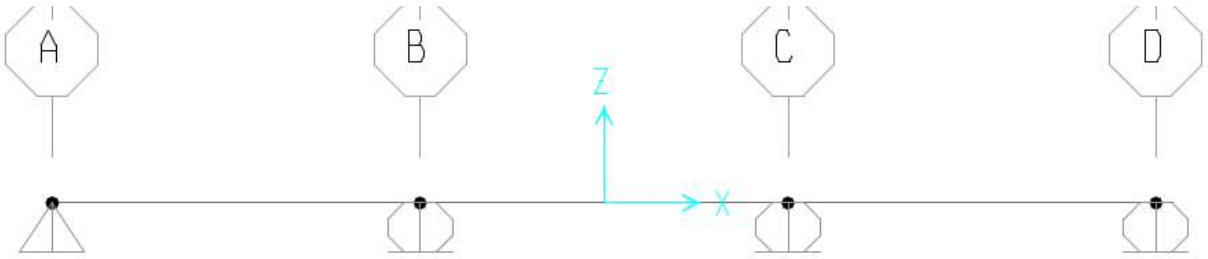

Figure 15: Three Spans Continuous Beam Model

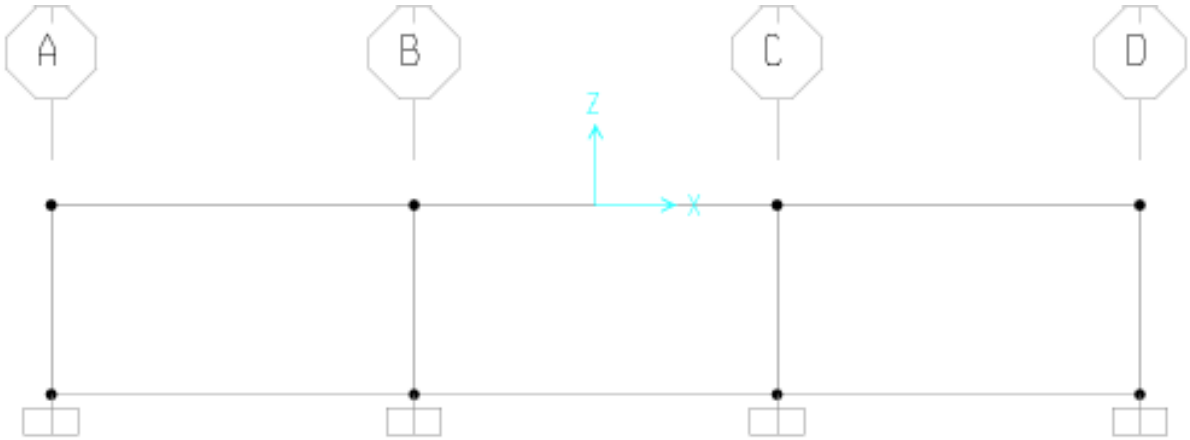

Figure 16: Fixed base at the columns model

4.5.Activity 4: Conduct Parametric Investigations of Base Model

After exploring the changes in structural redundancy of the base model, changes to different parameters were considered. These parameters included girder size, bay size, number of bays and the number of stories.

4.5.1. Investigate the influence of Changing Member Size

In this section, different girder and column sizes were defined to explore their effects on the collapse loads and mechanisms. Since changing member sizes would lead to changing the stiffnesses of the members; bending moments would be distributed differently. In addition, as the member size changed, the plastic section modulus of the member also changed. These effects could lead to different collapse loads and mechanisms.

In the first model, the column size didn't change while the girder size changed. The girder of the structure was designed as a simply supported beam. The new girder size was expected to be bigger than the base case. As the girder size was increased, the plastic limit loads for the new model also were expected to be larger than the base case. The analysis for this model was the same as the base case: three different fire locations, and snap-shot evaluation of the loading capacity at seven different temperatures.

The column sizes in the second model were changed simultaneously with the girder sizes. The girder was still designed as a simply supported beam. However, the column sizes were defined based on maintaining a constant stiffness ratio between the girders and columns. For the base case, the relationship of girder and column stiffness was established based on their moment of inertia and length, $\frac{I_g}{L_g}$ and $\frac{I_c}{L_c}$, respectively. The idea behind focusing on these relationship was to capture the moment redistribution within the frame. The column size for the new model was picked based on Equation 5

$$\frac{\alpha_1}{\beta_1} = \frac{\alpha_2}{\beta_2}$$

where $\alpha = \frac{I_g}{L_g}$ $\beta = \frac{I_c}{L_c}$

I_g: Moment of inertia of the girder
I_c: Moment of inertia of the column
L_g: Length of the girder
L_c: Length of the column

Equation 5: Relationship between girder and column

The collapse analysis of these two new models would provide a good idea of the role of girders and columns in structural continuity effects. The new results from these two new models would be compared to the base model to explore the importance of girders and columns on performance of the frame under fire conditions.

4.5.2. Investigate the Influence of Bay Size

The purpose of this portion of the study was to determine whether or not changing the length of the girder would affect the structural collapse loads and mechanisms. In this study, the length of the girder was changed from 25ft to 40ft but the column height stayed the same at 13ft. By increasing the length of the girder, a new girder design was need to ensure to have sufficient strength to carry the office load at normal temperature. Similar to previous section, the column size was revised by using Equation 5 to maintain a constant stiffness ratio. The analysis process was the same as the base case: three different

models which were three-span continuous beam, pinned base frame, and fixed base frame and the fire locations shown in Figure 14. The results for this study were compared to the base case to determine if bay size has any effect on structural continuity.

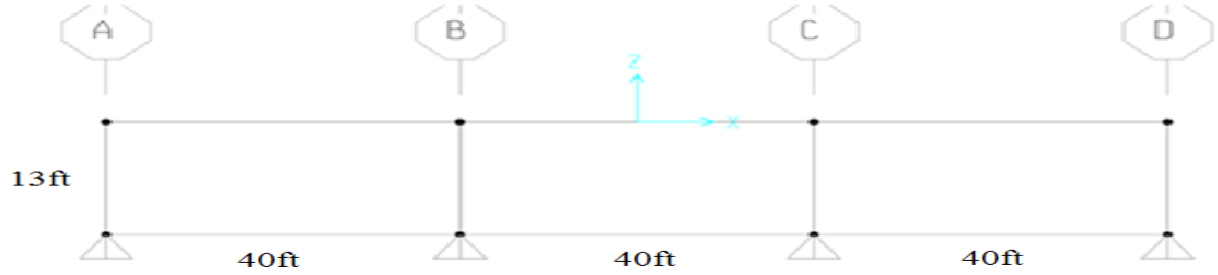

Figure 17: 40 feet-bay model

4.5.3. Investigate the Influence of Adding Another Bay

Similar to previous activities, the purpose of this study was to explore the performance of the structure for a different number of bays. One more bay was added to the base model to create a new frame with 4 bays. The girder and columns sizes were the same as those for the base model. However, because there were 4 bays in this frame, the fire location was assumed very similar to the base case. The first fire location would be the exterior bay, and the second location was in the interior bay next to the first location. Finally, in the third scenario, fire was assumed to occur in both of these two bays simultaneously. Similar to the base model, three different settings (4-span continuous beam, pinned-base frame, and fixed-base frame) were investigated to compare with the base case.

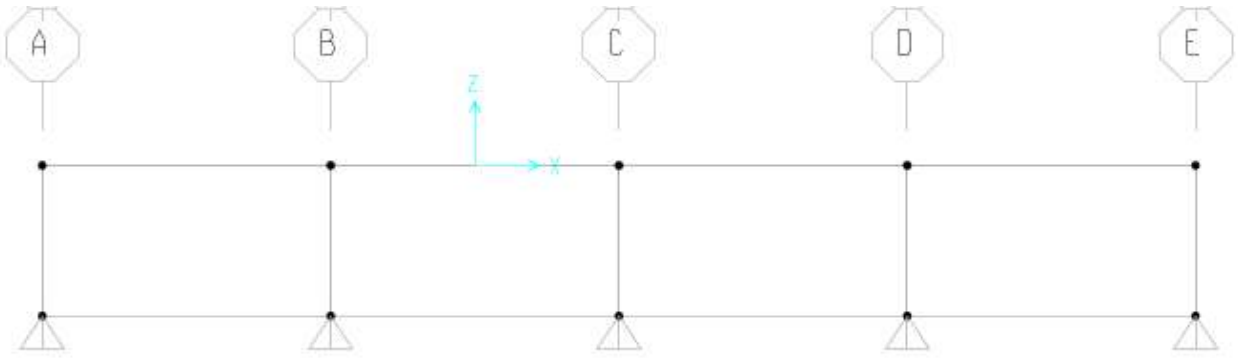

Figure 18: 4 bays frame model

4.5.4. Investigate the Influence of Adding Another Stories

In this study, another story was added to the base model to determine whether or not the associated moment distribution within the frame would affect the collapse loads and mechanisms. At the interior joints, for the base model, three members were concurrent; however, when another story was added to the model, at each interior joint, there were now four concurrent members. Thus the moment would be redistributed to four members instead of three, and the maximum moment in each member would be less than for the base model. Only two boundary conditions were considered for this study which were the pinned-end columns and fixed-end columns. The continuous beam would not be analyzed since it was the same as the base model. In this investigation, there were six different fire location models as shown in Figure 21: three on the first story and three on the second story. For the models with fire on the first story, the outcome was expected to be different than for the base case; however, when the fire locations were on the second story, the result would be comparable to the base case.

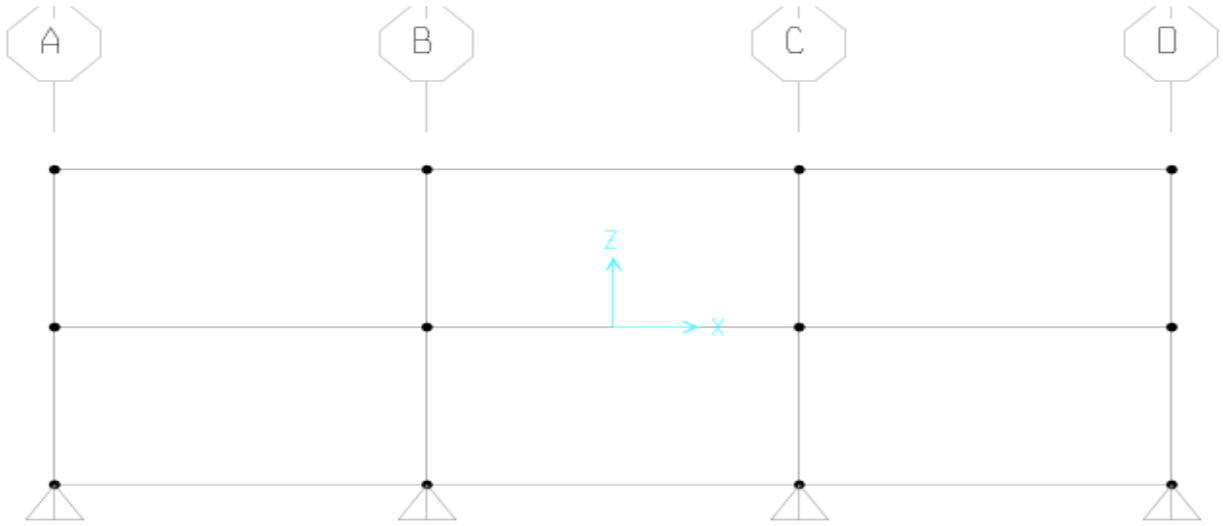

Figure 19: Two story model

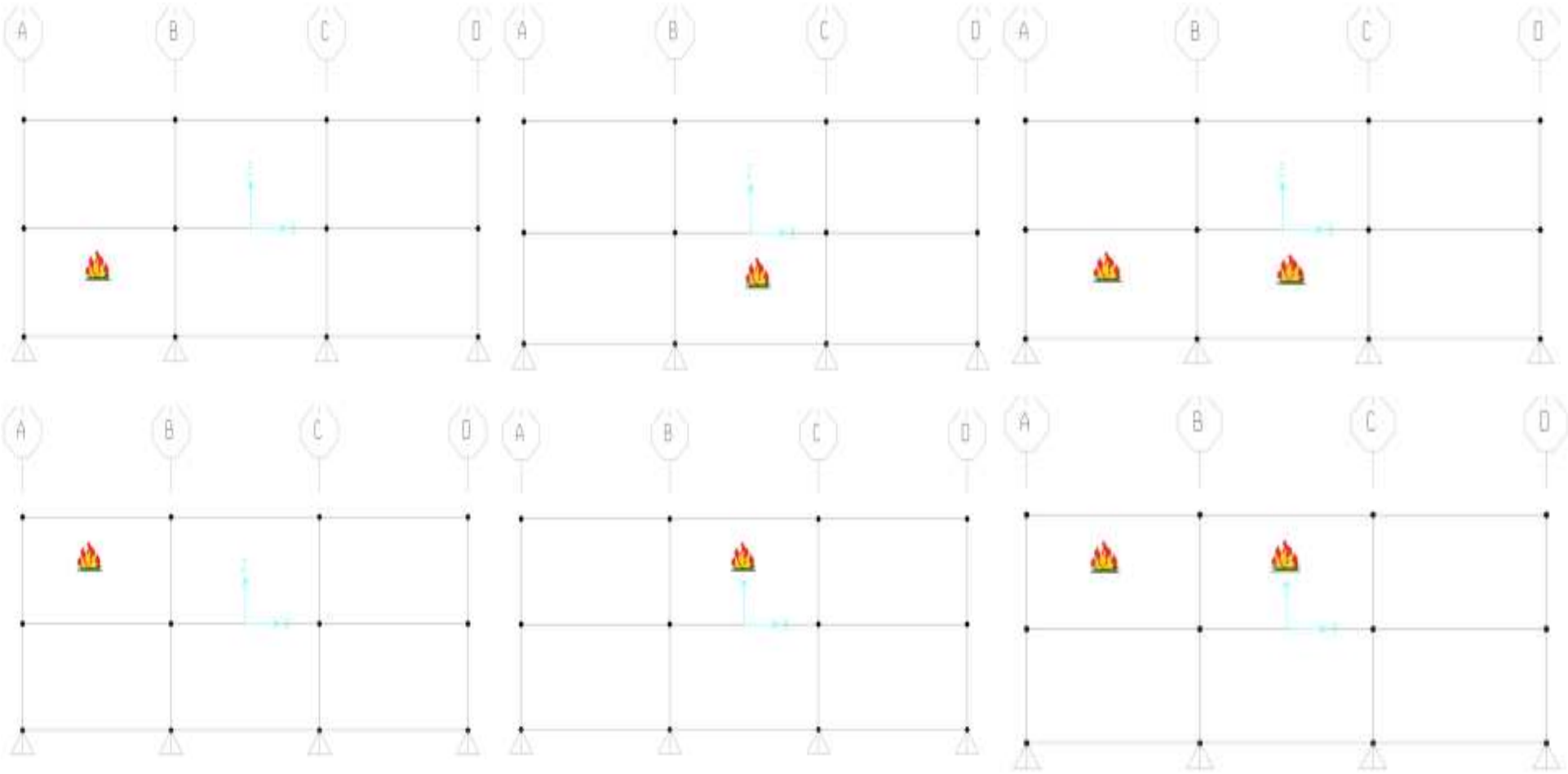

Figure 20: Six fire scenarios for two-story model

4.6.Activity 5: Design Aid Tool

The design aid tool was developed to help structural engineers in a design office readily assess the fire performance of steel frames. The tool was based on the idea of predicting complex structure behavior under fire condition from the results for a simpler model, such as simply supported beam. This notion is very similar to the adaption factor from *Eurocode 3* and the graphs from *Swedish Design Manual*. The tool was created based on the results from activity 2. The results from activity 2 established the collapse load capacities for different cases and different combination of parameters. These collapse loads were normalized by dividing the collapse load of a simply supported beam at the normal temperature to establish β factor. After that, graphs were developed by plotting β values as a function of temperature to observe the trends and to establish a reasonable, conservative approximation.

$$\beta = \frac{Collapse\ Load\ of\ the\ structure\ at\ elevated\ temperature}{Collapse\ Load\ of\ simply\ supported\ beam\ at\ normal\ temperature}$$

Equation 6: β Factor

5. Results

This chapter compares and summarizes the results from ANSYS and SAP2000 models to explore the structural continuity effects of steel frame. First, the collapse loads of simple model were determined by using ANSYS and SAP2000, and then they were compared to hand calculations to validate the plastic analysis ability. Second, the collapse loads and mechanism of different parametric models were investigated by using these finite element software programs. The graphs of the collapse loads for different models were generated by using Excel spreadsheets in order to explore visually the similarities and differences. The numerical data is presented in the *Appendix B* to *L*.

5.1.Moment Redistribution at Elevated Temperature

The engineering properties of steel change with temperature change, especially the modulus of elasticity and yield strength. The result of the changing in modulus of elasticity could lead to the redistribution of moment among members of the structural frames. First, a simple model of three-span continuous beam was investigated to explore the differences in value of the moment at each joint due to changes in the steel member's properties. This models has three spans and each one is 25 ft long. A W18x50 was selected as the member size for all three spans. The uniform loads of 3.4 kips/ft was assigned to all three spans. Figure 21 shows the moment diagram of the structure as it's subjected to the uniform loads, and Table 7 summarizes the moment and support reactions value at each joints at 20°C and 600°C.

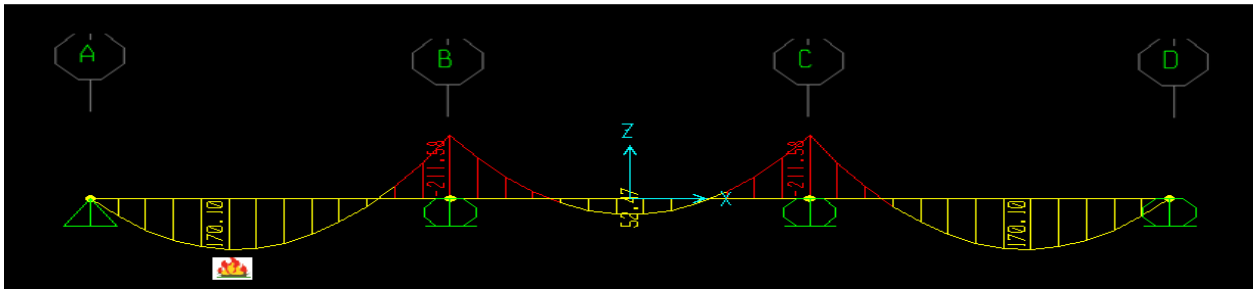

Figure 21: Continuous beam - Moment redistribution

Table 7: Moment values at different temperature of a three span continuous beam

Location	Moment (kips-ft)		Support Reactions (kips)	
	20°C	600°C	20°C	600°C
A	0	0	34.04	33.34
B	211.58	229.1	93.46	95.03
C	211.58	207.34	93.46	92.42
D	0	0	34.04	34.21

Table 7 shows that the moment at joint B changed significantly as the temperature of member AB increased to 600°C. The change in moment value at joint B was about 10% and about 2% at joint C. The moment value at the end of member AB increased as its elasticity of modulus and yield strength were decreased. However, looking at the support reactions, there were some changes in the magnitude but they were not significant. These results indicates that for the three-span continuous model, the moment is redistributed as the temperature of the member changes.

The moment redistribution phenomenon in structural frames was also investigated. W12x40 column sections were added to the three-span continuous beam model. The loading and boundary conditions of the frame model were the same as for the continuous beam model. Similar to Figure 21, Figure 22 shows the moment diagram of the structure, and Table 8 illustrates the differences in moment value at each joints, support reactions and shear reactions at the column bases.

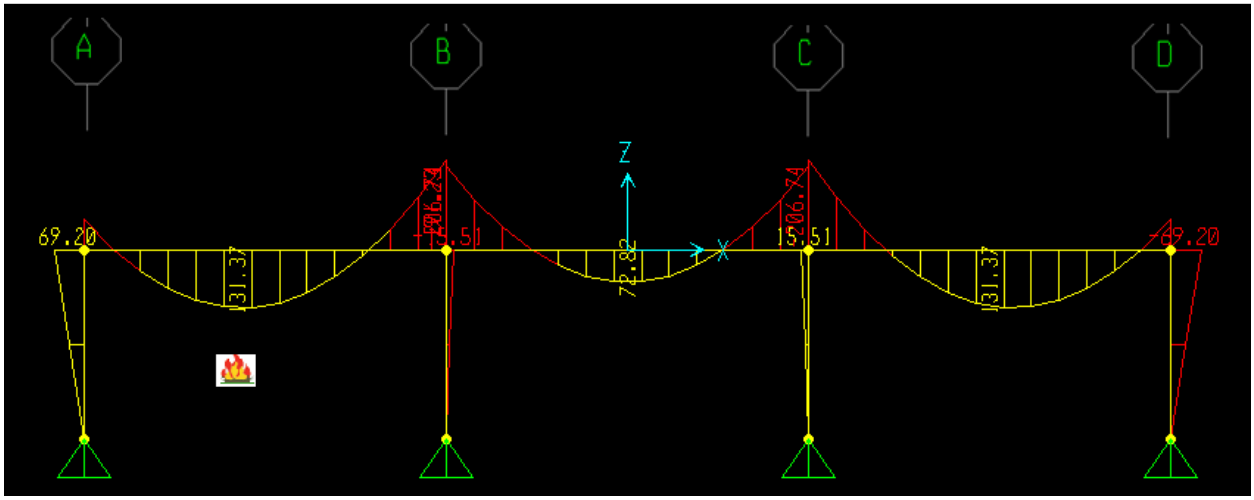

Figure 22: Structural Frame - Moment redistribution

Table 8: Frame Moment, support reaction, support shear value at different temperature

	Joint A		Joint B			Joint C			Joint D	
	Column	Girder AB	Girder AB	Column	Girder BC	Girder BC	Column	Girder CD	Girder CD	Column
20°C	69.2	69.2	206.74	15.51	191.23	191.23	15.51	206.74	69.2	69.2
600°C	91.77	91.77	208.73	22.84	185.88	195.26	6.83	202.09	76.76	76.76

Support Reactions	Base of column A	Base of column B	Base of column C	Base of column D
20°C	37.16	90.34	90.34	37.16
600°C	37.89	89.37	90.08	37.66

Shear Reactions	Base of column A	Base of column B	Base of column C	Base of column D
20°C	5.37	-1.38	1.38	-5.37
600°C	7.08	-1.93	1.75	-5.9

Table 8 shows that with the presence of the columns in the model, it's obvious that the moments were redistributed. There was significant increase in moment at the exterior joints A and a slight increase at joint D. The moment at the interior joints (B and C) however didn't change much. By looking at Table 8, the moment at the ends of the heated member generally increased. Similar to the continuous beam model, the support reactions and shear reactions at the base of the columns did change however, the change in magnitude was not significant.

The investigations of two models at two different temperatures showed the phenomenon of moment redistribution happening within the structural frames. For the members subjected to increased temperature, the moment along the beam also increased. By increasing the temperature of the member, the collapse mechanism of the structure not only depends on the reduction of yield strength of the member but also the moment redistribution effects.

5.2.Plastic Analysis of Simple Model by Using ANSYS, SAP2000 and Hand Calculation

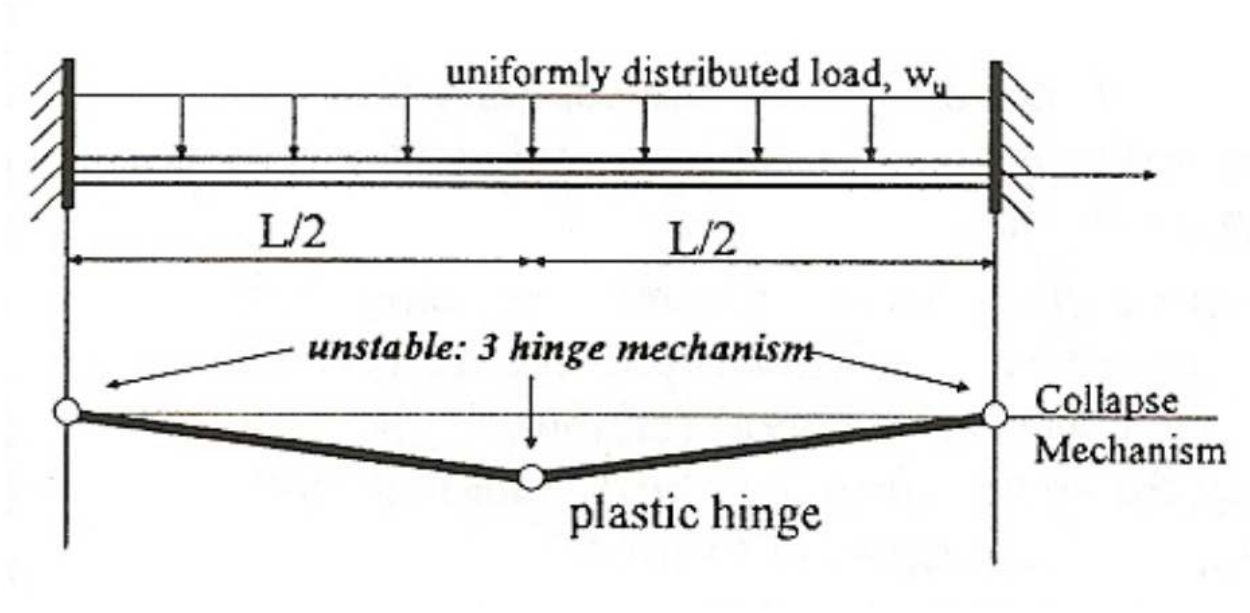

Figure 23: Fixed-end beam collapse mechanism

A fixed-end beam model was established to validate the plastic analysis capabilities and accuracies of two finite element software programs. Figure 23 illustrates the collapse mechanism of the fixed-end beam model. When the beam was subjected to increasing loads, the first two hinges would occur at the ends of the beam as it's shown in Figure 23. As the loads is increased, a third hinge would form at the mid-span of the beam resulting in a collapse mechanism. Table 9 presents the collapse loads of the beam model which were calculated by hand calculation, SAP2000 and ANSYS. The hand calculation was based on the virtual work method

Table 9: Collapse Load of Simple Model

	Hand Calculation	SAP2000	ANSYS
First and Second hinges	3.25 k/in	3.246 k/in	3.375 k/in
Third Hinge	4.33 k/in	4.329 k/in	4.375 k/in

Based on the hand calculation, the first and second hinges would form at the loads $w = \frac{12M_p}{L^2} = 3.25$k/in and the final hinge would occur at the loads $w = \frac{16M_p}{L^2} = 4.33$ k/in. The SAP2000 and ANSYS models provided similar results. With SAP2000, the results were about 0.1% less than the hand calculation while

the ANSYS results were slightly higher. The differences in results among these models were less than 5%. Thus, use of SAP2000 and ANSYS for plastic limit method analyses was considered appropriate.

5.3.Establish and Analyze the Base Model

The base model was designed for a pinned-base frame of an office building. The girders were assumed to be continuous and had a constant member size of W12x53. The interior and exterior columns of the frame were also assumed to have a constant member size of W12x22.

The data for collapse loads of the frame at different temperature exposures are presented in Figure 24. The collapse loads were calculated for three different fire location scenarios which were first span, middle span, and first and middle span. Looking at the data in Figure 24, it's obvious to see the differences in collapse loads among the fire locations. In the case where the fire occurred in the middle span, the collapse loads didn't change from 20°C to 300°C. The reason for this phenomenon was that the collapse mechanism for this case didn't change as the temperature increased from 20°C to 300°C: collapse always occurred in the girder of the exterior bays. After 300°C, the collapse loads started to drop significantly as the collapse mechanism changed. Because of the considerable reduction in strength of the interior girder, a beam mechanism would occur in the interior girder as the temperature went beyond 300°C.

In the cases where the fire occurred in the first span and both first span and middle span, the collapse loads show a general decreasing trend. There were only slight differences in the cases where fire occurred in the first span and the fire occurred in both first and middle span. The collapse mechanisms for these two cases were similar as the beam mechanism always occurred in the girder of the first span. This results indicate that fire in the exterior bay was the critical location.

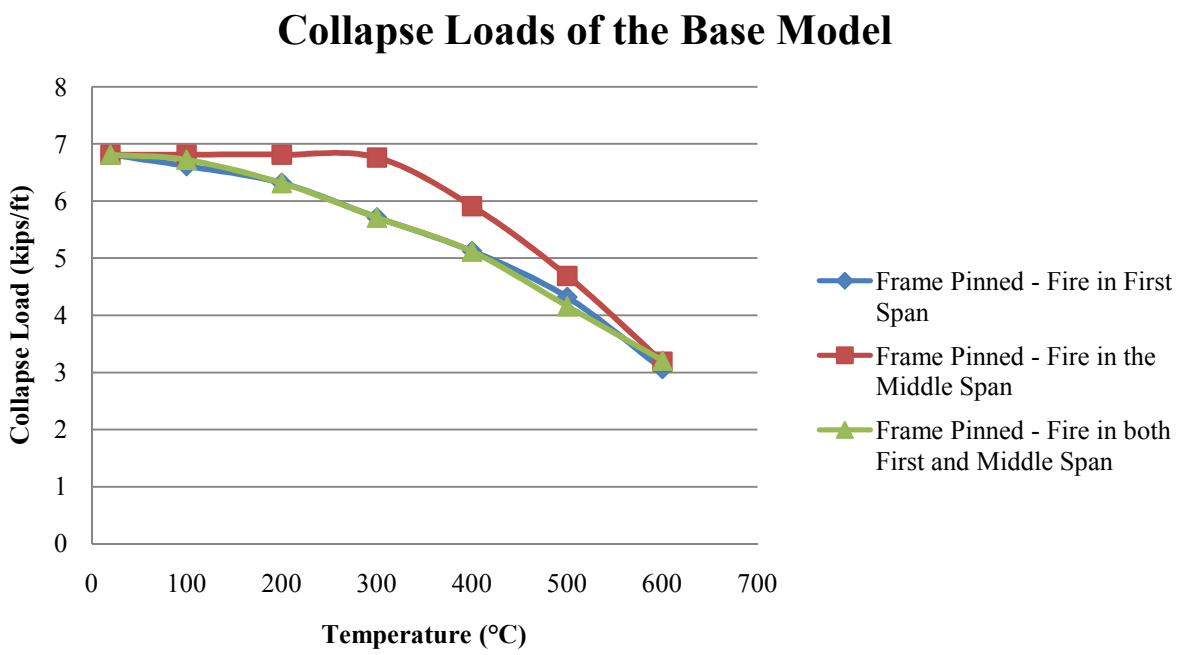

Figure 24: Collapse Loads of the Base Model

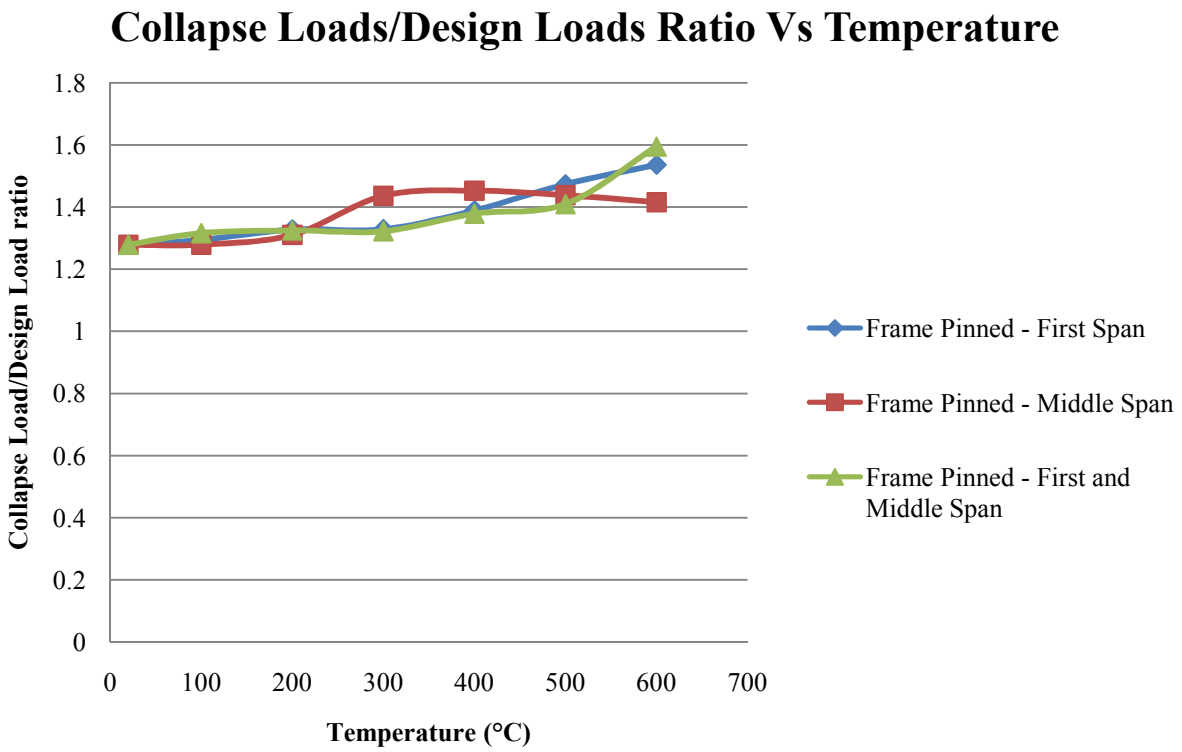

Figure 25: Collapse Loads/Design Loads Ratio Vs Temperature Pinned-base Frame

Figure 25 shows the collapse loads/design loads ratio of the pinned-base frame at elevated temperatures. The design loads are defined as the loads that the structural engineering would use to design at the elevated temperature. It was the level of load that causes the first hinge to form in the system. The engineering design is based on the elastic behavior. Therefore, once the first hinge occurs, the structural failure was considered. The purpose of the collapse loads/design loads ratio was to show the ability of carrying additional loads after initial yielding of the structures. In the case where the fire occurred in the middle span, it's obvious that there is a jump in the ratio at 300°C and this change is due to the change in the collapse mechanism. Above 300°C, the ratio value for this case slightly decrease. For the other two cases, the ratio was gradually increase as the temperature increased. The graph of these two cases are almost identical, though, there is still a small different at 500°C.

5.3.1. Analyze the Three-span Continuous Beam Model

The three-span continuous beam model was established by removing the columns from the base model. By removing the columns, the degree of redundancy of the structure decreased, thus, the load carrying capacity of the structure was expected to be decreased. After investigation, the collapse loads of the continuous beam models are plotted in Figure 26.

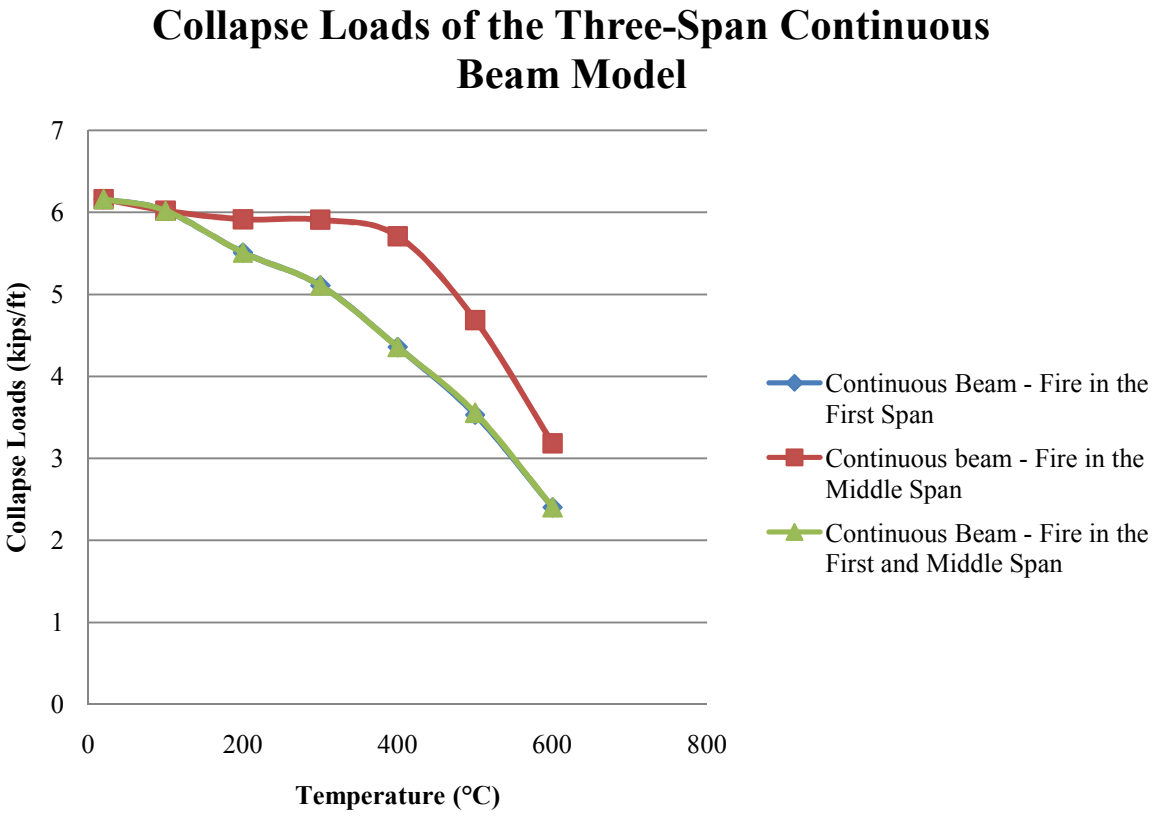

Figure 26: Collapse Load of the three-span continuous beam Model

Figure 26 shows similar trends in collapse loads at elevated temperature as were observed for the base model. The changing collapse mechanism phenomenon when fires occur in the middle span was also the reason for the drop of collapse load in this case. Moreover, the load capacity curves for fire in the first span and for fire in the first and middle span are almost identical. They are overlap each other. However, the load capacity curves does not converge as they approach 600°C while for the base model, the three curves converge.

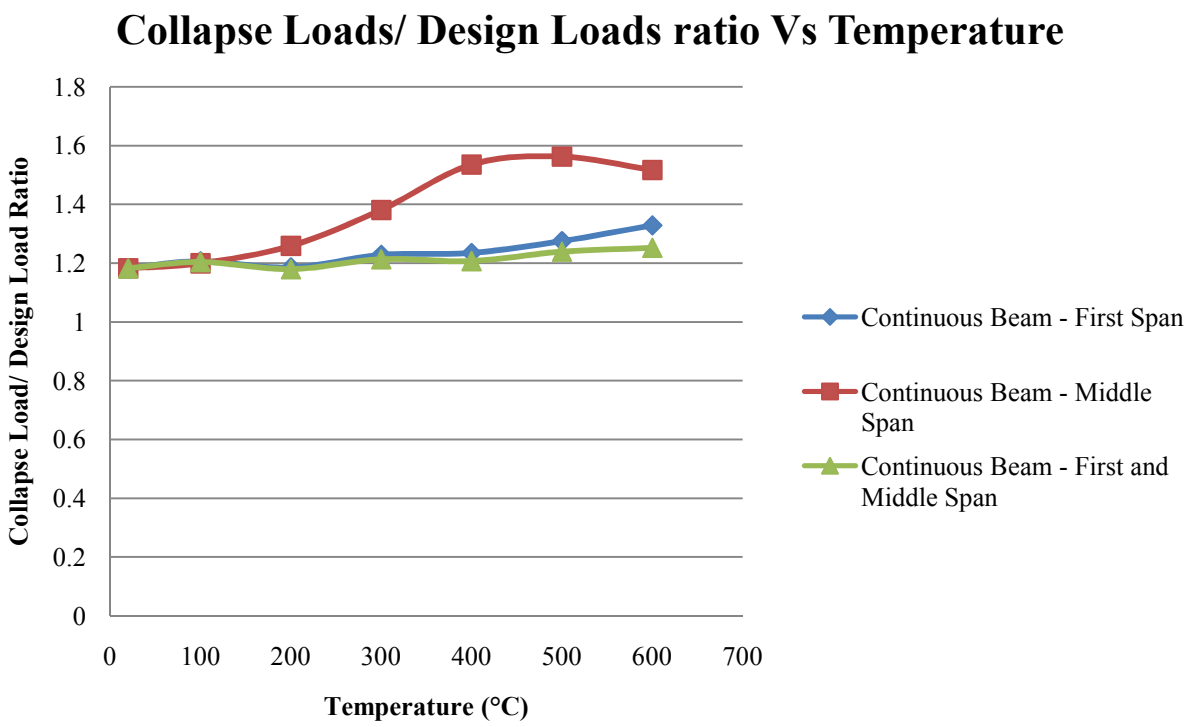

Figure 27: Collapse Loads/Design Loads Ration Vs Temperature - Continuous Beam

Figure 27 shows the collapse loads/design loads ratio of the continuous beam model at elevated temperature. It shows the ability carrying additional loads after initial yielding of the structure. Figure 27 illustrates that after the first hinge was formed, the structure could carry at least 20% additional load for the cases where the fire occurred in the first span and both the first and middle span. The data for the first span case and both first and middle span fire case was similar up to 300°C. After 300°C, the collapse loads/design ratio for the first span fire start to pick up and gradually grow away from the first and middle span fire case Moreover, in the case where fire occurred in the middle span of the three-continuous beam system, the structure could carry up to 57% additional load at 500°C.

5.3.2. Analyze the Fixed-base Frame Model

The support conditions of the base model were changed to increase the degree of redundancy of the structure. The purpose of this investigation was to determine the sensitivities of the column support condition to the structural collapse mode. It was initially expected that the load-carrying capacity of the

system would increase because the degree of redundancy for this model was greater than for the base model.

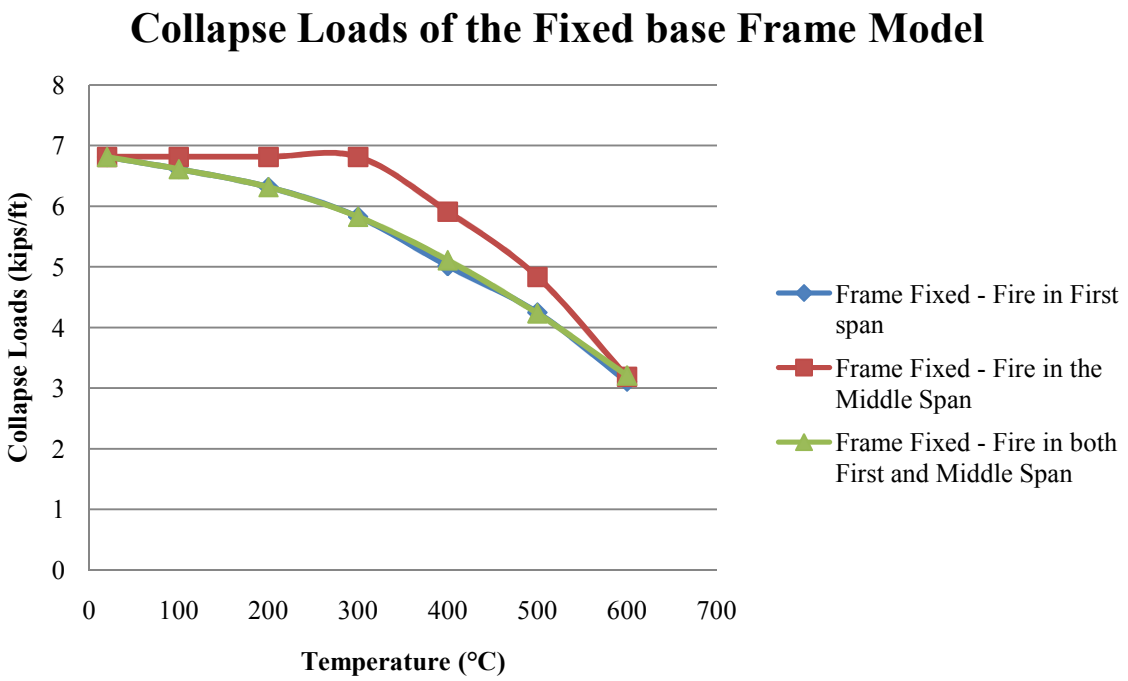

Figure 28: Collapse Loads of the Fixed Base Frame Model

However, Figure 28 demonstrates that the collapse loads for this model were almost identical to the base model's. Comparing this model to the base model, there were only a few cases where this model had a slightly different value of the collapse load such as fire occurred in the middle span with the temperature of 300°C and fire occurred in both first and middle span with temperature of 100°C, 300°C, and 500°C.

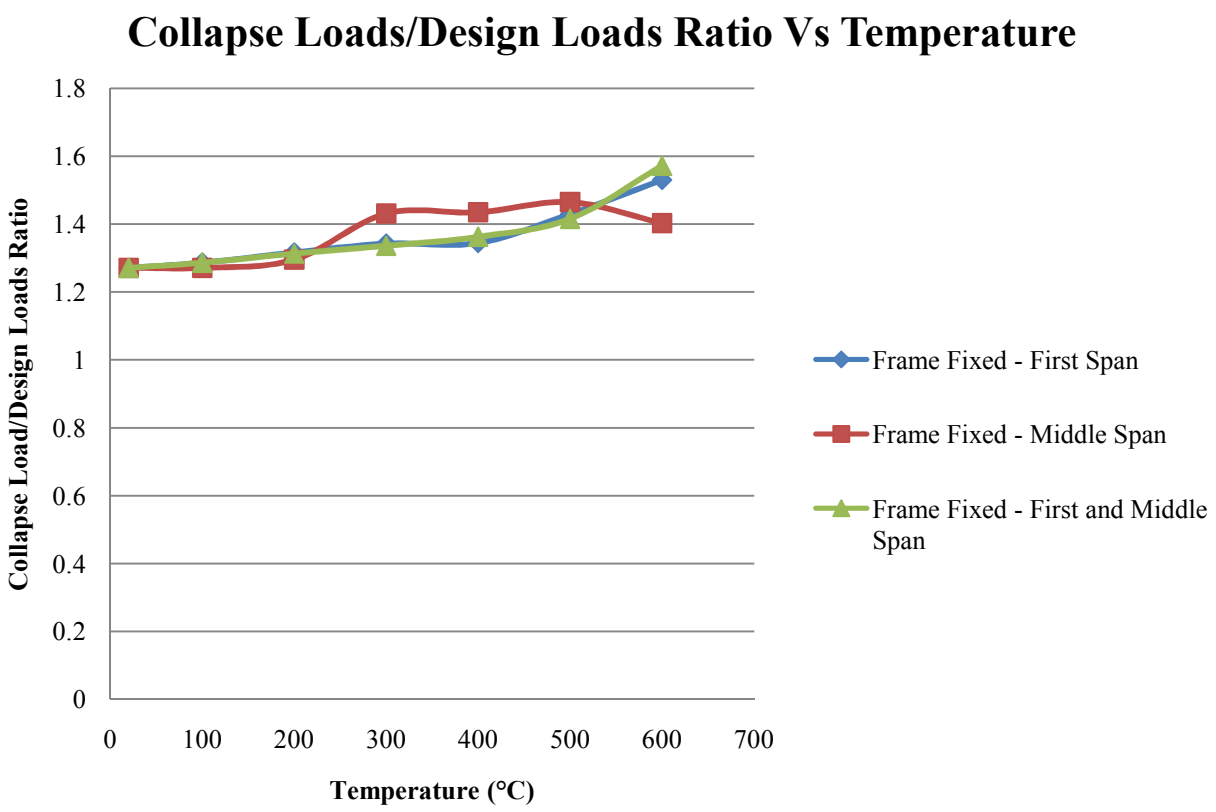

Figure 29: Collapse Loads/Design Loads Ratio Vs Temperature - Fixed-Base Frame

The collapse loads/design loads ratio of the fixed-base frame model is presented in Figure 29. Comparing to the base model, the graphs for fixed-base frame model had similar trends. For example, both graphs have a jump in the curves for fire in the middle span. In addition, gradually increasing trends for fire in the first span and for fires in the first and middle span are presented in both Figure 25 and 29. Thus, it can be concluded that changing the support condition of the base model had little effects on the collapse loads of the structure

5.3.3. Redundancy Effects of the Base model Results Summary

This section summarize the results from the investigation of the redundancy of the base model. The collapse loads curves for different models were combined in order to illustrate better comparisons among there models. The same concept would be applied for the collapse loads/design loads ratio graphs.

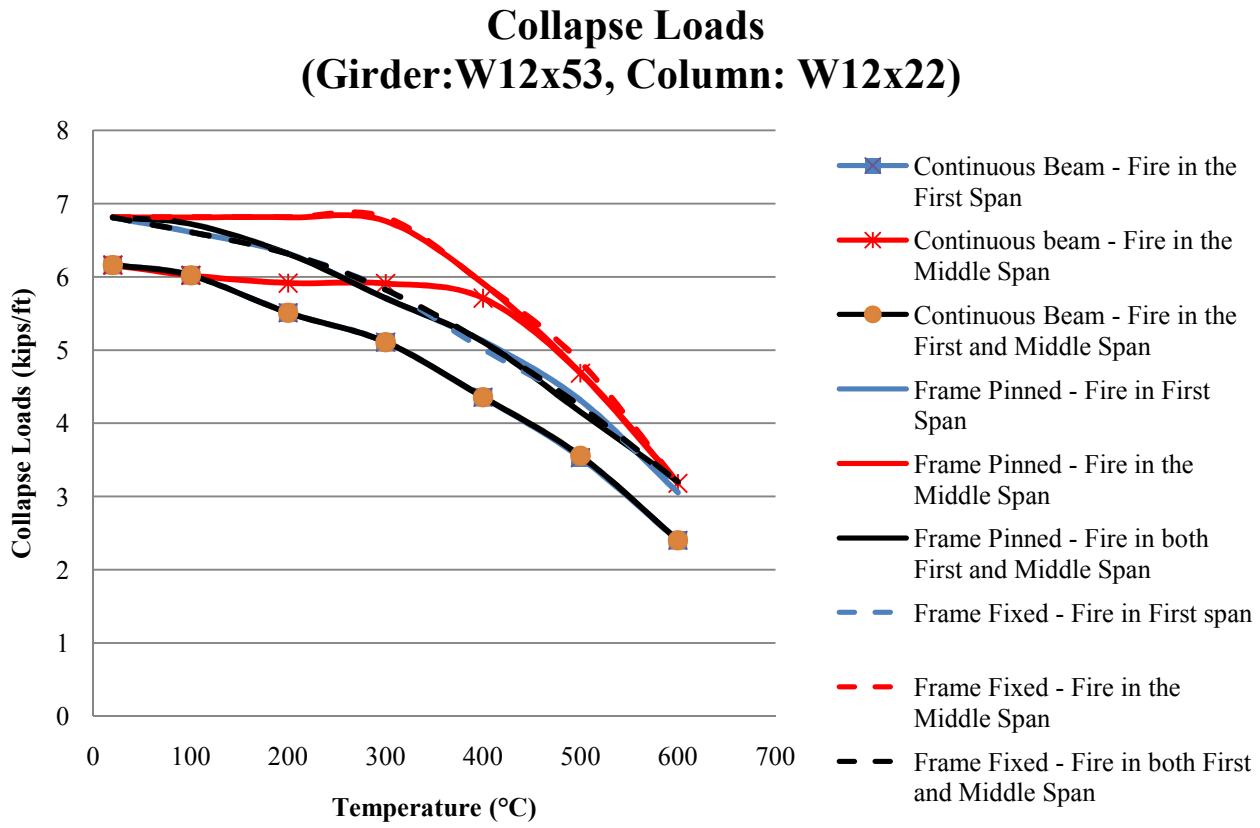

Figure 30: Collapse Loads of Redundancy Investigation for Base Model

The collapse loads investigation of three different models for degree of redundancy were combined and presented in Figure 30. The collapse loads of the frame models are larger than for the continuous beam model. It can be concluded that the columns help to improve the load carrying capacity of the structure. It's also noticeable that the load capacity curves for pinned-base frame and the fixed-base frame models overlap each other, indicating that the collapse loads for these two structures are the same in most of the case. The plastic limit loads differences for these two cases were only less than 2%. In the cases involving fire in the middle span, the collapse mechanism changed after the temperature reached 300°C. The collapse loads stayed at a constant value when the temperature was less than 300°C because the collapse consistently occurred at the exterior girder instead of the fire exposed girder. One more noticeable observation is that all the curves for the frame collapse loads graph converge to one point at 600°C. This

convergence indicates that the fire locations and column support boundary condition have little sensitivities in collapse loads of the structure.

Figure 31 shows the collapse loads/design loads ratio for three models at the elevated temperature. In most cases, the ratio start to increase as the temperature rises; however, for cases with fires in the middle span, the ratios decrease after the big jump. In the case for the continuous beam, a increased load capacity of 20% of the design loads would be a conservative number for all three fire locations. The frame system could have a slightly higher value of 30% of the design loads at the elevated temperature.

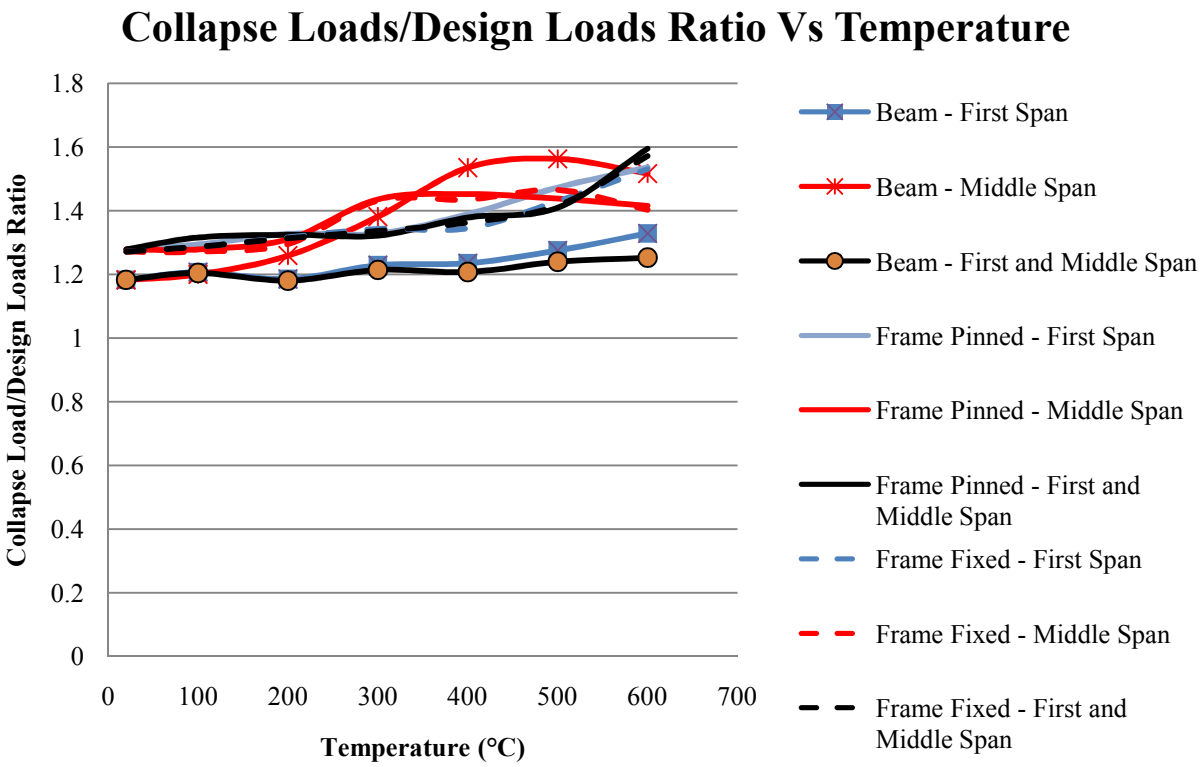

Figure 31: Collapse Loads/Design Loads Ratio Vs Temperature of Redundancy Investigation for Base Model

Some observations for the redundancy investigation results are listed below:

- The presence of columns in the structure helps to increase the load-carrying capacity of the structure.
- The column support conditions have little effects on the structure's collapse loads.

- At 600°C, the collapse loads of the structure have little senilities to the fire locations and column support conditions.
- For fire occurring in the interior bay of the structure, there is a change in collapse mechanism of the frame model as the temperature reaches 300°C.
- Except for cases of fires in the middle span, the collapse loads/design loads ratios gradually increase as the temperature rises.
- In the continuous beam model, the collapse loads/design loads ratios for fire in the first span and for fires in the first and middle span start to diverge from each other as the temperature reaches 300°C.

5.4.Conduct Parametric Investigations of Base Model

This section presents the results for different parametric investigations of the base model. The investigations included the effects of changing member sizes, bay sizes, number of bays, and number of stories. Because of the moment redistribution effects at the elevated temperature, in the investigations of influence of the member size and bay size, a model was established with constant stiffness ratio between the girders and columns, and the ratio was hold equal to that for the base model. The collapse loads and collapse loads/design ratio of these parametric cases are compared to the base case in order to determine the sensitivity of the collapse of the structure to each of the effects.

5.4.1. Influence of Changing Member Size

This section presents two new set of models. In both of the new sets, the girders of the base case were changed into larger sections based on the design for simply-supported beam. With larger sections, the collapse loads for these cases were expected to be larger than for the base model. For the first model, the new section was selected to be W18x50 based on the design for a simply-supported beam to carry the office loadings. The columns for this model were not changed. It was expected that the collapse loads and collapse mechanism for this model would be different from the base model since the stiffness ratio

between the girders and columns of the structure was changed which would change the distribution of moments at each joint.

In the second model, the same girder size, W18x50. was also selected. In order to maintain the stiffness ratio between the girders and columns of the structure, the new column section was determined to be W14x30. The collapse loads/design loads ratios for this model were expected to be similar to the base model; however, the ratio values were a bit off because of the error in the member modeling. This error is explained in Appendix A.

Figure 32 illustrates the influence of changing girder size on collapse loads. The collapse loads for two new sets of models are compared to the base model to compare the trends amongst these models. The patterns of the curves are similar; however, the level of loads are different. As expected, the models that have larger girder size have more load-carrying capacity. The change in collapse mechanism is still presented in all these models for the case of fire in the middle span. In addition, the fires occurring in the exterior bays were always the critical case. As the temperature rises, the curves for the frame models start to converge.

Figure 33 shows the comparison of collapse loads/design loads ratio among three models. The graphs for these cases are not identical but exhibit the same pattern. The value for ratio of the base model ranges from 1.2 to 1.6 while the other two models range from 1.1 to 1.5. In the case where a constant stiffness ratio is maintained, all the data trends are very much similar to the base model. Both Figures 31 and 33 also show that as the temperature rises, the collapse loads/design loads ratio also increases.

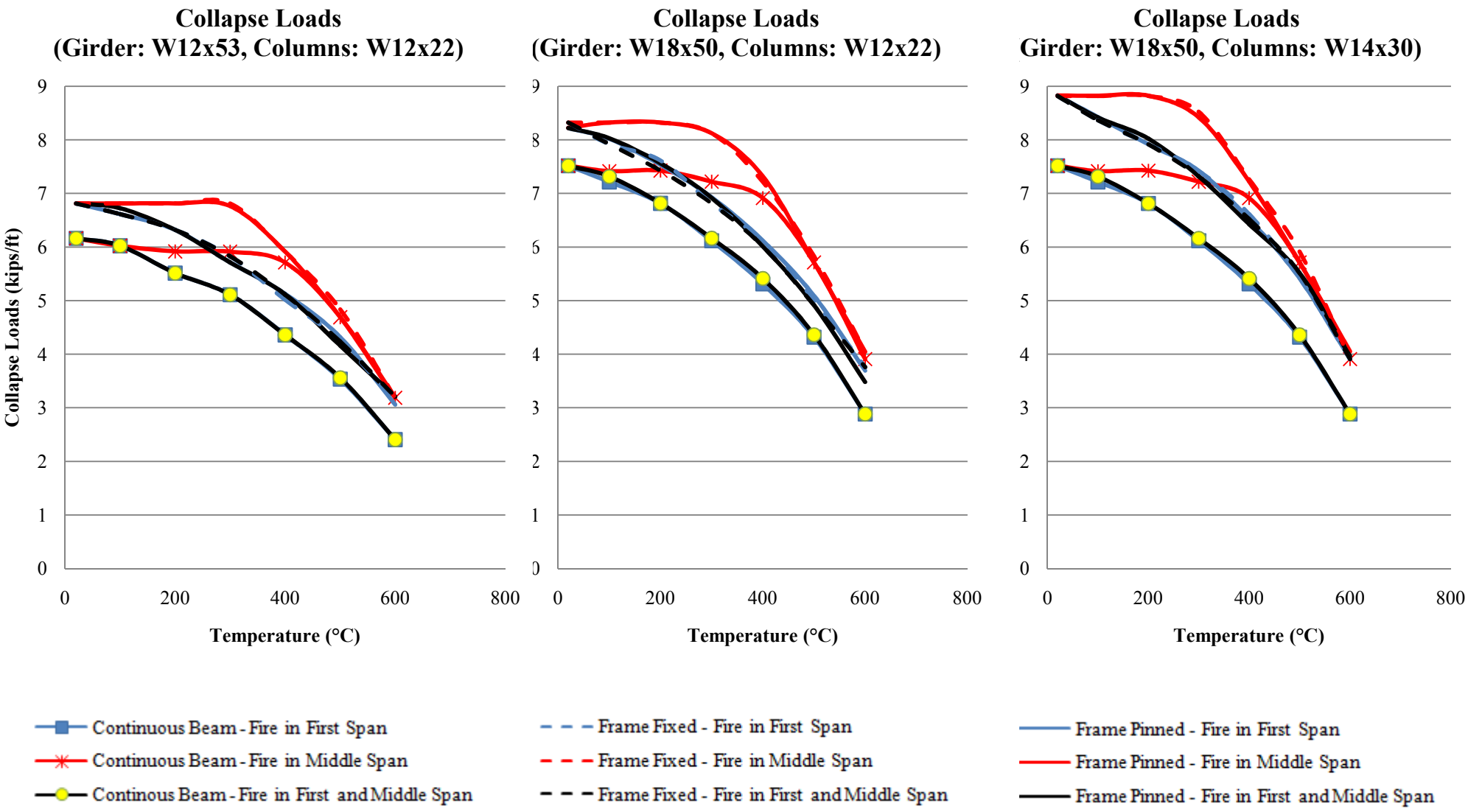

Figure 32: Influence of changing member size - Collapse Loads

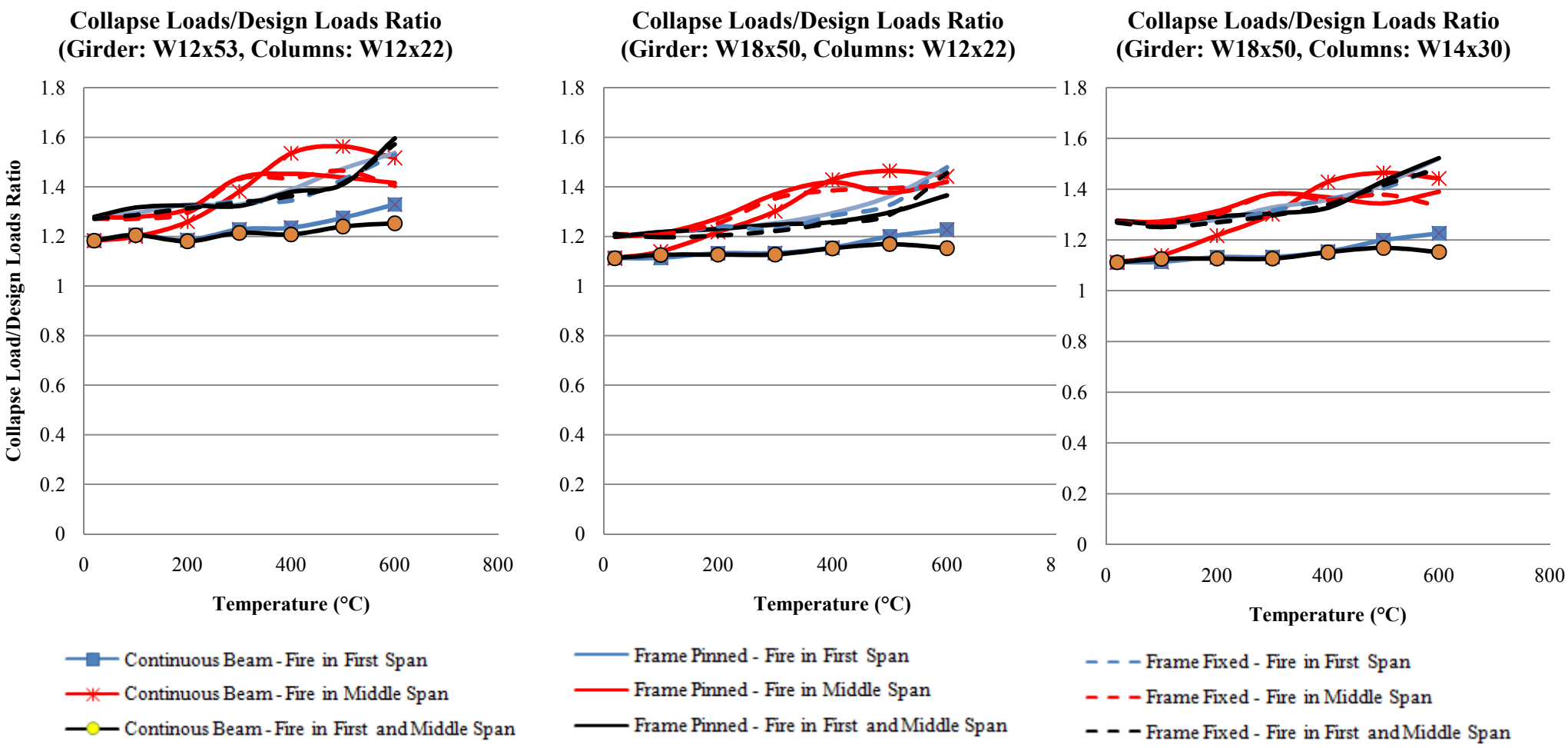

Figure 33: Influence of changing member size - Collapse Loads/Design Loads Ratio

5.4.2. Influence of Changing the Bay Size

In order to investigate the influence of changing the bay size, the girder span of the base model was increased from 25ft to 40ft. As the girder length increased, a new set of girder and column size were established. This set of design also maintains the stiffness ratio between girders and columns. First, the girder size was established by selecting member with the same collapse load of simply supported beam of the base model. The column size was determined by using a constant stiffness ratio of the base model. After the design procedure, an W16x100 beam and an W14x34 section were selected for the girders and the columns respectively.

Figure 34 compares the collapse loads of the new model compared to the base model. The graphs for 40-foot models displayed almost identical behavior for all the fire exposure cases, although there were slight differences in the magnitude of the loads. The patterns of the new model curves are the same as the base model shown in Figure 30. This results shows the relationship of the influence of changing they bay size and the stiffness ratio of the girder and column along with the plastic section modulus of the member.

Figure 35 compares the ability to carry additional loads after the first hinge was formed of the base model and the 40-foot model. The curves for the 40-foot model resemble the base case except for the case with fire in the middle span. The case with fire in the middle span in both new model and base model experienced the shift of the jump. In the base case, the jump usually occurred at 300°C; however, for the 40-foot model, the jump occurred at 400°C. Other curves still experienced the same gradually increasing trends as the temperature rises to 600°C.

In summary, with the increase in bay size, the new model demonstrated the same behavior as the base case. There was a change in collapse mechanism that caused the change in curve pattern for the cases with fire in the middle span. Additionally, fires in the first bay always created critical situation. As the temperature reached 600°C, all the curves for frame structure converged to one point as it shown in Figure 34.

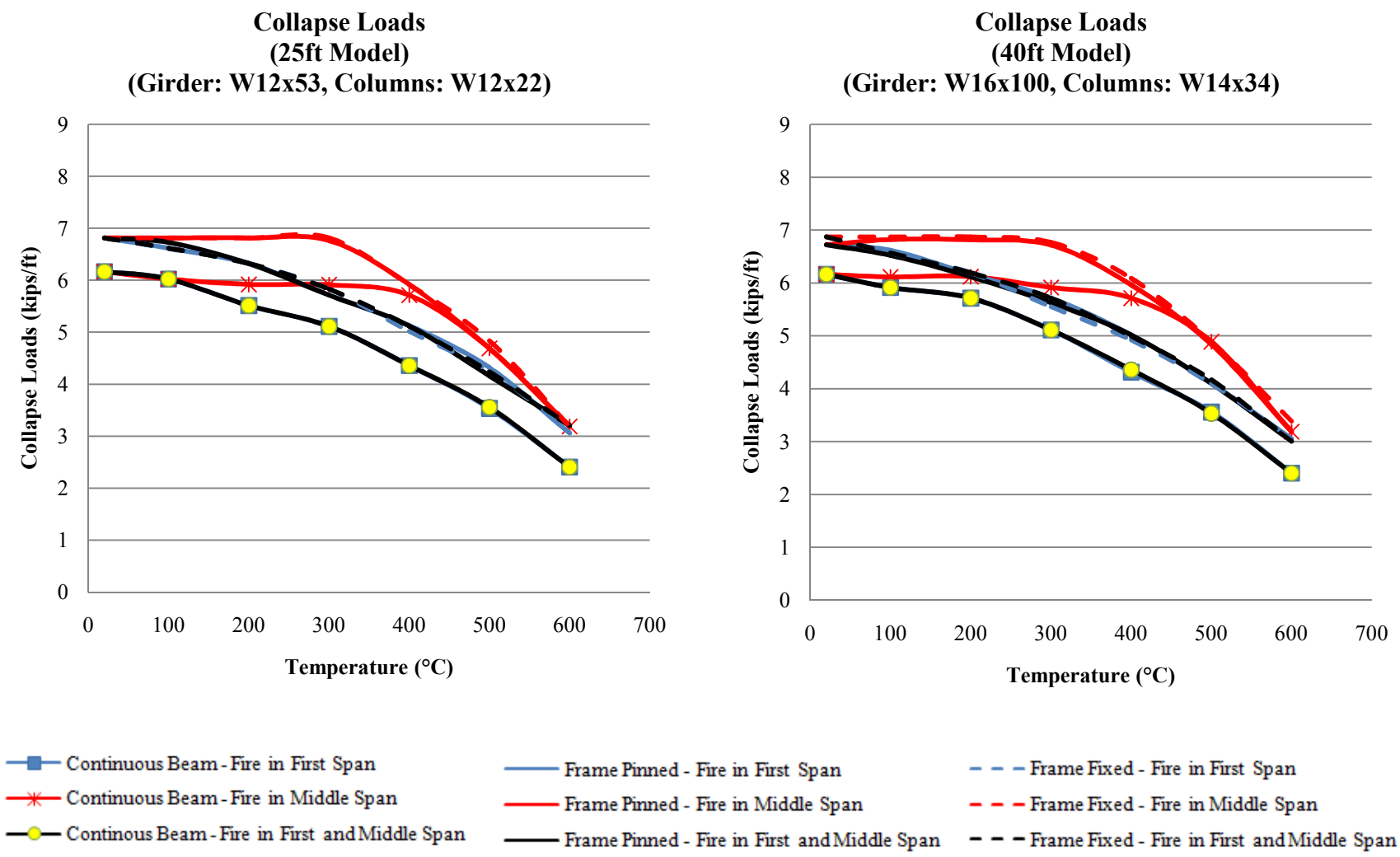

Figure 34: Influence of changing the bay size - Collapse Loads

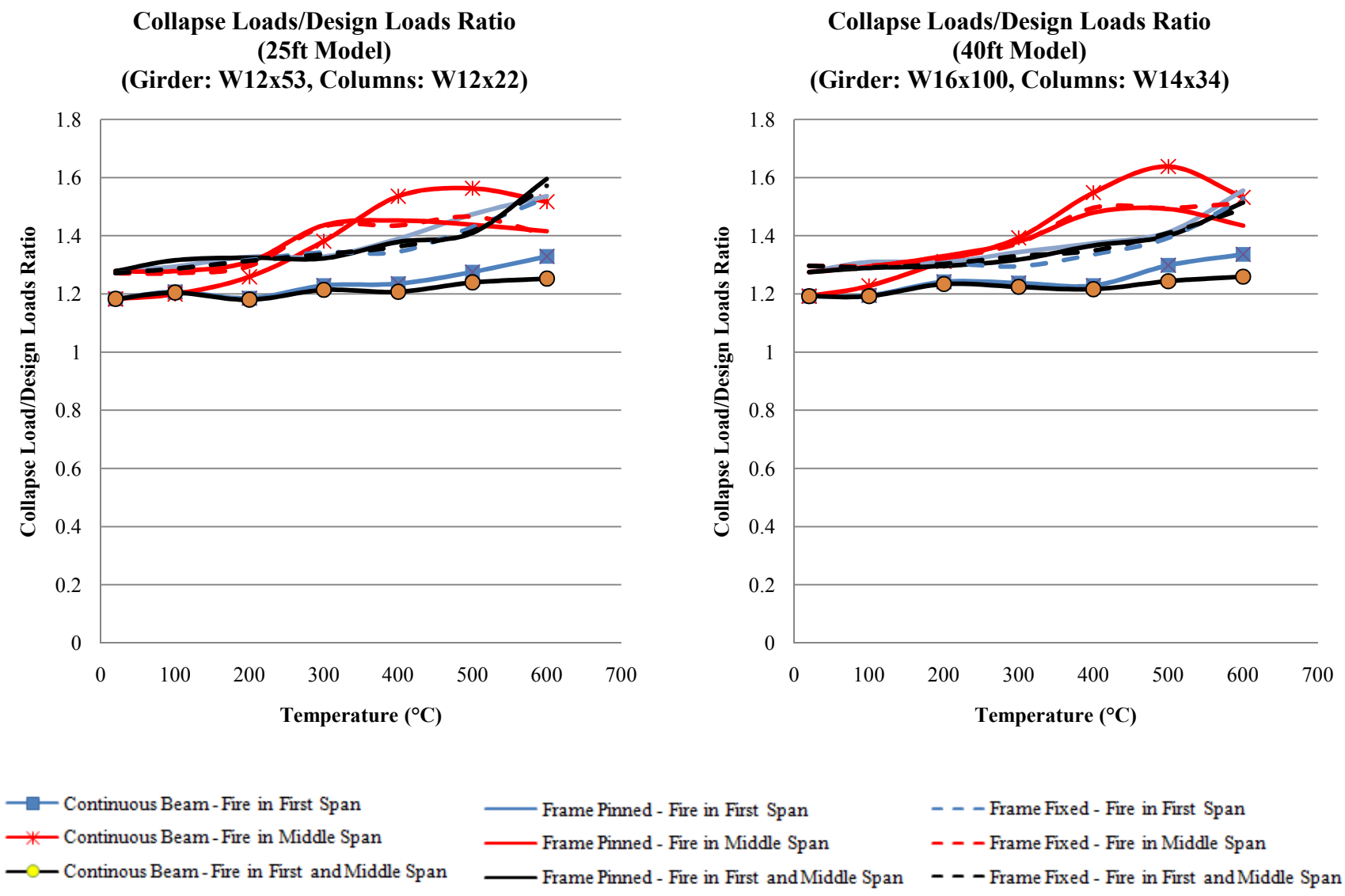

Figure 35: Influence of changing the bay size - Collapse Loads/Design Loads Ratio

5.4.3. Influence of Changing Number of Bays

In this investigation, another bay was added to the base model while maintaining the same girder and column sizes. The purpose of this study was to determine whether or not the number of bay has substantial influence on the collapse of the structure. In addition, the critical fire location can be confirmed. As another bay was added to the base model, there was a moment redistribution within the structure; however, the moment redistribution effects in this case were fairly small. Thus, the collapse loads and mechanism of the 4-bay structure are approximately identical to those for the base model. Figure 36 and Figure 37 compares the collapse loads and the collapse loads/design loads ratio of the 4-bay model to the base model.

Figure 36 shows that the graph of the collapse loads for the 4-bay structure is identical as the 3-bay structure. There are some differences between the 3-bay and 4-bay structures in Figure 37 as the ratio curves for the 4 span continuous beam model rise up. This is due to the fact that the moments at the interior support became larger for the 4-span model. The increasing moment value at the supports resulted from the formation of the first hinge at lower level of loadings.

By adding one more bays to the structure, the collapse loads and mechanism of the structure did not change considerably. From this investigation, it may be concluded that, for one-story buildings, fires occurring in the exterior bay of the structure would cause the most critical situation.

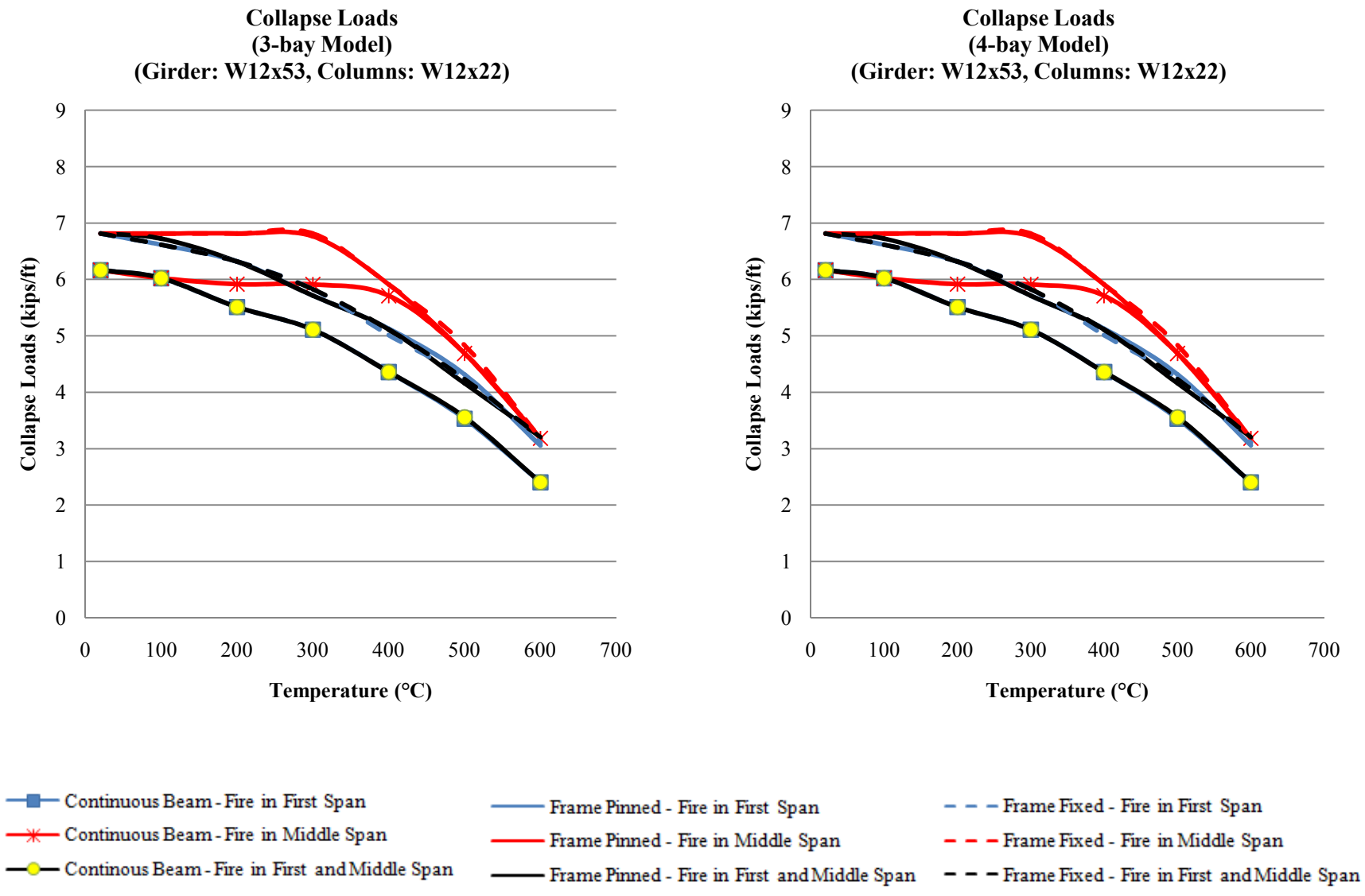

Figure 36: Influence of changing number of bay - Collapse Loads

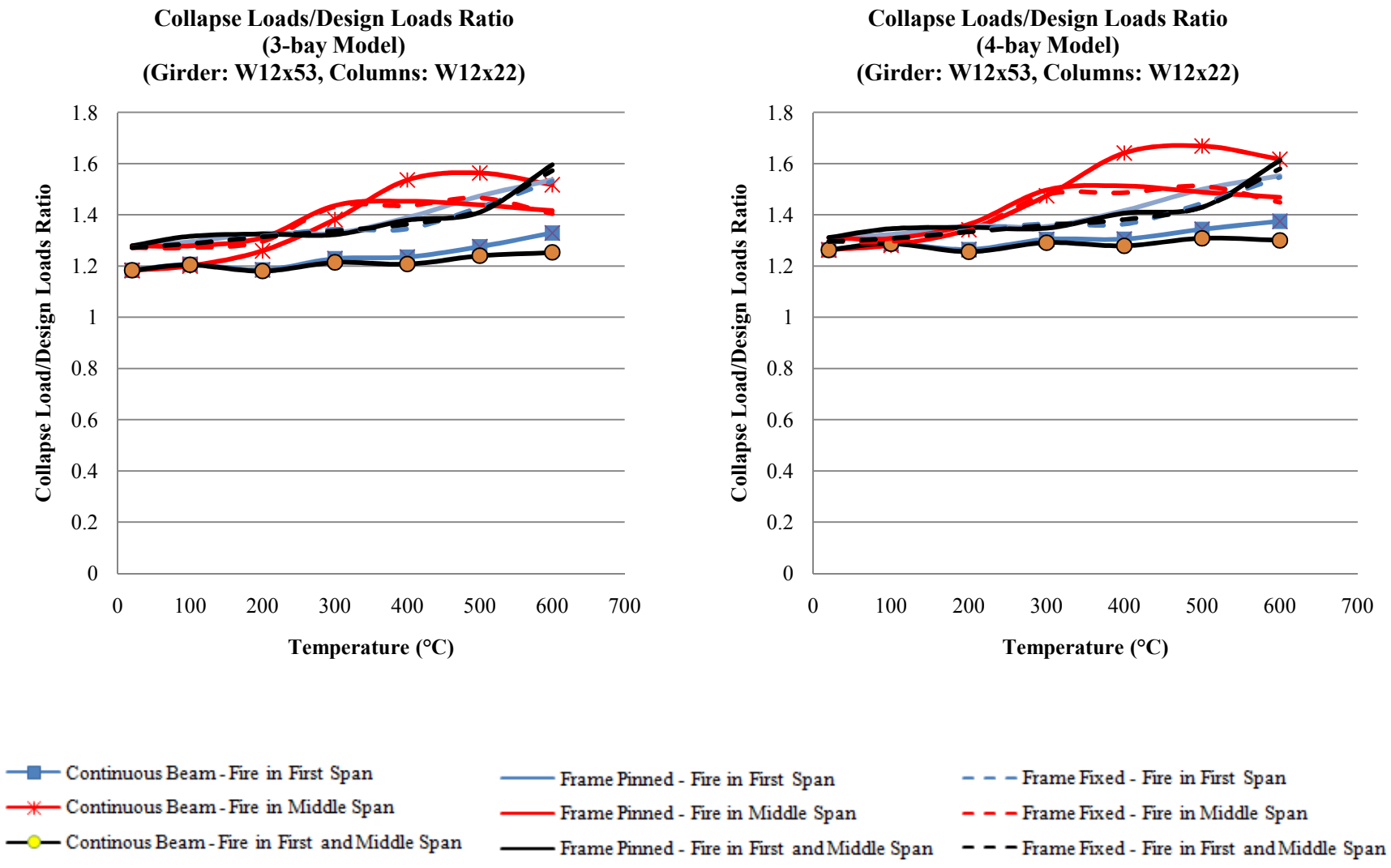

Figure 37: Influence of changing number of bay - Collapse Loads/Design Loads Ratio

5.4.4. Influence of Adding Additional Stories

This section presents the investigation of the influence of adding an additional story. One more story was added to the base model while maintaining the same column and girder sizes. By adding one story to the base case, the moments at the first floor joint would be redistributed. Originally, there were only three members connected to each other at the interior joints. The interior joints on the first floor of the new model involve four members and thus, the moment would be redistributed among four members instead of three. The fire locations varied from the first floor to the second floor. Therefore, there were two set of new models. The first model included all fire locations scenarios that occurred on the first floor, and the second model included all fire locations scenarios that occurred on the second floor.

Figure 38 and Figure 39 compare the results of two new models to the base model. It's noticeable that the all the curves in the collapse graph of the case with fire on the first floor (Figure 38) were merging to each other. There were little differences in collapse load values at 300°C and 400°C. The reason for this behavior was due to the redistribution moment phenomenon at the interior joints of the first model. In both Figure 38 and Figure 39, the second model shows comparable results to the base model. Because all the fires were assumed to occur on the second floor, the upper part of the structure behaved much like the base model; however, the levels of collapse loads for the second models were less than the base model.

As one story was added to the base model, the collapse loads slightly decreased even though the curve trends were quite similar to those for the base model. The fires in the exterior bay always caused the most critical events up to 600°C. At 600°C, the collapse loads curves merged together indicating that the fire locations and boundary conditions have little influence on the collapse of the structure beyond 600°C

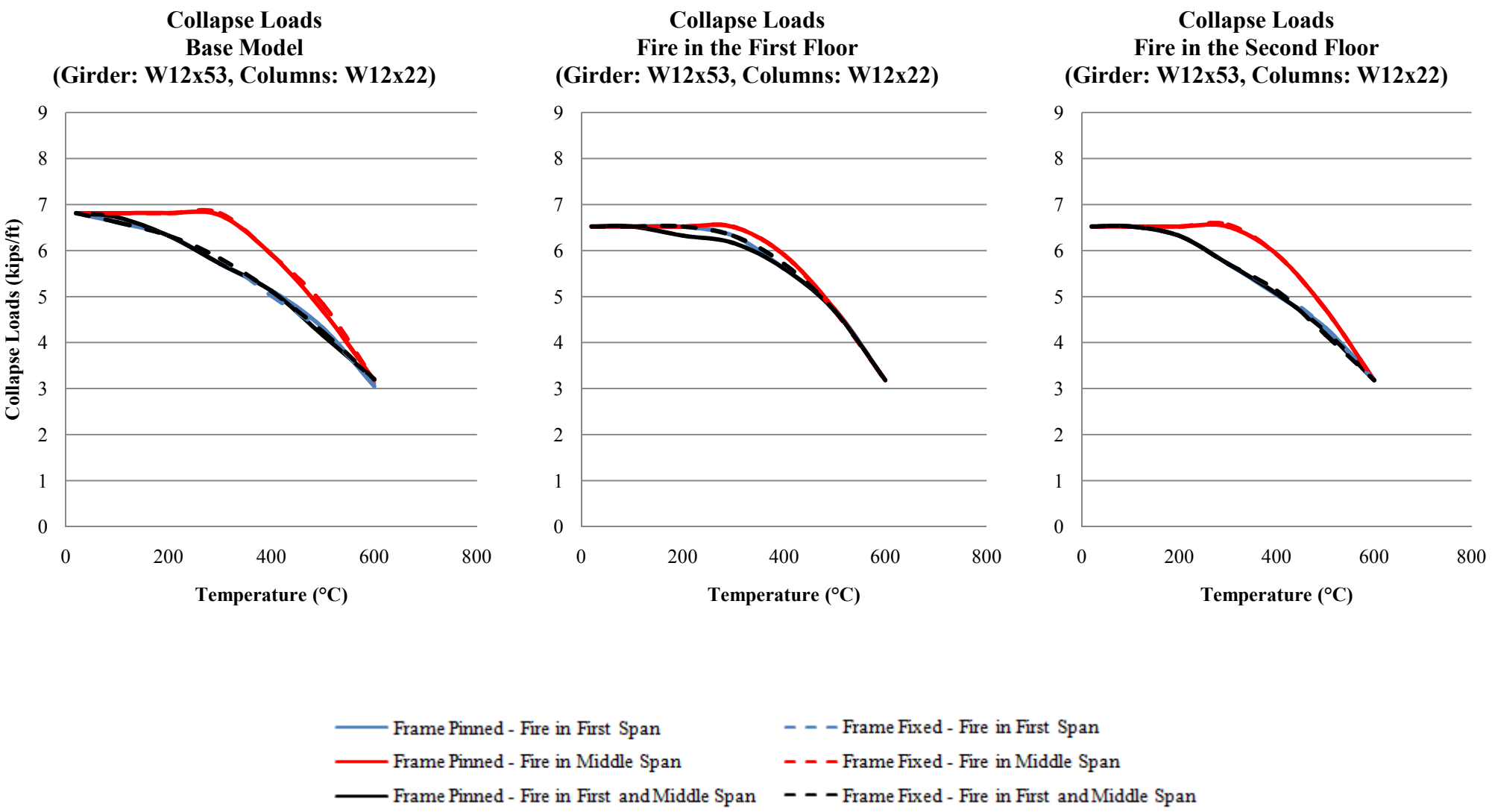

Figure 38: Influence of adding an additional story - Collapse Loads

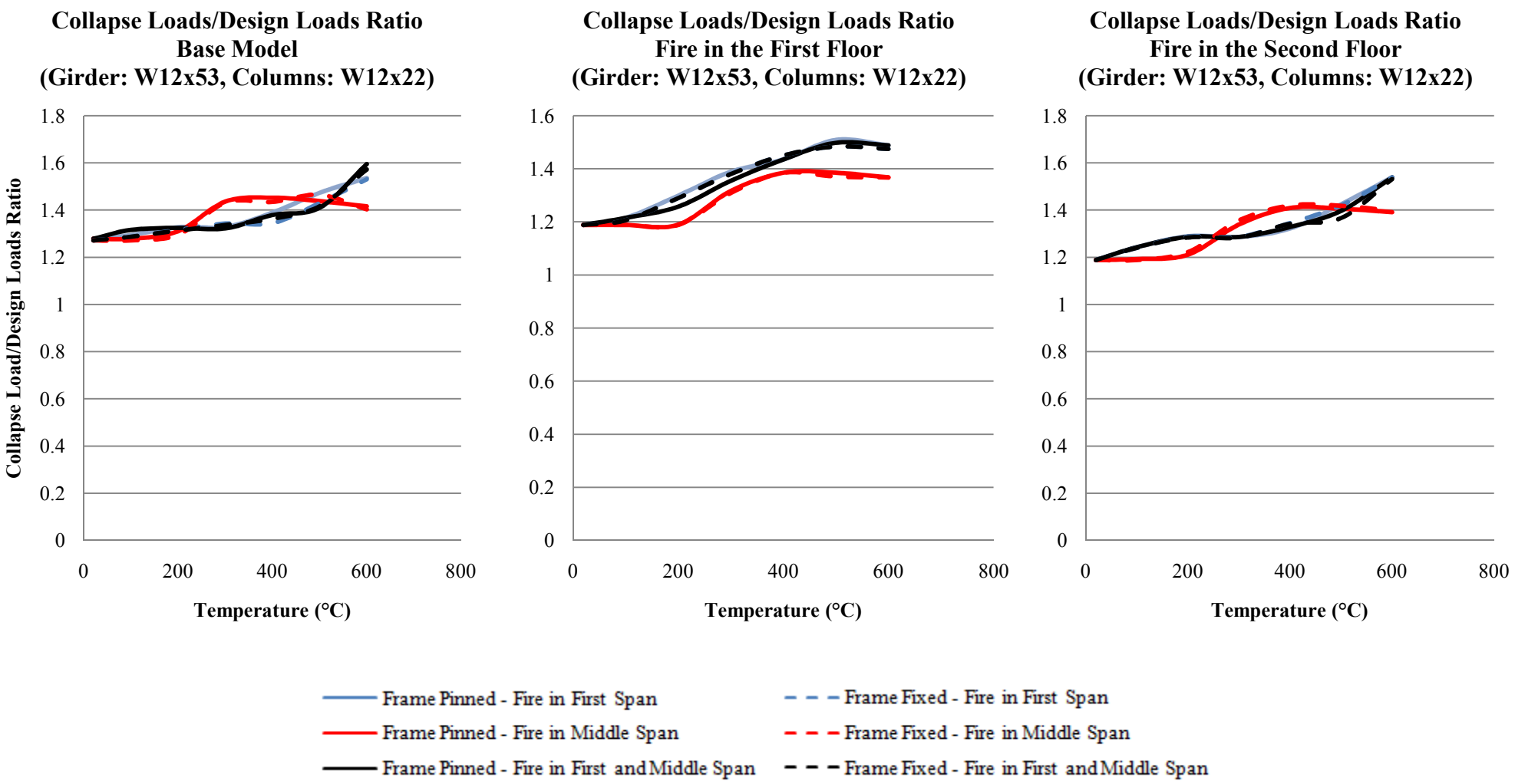

Figure 39: Influence of adding an additional story - Collapse Loads/Design Loads Ratio

5.5.Design Aid Tool

The design aid tool was developed using data from the previous section. The proposed tool is intended to help the structural engineers in a design office assess the fire performance of a steel frame using a simplified approach. The tool was inspired by the adaption factor from *Eurocode 3* and the graphs from *Swedish Design Manual.* For practicing engineers, this tool could provide an approximation on the strength of steel frames at elevated temperatures. An engineer would first have to determine the collapse limit load of a simply supported beam which can be calculated as $\frac{8M_p}{L^2}$ (M_p is the plastic moment of the beam; L is the span length of the beam). For a given fire-induced temperature, a factor β can be found from the graphs. Multiplying this factor β by the collapse limit load of the simply supported beam gives an estimate of the collapse load at the elevated temperature. This tool doesn't fully capture the behavior of the structure because it's only based on consideration of collapse strength.

5.5.1. Developing the Tool

In order to find the similar trend among the investigated models, a series of β graphs was established based on the collapse loads for all the models that were studied. Figures 40 to 46 present the graphs of β values for all of the different parametric investigation. In this series, Figure 41 is the only case for which a constant stiffness ratio between girder and column of the structure is not maintained. All of the graphs have very similar patterns for all the curves. The differences among these graphs are only the magnitude of the β. After investigation, the β factor is very sensitive to the collapse load of the simply supported beam model and the girder to column stiffness ratio. As the collapse load of the simply supported beam model changes, the value of β tends to change. For example in Figure 41, the β curves for the case in which the girder size was changed were generally less than for the base case. For the base case, at normal temperature, the β factor for frame was above 1.6 while for the W18x53 case, the β of the frame was less than 1.6. Figure 40 shows a similar situation in which the β factor for the continuous beam model was less than for the base model.

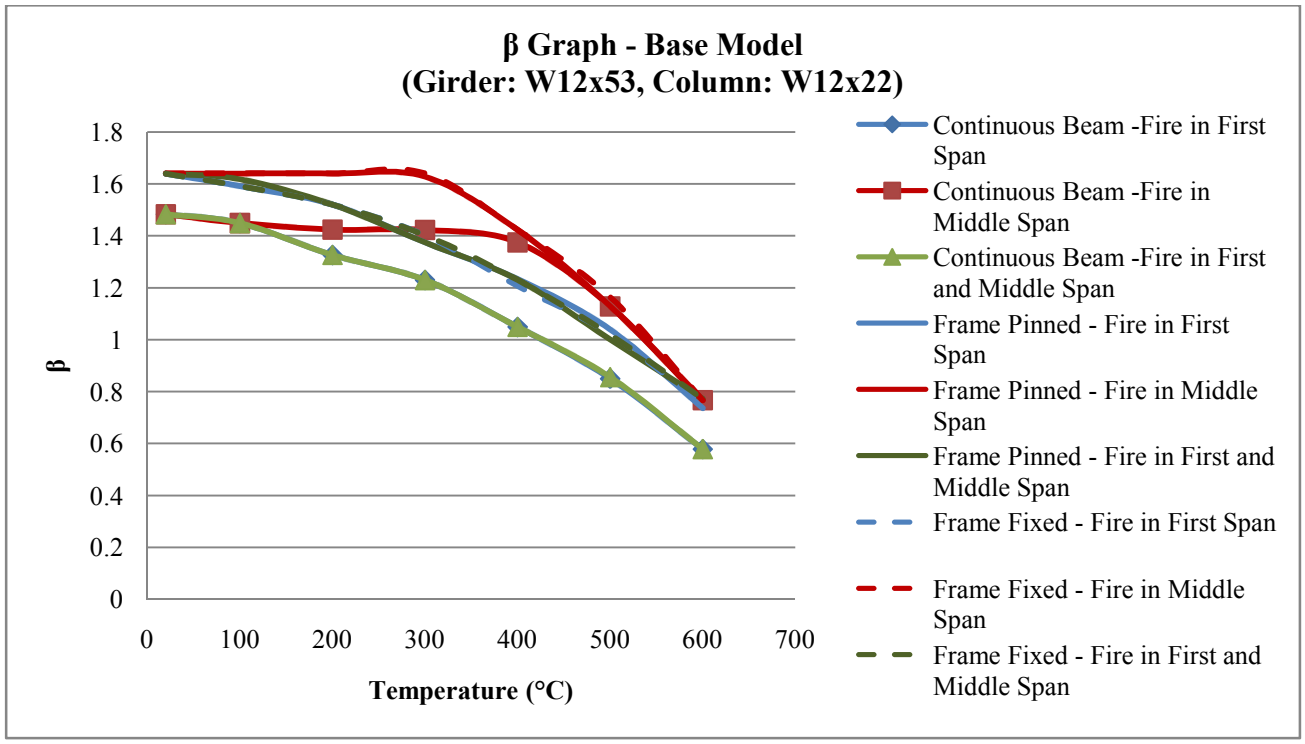

Figure 40: β Graph - Base Model

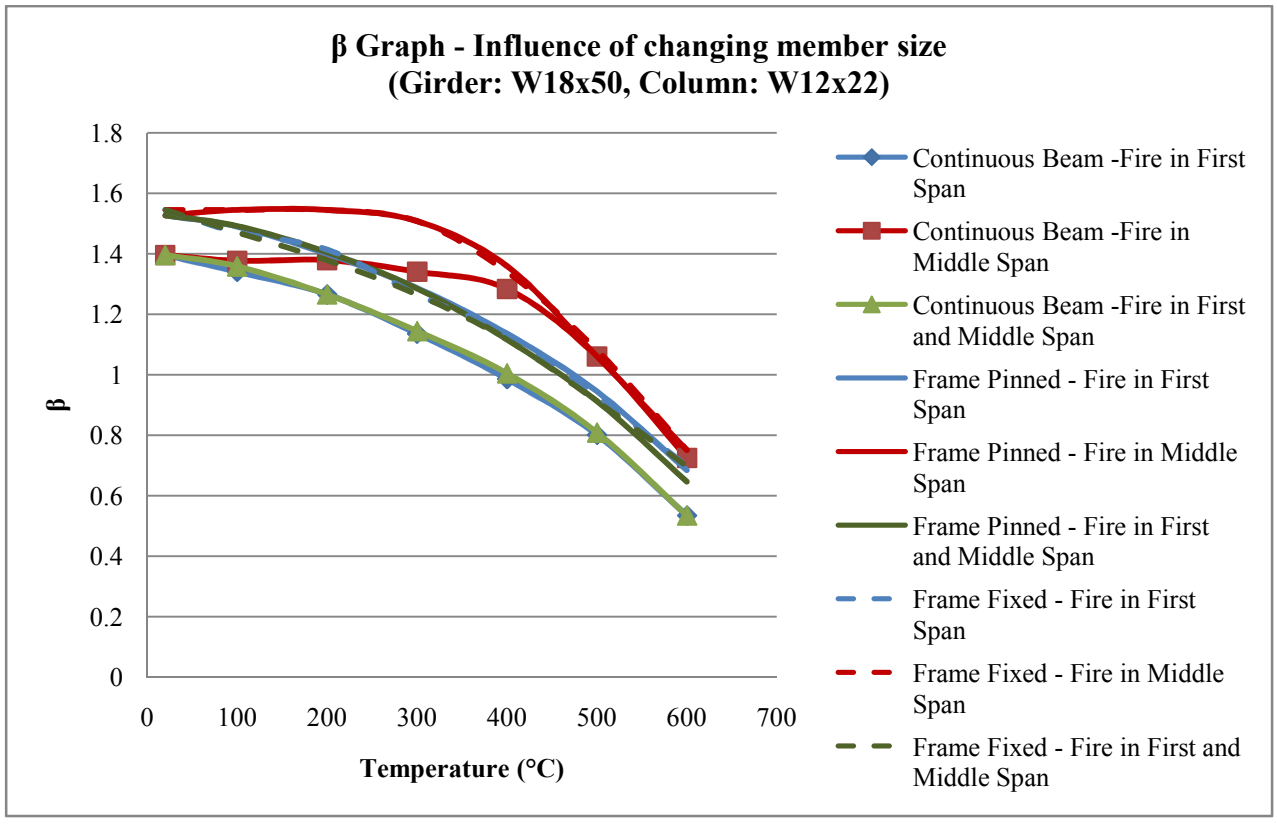

Figure 41: β Graph - Influence of changing member size

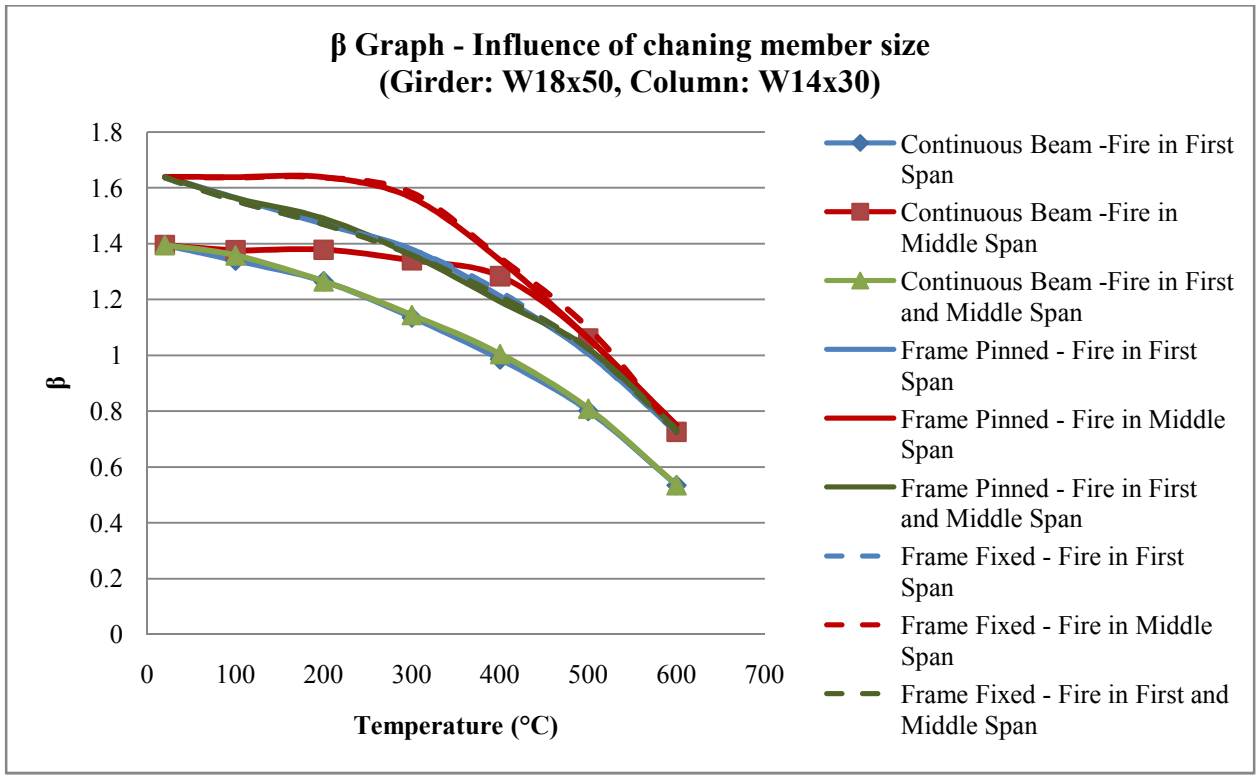

Figure 42: β Graph - Influence of changing member sizes

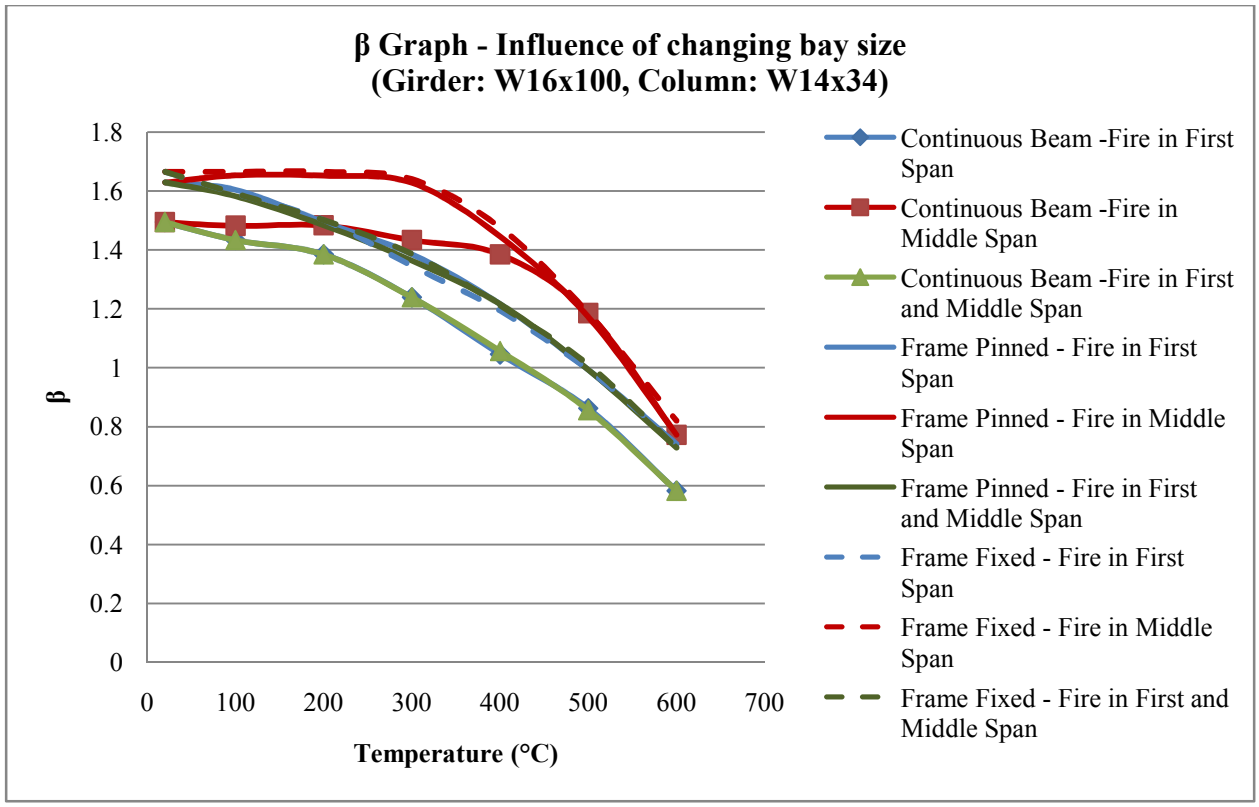

Figure 43: β Graph - Influence of changing bay size

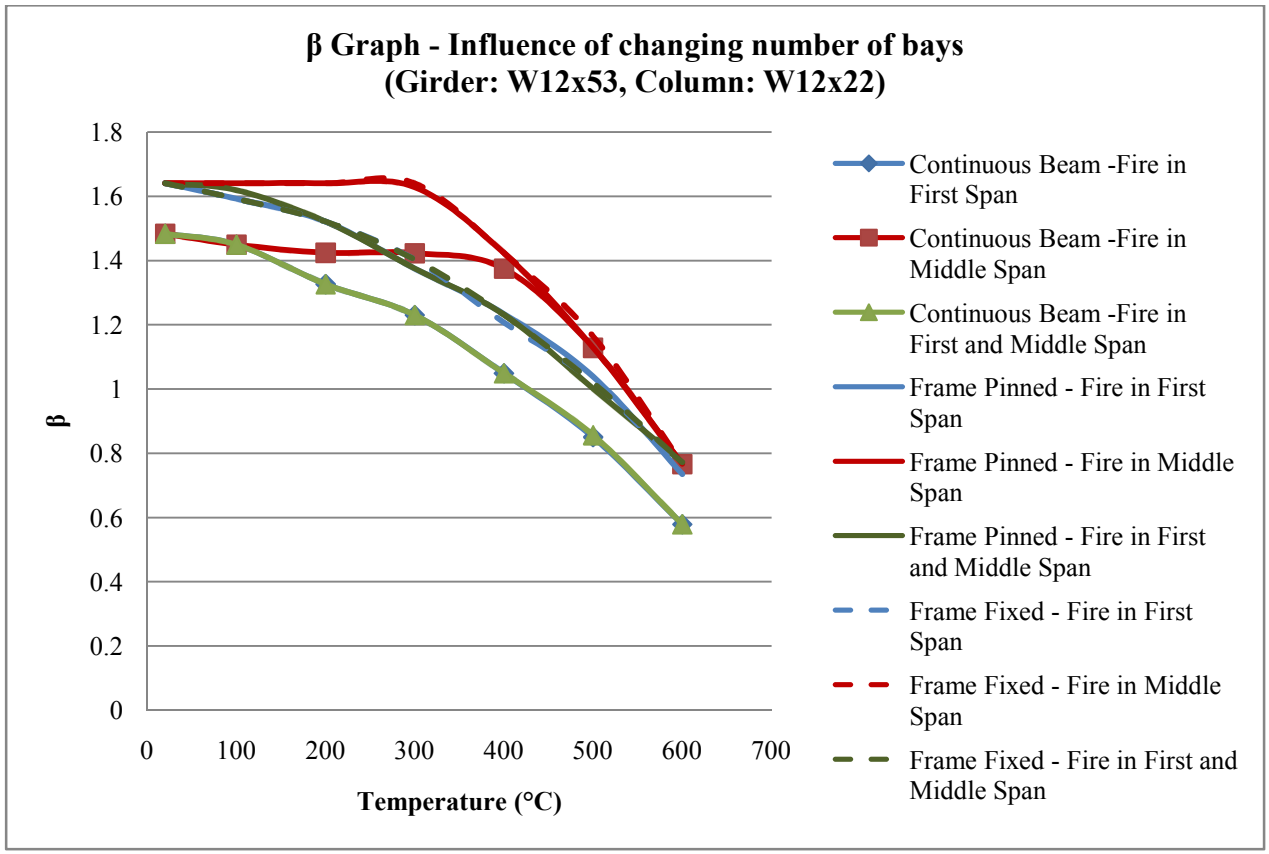

Figure 44: β Graph - Influence of changing number of bays

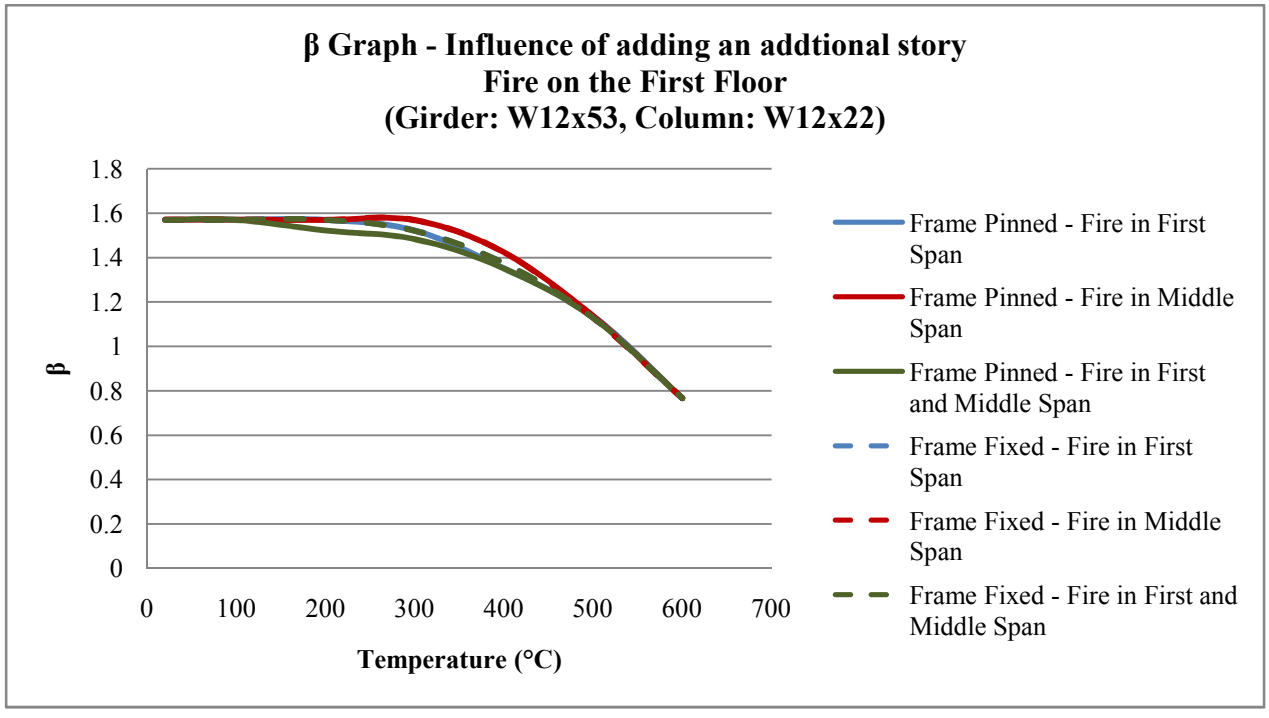

Figure 45: β Graph - Influence of adding an additional story

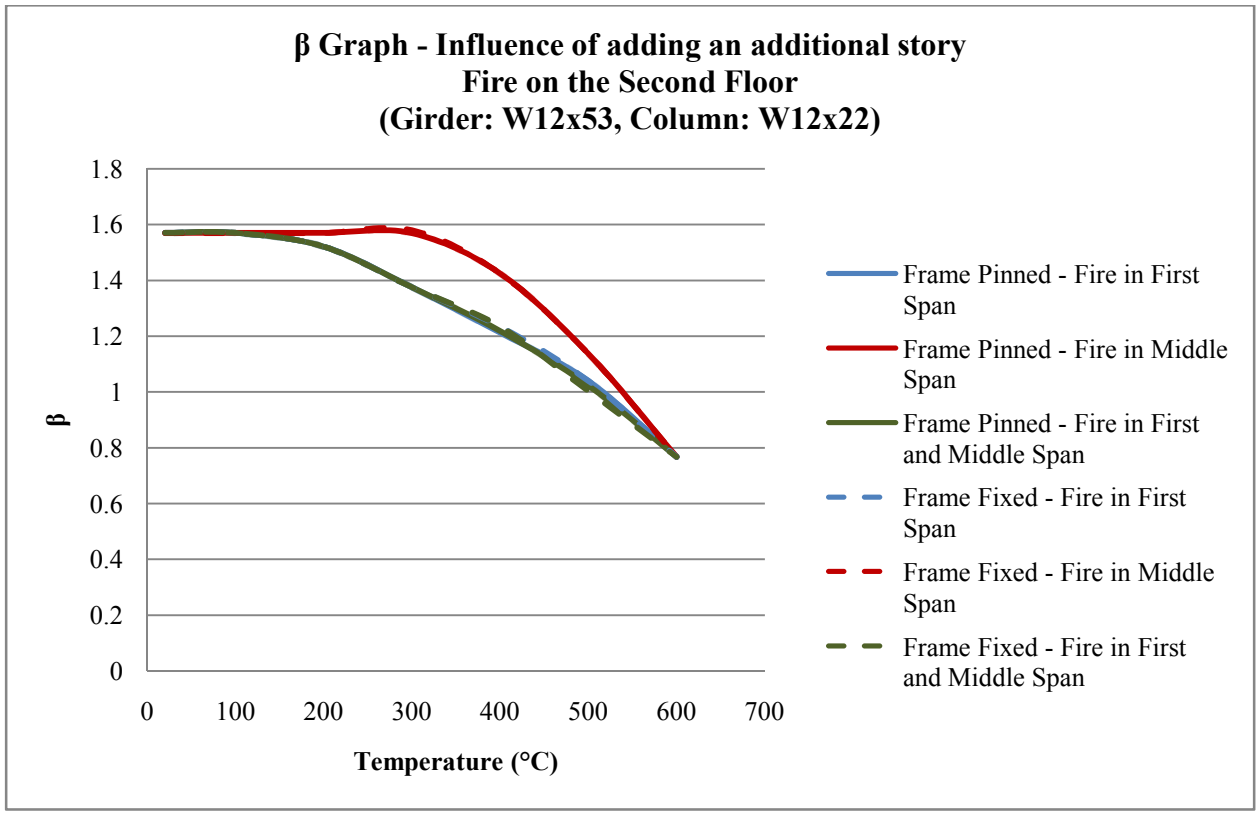

Figure 46: β Graph - Influence of adding an additional story

5.5.2. Design Tool and the Usage Condition

Since all the β graphs of different effects are relatively similar to the base model β graph, the β graph for the base model could be use as a design tool to aid the structural engineering in predicting the collapse strength of steel frames under fire conditions. In order to predict the collapse load of the structure at the elevated temperature, the collapse load of the simply supported case of the girder at the room temperature must first be calculated. This collapse load can be multiplied by the factor β which can be found by looking up in the design tool to find the critical load at the temperature of interest. By finding the critical loads at the temperature of interest, structural engineers can also determine the survival time of the structure by conducting a heat transfer analysis of the structure under design fire conditions. The survival time then can be compared with the ratings from standards and building codes. Changes in member design or insulation may be made to increase survival time as appropriate.

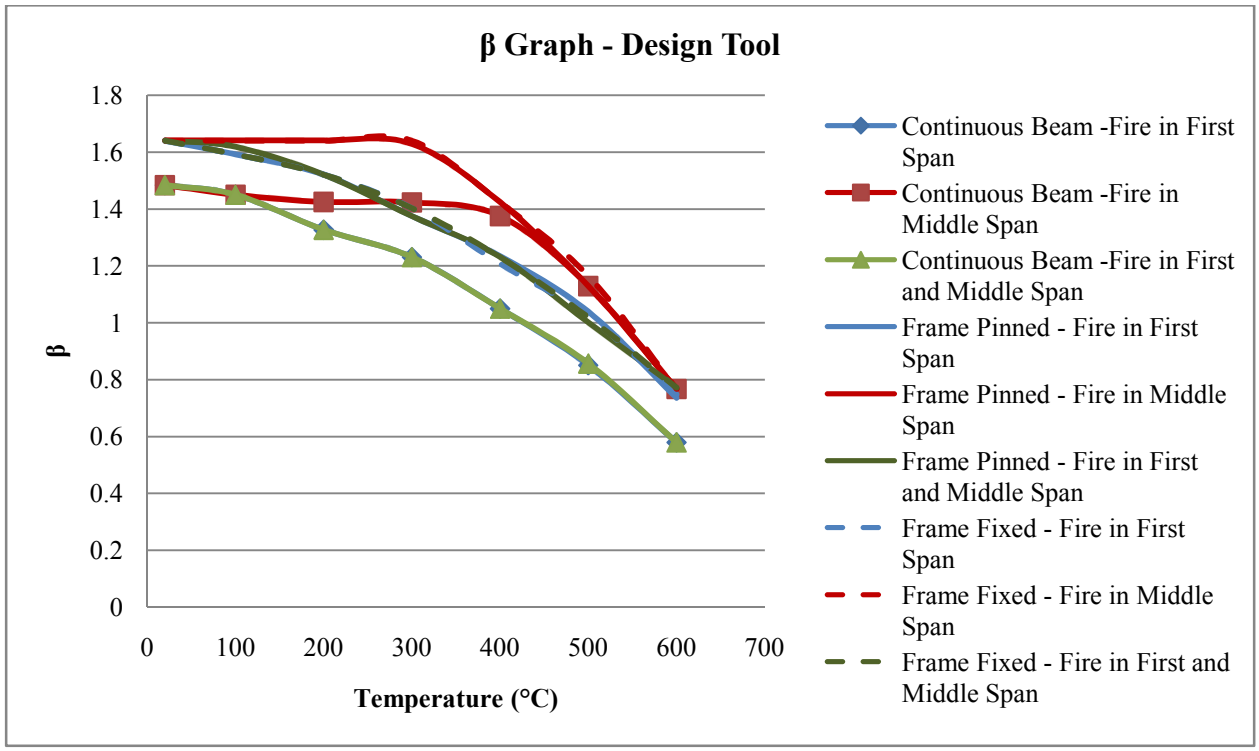

Figure 47: Design Aid Tool

Figure 47 illustrates the proposed tool that can be use to predict collapse strength of the steel structures under fire conditions. The value of β can be determined at different temperature exposures in this Figure. The proposed tool is not fully developed since it does not capture the effects of member section properties. This design tool is valid under certain conditions which are listed in the following:

- The collapse load of the simply supported beam of the girder is equal to 4.107 k/ft
- The stiffness ratio between the girders and columns is equal to 1.416667

This tool works best for the one-story building frame. It also can be applied to different bay sizes and different number of bay as long as two conditions above are maintained.

6. Conclusion

Traditionally, fire design of steel buildings is only based on the testing and performance of single element subjected to standard fires. However, if the single column or beam element is part of a highly redundant frame, then its individual behavior may not resemble failure of the frame. Thus, in order to understand and predict the behavior of steel frames under fire conditions, structural engineers need to analyze the structure as an entity and not as a collection of isolated members. Structural continuity effects in steel frames play an important role in collapse limit loads and mechanisms of the structure

6.1.Summary of Results

The objective of this thesis is to understand structural continuity effects in steel frames by parametric investigations of different factors that might change the collapse loads and mechanisms. After exploring different effects such as changes in member size, bay size, the number of bay, and the number of stories, some key findings are listed below

1. For the continuous structure, the collapse loads and mechanism are not only based on the reduction in material strength of the structure but also moment redistribution effects. As a member is subjected to fire, the change in stiffness of the member results in changing the distribution of bending moment within the structure.
2. Fires that occurred in the exterior bay of the structure always cause the critical situation. It suggests that designers should increase the fire proofing material for both the girders and columns in the exterior bay to increase survival time of the frame.
3. The presence of columns in the structure help to increase the load-carrying capacity of the structure. By having the columns, the degree of redundancy increases and also the moment is distributed to both girders and columns, which results in increasing the load-carrying capacity of the structure.

4. Column support conditions had little effect on the collapse loads of the structure. After investigation, the collapse loads and mechanisms of the structure for both pinned-based columns and fixed-based columns were almost identical. There are some minor changes in the order of plastic hinge formation and slight differences in magnitude of the collapse load as the temperature increased; however, there effects were insignificant.
5. At 600°C and beyond, collapse loads of the structural frame have little sensitivities to fire locations and column support boundary conditions. After investigations, the collapse load curves at 600°C for all fire locations converged to one value.
6. As the fire occurs in the interior bay of the structure, there was a change in collapse mechanism as the temperature increased. At normal temperatures, the failure of the structure always occurred in the exterior girders; however, as the interior girders are subjected to fire, the collapse mechanisms occurred in the interior bay.
7. With an appropriate design, the bay size and number of bays in the structure do not affect the collapse load. Also, if the stiffness ratio between girders and columns is maintained, the structural behavior under fire condition does not change
8. The proposed tool is most applicable to use for understanding the steel structural behavior for one-story buildings. These structures need to have a constant girder to column stiffness ratio of 1.41667 and 4.107 kips/ft as the collapse load of simply supported beam of the girder.

6.2.Limitation of the Work

The above observations must be considered in the context of the limitations to this thesis.

- First, the column for the base case was designed by using K factor of 1 which is the ideal Euler column. The column sizes needs to be redesigned including side sway effects to have more accurate results of the collapse loads and β graphs.

- Second, there were limited cases in the member size investigation. In order to fully establish the relationship of member size and collapse loads and mechanisms of the structure, more models need to be established.
- Third, there were some errors in modeling technique in ANSYS since ANSYS is not an accessible structural analysis program. The section properties that were calculated automatically in ANSYS show some errors compared to values tabulated in the *AISC Steel Manual* (AISC, 2005)

6.3. Recommendations for Future Work

Since there were still some limitations that the thesis could not cover, this section presents recommendations for future work

- This thesis only investigated 2D steel frame models. In reality, the structural frames are 3D systems. Thus, future investigation of 3D models would be desirable.
- Because of the limited cases in member size effects investigation, more cases are needed to explore the relationship of the columns and girders in collapse analysis.
- This thesis only explored the collapse of the structure from the strength point of view. Future work should investigate other effects that could lead to failure of the structure such as thermal expansion, creep, and deformation.
- This thesis only looked at different snap-shots of temperature and assumed that the temperature within the member was uniform. Further investigations could involve full heat transfer analysis when the structure is subjected to ASTM E-199 standards fire. The calculations could involve modeling in finite element software program that is capable of doing advanced heat transfer analysis.
- Since the design aid tool was not fully developed, it needs to be modified by incorporating section properties into the equation for β.

- Lastly, there is always a need for fire physical tests for benchmarking numerical approaches and results.

Bibliography

ANSYS Academic Teaching Advance (2009), version 11, ANSYS Inc.

AISC. (2005). *Steel Construction Manual.*

Bailey, C. (1997). *Computer modeling of the corner compartment fire test on the large-scale Cardington test frame.* Journal of construction steel research.

British Standards Institution. (2001). *Eurocode 3: Design of Steel Structure.* London, UK: European Committee for Standardization.

British Steel plc. (1999). *The behavior of multi-storey building framed buildings in fire.* South Yorkshire, United Kingdom: Bristish Steel plc, Swiden Technology Centre.

De Chiara, J., & Callender, J. H. (1973). *Time-Saver Standards for Building Types.* New York: McGraw-Hill Book Company.

Ghaffarzadeh, H., & Ghalghachi, R. N. (2009). *Redundancy of the Steel Frames with Masonry Infill Walls.* World Academy of Science, Engineering and Technology.

Grant, C., & Pagni, P. J. (1986). *Fire safety science: proceedings of the first international symposium.* Hemisphere Publishing Corporation.

Hall, J. R. (2009). *High-rise building fires.* Quincy, MA: National Fire Protection Association.

Hibbeler, R. (2005). *Mechanics of Materials.* New Jersey: Pearson Prentice Hall.

Horne, M. R. (1979). *Plastic Theory of Structure.* New York: Pergamon Press Inc.

Lamont, S. (2001). *The Behavior of Multi-storey Composite Steel Frame Structures in Response to Compartment Fires.* Edinburgh, United Kingdom: University of Edinburgh.

Lamont, S., Lane, B., Flint, G., & Usmani, A. (2006). *Behavior of Structures in Fire and Real Design - A Case Study.* Journal of fire protection engineering.

McCormac, J. C. (2008). *Structural Steel Design.* New Jersey: Pearson Education, Inc.

Moore, A. (2003). *Development of a Process to Define Design Fires for Structural Design of Buildings for Fire.* Worcester: Worcester Polytechnic Institute.

Neal, B. (1977). *The plastic Methods of Structural Analysis.* New York: John Wiley & Sons.

NIST. (2008). *Analysis of Needs and Existing Capabilities for Full-Scale Fire Resistance Testing.*

Pettersson, O., Magnusson, S.-E., & Thor, J. (1976). *Fire Engineering Desing of Steel Structures.* Lund, Sweden: Swedish Institute of Steel Construction.

Petterssona, O., & Witteveen, J. (1980). *On the fire resistance of structural steel elements derived from standard fire tests or by calculation* . Fire safety journal.

SAP2000 Structural Analysis Program (2009), Version 14, Computers and Structures, Inc.

Society of Fire Protection Engineers. (1988). *SFPE Handbook of Fire Protection Engineering.* Massachusetts: Society of Fire Protection Engineers.

United States Fire Administration. (2010, February 2). *Structures fire*. Retrieved March 29, 2010, from U.S. Fire Administration: http://www.usfa.dhs.gov/statistics/national/all_structures.shtm

Wang, Y.C.; Moore, D.B. (1994). *Steel frames in fire: analysis.* Watford, UK: Structural Design Division, Building Research Establishment.

Wong, M. (2006). *Adaptation factor for moment capacity calculation of steel beams subject to temperature gradient.* Melbourne, Australia: Journal of Constructional Steel Research.

Wong, M. (2000). *Elastic and plastic methods for numerical modeling of steel structures subject to fire.* Melburne, Australiaa: Journal of Constructional Steel Research.

Appendix A: SAP2000 and ANSYS Models

This section outlines how to model and perform the plastic analysis with SAP2000 and ANSYS finite element software programs. They both have their advantages and disadvantages in determining the collapse loads and mechanisms.

SAP2000 Model

Modeling in SAP2000 was rather easy since the program was developed for structural analysis. The member size and geometry of the structure was already in template and library. The only thing that needed to be modified was the material property of the steel at the elevated temperature. The modeling in SAP2000 generally took less than 30 minutes. However, SAP2000 doesn't have the ability to do the collapse analysis automatically. In fact, it doesn't have the ability to insert plastic hinges which allow the rotation of the member. However, the moment can be released from the end of the member. Once the moment is release, the member is free to rotate. Therefore, the only way to work around this problem was to insert a conventional hinge at the point of interest. Then the member was cut at the hinge into two parts so that the moment could be released from the end of each part. Every time the plastic hinge was formed, the same procedure was repeated. In order to find the collapse load of the structure, an Excel spreadsheet was needed to keep track of the moment and loads.

For collapse analysis, SAP2000 acted as a calculator to find the moment capacity of the structure. The Excel spreadsheet was used as a tool to keep track of maximum moment and loads. Since, the process of doing plastic analysis in SAP2000 was tedious; it took a considerable amount of time to investigate one model. However, with this method, the sequence of plastic hinges and collapse mechanism were recorded.

ANSYS Model

Since ANSYS is a general-purpose program with application outside of structural analysis, modeling in ANSYS required considerable time and efforts. Modeling girders and columns required input of several points on the cross section of the members. From these points, ANSYS automatically calculates

all the properties of the section, and as a result, there are some errors compared to published values in the *AISC Steel Manual*. The procedure of modeling in ANSYS is much more complicated than SAP2000: it could take more than 30 minutes to model the frame. However, ANSYS has the ability to perform plastic analysis. It could determine the collapse load much faster than SAP2000 because the program did all the work. One major drawback of using ANSYS was it only gave the final collapse load and it was complicated to find the collapse mechanism.

ANSYS was used most of the time in this thesis to find the collapse loads of the structure. However, initially SAP2000 was used to understand the collapse mechanism of the structure using the hinge-by-hinge method of plastic analysis.

Appendix B: 25-foot Model (Girder: W12x53; Column: W12x22 case)

3-span continuous beam

Temperature	Collapse Loads (kips/ft)		
	Fire in the exterior bay	Fire in the interior bay	Fire in both the exterior and interior bays
20°C	6.1623	6.1623	6.1623
100°C	6.02202	6.02202	6.02202
200°C	5.511	5.91681	5.511
300°C	5.1102	5.9118	5.1102
400°C	4.3587	5.7114	4.3587
500°C	3.53205	4.68809748	3.5571
600°C	2.4048	3.18511752	2.4048

Temperature	First hinge formation (kips/ft)		
	Fire in the exterior bay	Fire in the interior bay	Fire in both the exterior and interior bays
20°C	5.21	5.21	5.21
100°C	4.99	5.02	5
200°C	4.65	4.7	4.67
300°C	4.16	4.28	4.21
400°C	3.53	3.72	3.61
500°C	2.77	3	2.87
600°C	1.81	2.1	1.92

Temperature	β values		
	Fire in the exterior bay	Fire in the interior bay	Fire in both the exterior and interior bays
20°C	1.483223684	1.483223684	1.483223684
100°C	1.449459243	1.449459243	1.449459243
200°C	1.326460205	1.424135911	1.326460205
300°C	1.229990372	1.422930039	1.229990372
400°C	1.049109435	1.374695122	1.049109435
500°C	0.850140404	1.128393168	0.856169769
600°C	0.578818999	0.766636117	0.578818999

Pinned-based frame

Temperature	Collapse Loads (kips/ft)		
	Fire in the exterior bay	Fire in the interior bay	Fire in both the exterior and interior bays
20°C	6.8136	6.8136	6.8136
100°C	6.6132	6.8136	6.6132
200°C	6.31761	6.8136	6.31761
300°C	5.82663	6.8136	5.82663
400°C	5.01501	5.9118	5.1102
500°C	4.245975	4.83465	4.23345
600°C	3.1062	3.1851075	3.2064

Temperature	First hinge formation (kips/ft)		
	Fire in the exterior bay	Fire in the interior bay	Fire in both the exterior and interior bays
20°C	5.33	5.33	5.33
100°C	5.11	5.33	5.11
200°C	4.76	5.2	4.77
300°C	4.3	4.71	4.32
400°C	3.69	4.07	3.71
500°C	2.93	3.26	2.95
600°C	1.99	2.25	2.01

Temperature	β values		
	Fire in the exterior bay	Fire in the interior bay	Fire in both the exterior and interior bays
20°C	1.639987163	1.639987163	1.639987163
100°C	1.591752246	1.639987163	1.618281451
200°C	1.520605745	1.639987163	1.520605745
300°C	1.374695122	1.627928434	1.374695122
400°C	1.233607991	1.422930039	1.231196245
500°C	1.038859515	1.128393168	1.000874519
600°C	0.735582478	0.766636117	0.771758665

Fixed-based frame

Temperature	Collapse Loads (kips/ft)		
	Fire in the exterior bay	Fire in the interior bay	Fire in both the exterior and interior bays
20°C	6.8136	6.8136	6.8136
100°C	6.6132	6.8136	6.72342
200°C	6.31761	6.8136	6.31761
300°C	5.7114	6.7635	5.7114
400°C	5.12523	5.9118	5.11521
500°C	4.316115	4.68809748	4.1583
600°C	3.0561	3.18511752	3.2064

Temperature	First hinge formation (kips/ft)		
	Fire in the exterior bay	Fire in the interior bay	Fire in both the exterior and interior bays
20°C	5.36	5.36	5.36
100°C	5.14	5.36	5.14
200°C	4.8	5.26	4.81
300°C	4.34	4.76	4.36
400°C	3.73	4.12	3.75
500°C	2.97	3.3	2.99
600°C	2.03	2.27	2.04

Temperature	β values		
	Fire in the exterior bay	Fire in the interior bay	Fire in both the exterior and interior bays
20°C	1.639987163	1.639987163	1.639987163
100°C	1.591752246	1.639987163	1.591752246
200°C	1.520605745	1.639987163	1.520605745
300°C	1.402430199	1.639987163	1.402430199
400°C	1.207078787	1.422930039	1.229990372
500°C	1.021977295	1.163667362	1.018962612
600°C	0.747641207	0.766633705	0.771758665

Appendix C: 25-foot Model (Girder: W18x50; Column: W12x22 case)

3-span continuous beam

Temperature	Collapse Loads (kips/ft)		
	Fire in the exterior bay	Fire in the interior bay	Fire in both the exterior and interior bays
20°C	7.515	7.515	7.515
100°C	7.2144	7.4148	7.3146
200°C	6.8136	7.42482	6.8136
300°C	6.11721	7.21941	6.1623
400°C	5.3106	6.9138	5.4108
500°C	4.316115	5.7114	4.3587
600°C	2.88075	3.9078	2.88075

Temperature	First hinge formation (kips/ft)		
	Fire in the exterior bay	Fire in the interior bay	Fire in both the exterior and interior bays
20°C	6.76	6.76	6.76
100°C	6.48	6.51	6.5
200°C	6.02	6.1	6.05
300°C	5.4	5.55	5.47
400°C	4.6	4.84	4.7
500°C	3.6	3.9	3.73
600°C	2.35	2.71	2.5

Temperature	β values		
	Fire in the exterior bay	Fire in the interior bay	Fire in both the exterior and interior bays
20°C	1.395111386	1.395111386	1.395111386
100°C	1.339306931	1.376509901	1.357908416
200°C	1.26490099	1.37837005	1.26490099
300°C	1.135620668	1.340237005	1.143991337
400°C	0.985878713	1.283502475	1.004480198
500°C	0.801258973	1.060284653	0.809164604
600°C	0.534792698	0.725457921	0.534792698

Pinned-based frame

Temperature	Collapse Loads (kips/ft)		
	Fire in the exterior bay	Fire in the interior bay	Fire in both the exterior and interior bays
20°C	8.32161	8.32161	8.32161
100°C	7.92081	8.32161	7.92081
200°C	7.6152	8.32161	7.42482
300°C	6.8136	8.12121	6.8136
400°C	6.11721	7.2144	6.012
500°C	5.01501	5.82663	4.91481
600°C	3.7575	4.045575	3.7575

Temperature	First hinge formation (kips/ft)		
	Fire in the exterior bay	Fire in the interior bay	Fire in both the exterior and interior bays
20°C	6.86	6.86	6.86
100°C	6.59	6.87	6.6
200°C	6.13	6.54	6.15
300°C	5.53	5.93	5.55
400°C	4.73	5.16	4.78
500°C	3.74	4.15	3.79
600°C	2.5	2.85	2.55

Temperature	β values		
	Fire in the exterior bay	Fire in the interior bay	Fire in both the exterior and interior bays
20°C	1.526251856	1.526251856	1.526251856
100°C	1.489048886	1.544853342	1.490909035
200°C	1.398831683	1.544853342	1.404412129
300°C	1.286292698	1.507650371	1.28443255
400°C	1.135620668	1.35883849	1.116089109
500°C	0.944721067	1.060284653	0.912402847
600°C	0.684999691	0.750848948	0.646401609

Fixed-based frame

Temperature	Collapse Loads (kips/ft)		
	Fire in the exterior bay	Fire in the interior bay	Fire in both the exterior and interior bays
20°C	8.22141	8.22141	8.22141
100°C	8.02101	8.32161	8.03103
200°C	7.53504	8.32161	7.5651
300°C	6.92883	8.12121	6.91881
400°C	6.11721	7.31961	6.012
500°C	5.08889748	5.7114	4.91481
600°C	3.689865	4.044573	3.48195

Temperature	First hinge formation (kips/ft)		
	Fire in the exterior bay	Fire in the interior bay	Fire in both the exterior and interior bays
20°C	6.88	6.88	6.88
100°C	6.61	6.89	6.62
200°C	6.14	6.64	6.17
300°C	5.55	6	5.58
400°C	4.77	5.21	4.8
500°C	3.78	4.18	3.82
600°C	2.54	2.88	2.58

Temperature	β values		
	Fire in the exterior bay	Fire in the interior bay	Fire in both the exterior and interior bays
20°C	1.544853342	1.544853342	1.544853342
100°C	1.470447401	1.544853342	1.470447401
200°C	1.413712871	1.544853342	1.37837005
300°C	1.26490099	1.507650371	1.26490099
400°C	1.135620668	1.339306931	1.116089109
500°C	0.931004332	1.081676361	0.912402847
600°C	0.697555693	0.751034963	0.697555693

Appendix D: 25-foot Model (Girder: W18x50; Column: W14x30 case)

3-span continuous beam

Temperature	Collapse Loads (kips/ft)		
	Fire in the exterior bay	Fire in the interior bay	Fire in both the exterior and interior bays
20°C	7.515	7.515	7.515
100°C	7.2144	7.4148	7.3146
200°C	6.8136	7.42482	6.8136
300°C	6.11721	7.21941	6.1623
400°C	5.3106	6.9138	5.4108
500°C	4.316115	5.7114	4.3587
600°C	2.88075	3.9078	2.88075

Temperature	First hinge formation (kips/ft)		
	Fire in the exterior bay	Fire in the interior bay	Fire in both the exterior and interior bays
20°C	6.76	6.76	6.76
100°C	6.48	6.51	6.5
200°C	6.02	6.1	6.05
300°C	5.4	5.55	5.47
400°C	4.6	4.84	4.7
500°C	3.6	3.9	3.73
600°C	2.35	2.71	2.5

Temperature	β values		
	Fire in the exterior bay	Fire in the interior bay	Fire in both the exterior and interior bays
20°C	1.395111386	1.395111386	1.395111386
100°C	1.339306931	1.376509901	1.357908416
200°C	1.26490099	1.37837005	1.26490099
300°C	1.135620668	1.340237005	1.143991337
400°C	0.985878713	1.283502475	1.004480198
500°C	0.801258973	1.060284653	0.809164604
600°C	0.534792698	0.725457921	0.534792698

Pinned-based frame

Temperature	Collapse Loads (kips/ft)		
	Fire in the exterior bay	Fire in the interior bay	Fire in both the exterior and interior bays
20°C	8.82762	8.82762	8.82762
100°C	8.42181	8.82261	8.4168
200°C	7.9158	8.82261	8.02101
300°C	7.42482	8.42181	7.31961
400°C	6.51801	7.21941	6.42282
500°C	5.41581	5.7114	5.511
600°C	3.9078	4.045575	3.9579

Temperature	First hinge formation (kips/ft)		
	Fire in the exterior bay	Fire in the interior bay	Fire in both the exterior and interior bays
20°C	6.92	6.92	6.92
100°C	6.65	6.93	6.66
200°C	6.19	6.72	6.21
300°C	5.59	6.1	5.61
400°C	4.8	5.28	4.84
500°C	3.81	4.25	3.85
600°C	2.57	2.91	2.6

Temperature	β values		
	Fire in the exterior bay	Fire in the interior bay	Fire in both the exterior and interior bays
20°C	1.638790842	1.638790842	1.638790842
100°C	1.563454827	1.637860767	1.562524752
200°C	1.469517327	1.637860767	1.489048886
300°C	1.37837005	1.563454827	1.35883849
400°C	1.210026609	1.340237005	1.192355198
500°C	1.005410272	1.060284653	1.023081683
600°C	0.725457921	0.751034963	0.734758663

Fixed-based frame

Temperature	Collapse Loads (kips/ft)		
	Fire in the exterior bay	Fire in the interior bay	Fire in both the exterior and interior bays
20°C	8.8176	8.8176	8.8176
100°C	8.3667	8.8176	8.3667
200°C	7.9158	8.8176	7.9158
300°C	7.41981	8.52201	7.31961
400°C	6.6132	7.2645	6.52302
500°C	5.41581	5.9118	5.511
600°C	3.9078	3.9078	3.9078

Temperature	First hinge formation (kips/ft)		
	Fire in the exterior bay	Fire in the interior bay	Fire in both the exterior and interior bays
20°C	6.95	6.95	6.95
100°C	6.68	6.96	6.69
200°C	6.23	6.78	6.24
300°C	5.64	6.17	5.65
400°C	4.86	5.35	4.87
500°C	3.86	4.29	3.89
600°C	2.62	2.93	2.64

Temperature	β values		
	Fire in the exterior bay	Fire in the interior bay	Fire in both the exterior and interior bays
20°C	1.636930693	1.636930693	1.636930693
100°C	1.55322401	1.636930693	1.55322401
200°C	1.469517327	1.636930693	1.469517327
300°C	1.377439975	1.582056312	1.35883849
400°C	1.22769802	1.348607673	1.210956683
500°C	1.005410272	1.097487624	1.023081683
600°C	0.725457921	0.725457921	0.725457921

Appendix E: 40-foot Model (Girder: W16x100; Column: W14x34 case)

3-span continuous beam

Temperature	Collapse Loads (kips/ft)		
	Fire in the exterior bay	Fire in the interior bay	Fire in both the exterior and interior bays
20°C	6.1623	6.1623	6.1623
100°C	5.9118	6.1122	5.9118
200°C	5.7114	6.11721	5.7114
300°C	5.1102	5.9118	5.1102
400°C	4.31361	5.7114	4.3587
500°C	3.5571	4.88851752	3.53205
600°C	2.4048	3.18511752	2.4048

Temperature	First hinge formation (kips/ft)		
	Fire in the exterior bay	Fire in the interior bay	Fire in both the exterior and interior bays
20°C	5.17	5.17	5.17
100°C	4.95	4.98	4.96
200°C	4.6	4.665	4.63
300°C	4.13	4.245	4.175
400°C	3.51	3.69	3.585
500°C	2.74	2.985	2.84
600°C	1.8	2.08	1.91

Temperature	β values		
	Fire in the exterior bay	Fire in the interior bay	Fire in both the exterior and interior bays
20°C	1.493890909	1.493890909	1.493890909
100°C	1.433163636	1.481745455	1.433163636
200°C	1.384581818	1.48296	1.384581818
300°C	1.238836364	1.433163636	1.238836364
400°C	1.045723636	1.384581818	1.056654545
500°C	0.862327273	1.185095156	0.856254545
600°C	0.582981818	0.772149702	0.582981818

Pinned-based frame

Temperature	Collapse Loads (kips/ft)		
	Fire in the exterior bay	Fire in the interior bay	Fire in both the exterior and interior bays
20°C	6.71841	6.71841	6.71841
100°C	6.6132	6.81861	6.52302
200°C	6.1623	6.8136	6.11721
300°C	5.7114	6.7134	5.62122
400°C	5.01501	5.9619	5.01501
500°C	4.095675	4.83465	4.095675
600°C	3.0561	3.1851075	3.006

Temperature	First hinge formation (kips/ft)		
	Fire in the exterior bay	Fire in the interior bay	Fire in both the exterior and interior bays
20°C	5.27	5.27	5.27
100°C	5.05	5.27	5.06
200°C	4.71	5.125	4.72
300°C	4.25	4.865	4.265
400°C	3.65	4.03	3.67
500°C	2.9	3.24	2.925
600°C	1.965	2.22	1.985

Temperature	β values		
	Fire in the exterior bay	Fire in the interior bay	Fire in both the exterior and interior bays
20°C	1.628705455	1.628705455	1.628705455
100°C	1.6032	1.652996364	1.581338182
200°C	1.493890909	1.651781818	1.48296
300°C	1.384581818	1.627490909	1.36272
400°C	1.21576	1.445309091	1.21576
500°C	0.992890909	1.172036364	0.992890909
600°C	0.740872727	0.772147273	0.728727273

Fixed-based frame

Temperature	Collapse Loads (kips/ft)		
	Fire in the exterior bay	Fire in the interior bay	Fire in both the exterior and interior bays
20°C	6.8674575	6.8674575	6.8674575
100°C	6.5631	6.8674575	6.5631
200°C	6.1911075	6.8674575	6.19111752
300°C	5.548575	6.7635	5.7151575
400°C	4.922325	6.08715	4.992465
500°C	4.093671	4.8885075	4.165815
600°C	3.0561	3.3855075	3.006

Temperature	First hinge formation (kips/ft)		
	Fire in the exterior bay	Fire in the interior bay	Fire in both the exterior and interior bays
20°C	5.295	5.295	5.295
100°C	5.08	5.295	5.08
200°C	4.745	5.19	4.75
300°C	4.285	4.92	4.295
400°C	3.685	4.07	3.7
500°C	2.94	3.27	2.955
600°C	2	2.24	2.015

Temperature	β values		
	Fire in the exterior bay	Fire in the interior bay	Fire in both the exterior and interior bays
20°C	1.664838182	1.664838182	1.664838182
100°C	1.591054545	1.664838182	1.591054545
200°C	1.500874545	1.664838182	1.500876975
300°C	1.345109091	1.639636364	1.385492727
400°C	1.193290909	1.475672727	1.210294545
500°C	0.992405091	1.185092727	1.009894545
600°C	0.740872727	0.820729091	0.728727273

Appendix F: 4-bay Model (Girder: W12x53; Column: W12x22 case)

3-span continuous beam

Temperature	Collapse Loads (kips/ft)		
	Fire in the exterior bay	Fire in the interior bay	Fire in both the exterior and interior bays
20°C	6.1623	6.1623	6.1623
100°C	6.01701	6.01701	5.9118
200°C	5.62122	6.02703	5.511
300°C	5.1102	5.9118	5.1102
400°C	4.38375	5.71516752	4.38375
500°C	3.5571	4.68809748	3.53205
600°C	2.4048	3.2064	2.4048

Temperature	First hinge formation (kips/ft)		
	Fire in the exterior bay	Fire in the interior bay	Fire in both the exterior and interior bays
20°C	4.88	4.88	4.88
100°C	4.68	4.7	4.68
200°C	4.36	4.41	4.39
300°C	3.92	4.01	3.96
400°C	3.34	3.48	3.41
500°C	2.63	2.81	2.72
600°C	1.75	1.97	1.85

Temperature	β values		
	Fire in the exterior bay	Fire in the interior bay	Fire in both the exterior and interior bays
20°C	1.483223684	1.483223684	1.483223684
100°C	1.449459243	1.449459243	1.449459243
200°C	1.326460205	1.424135911	1.326460205
300°C	1.229990372	1.422930039	1.229990372
400°C	1.049109435	1.374695122	1.049109435
500°C	0.850140404	1.128393168	0.856169769
600°C	0.578818999	0.766636117	0.578818999

Pinned-based frame

Temperature	Collapse Loads (kips/ft)		
	Fire in the exterior bay	Fire in the interior bay	Fire in both the exterior and interior bays
20°C	6.8136	6.8136	6.8136
100°C	6.6132	6.8136	6.6132
200°C	6.31761	6.8136	6.31761
300°C	5.7114	6.81861	5.7114
400°C	5.11521	5.9118	5.11521
500°C	4.316115	4.78455	4.291065
600°C	3.0561	3.18511752	3.2064

Temperature	First hinge formation (kips/ft)		
	Fire in the exterior bay	Fire in the interior bay	Fire in both the exterior and interior bays
20°C	5.2	5.2	5.2
100°C	5	5.21	5
200°C	4.66	5	4.68
300°C	4.22	4.52	4.24
400°C	3.62	3.91	3.64
500°C	2.88	3.15	2.91
600°C	1.97	2.17	1.99

Temperature	β values		
	Fire in the exterior bay	Fire in the interior bay	Fire in both the exterior and interior bays
20°C	1.639987163	1.639987163	1.639987163
100°C	1.591752246	1.639987163	1.618281451
200°C	1.520605745	1.639987163	1.520605745
300°C	1.374695122	1.627928434	1.374695122
400°C	1.233607991	1.422930039	1.231196245
500°C	1.038859515	1.128393168	1.000874519
600°C	0.735582478	0.766636117	0.771758665

Fixed-based frame

Temperature	Collapse Loads (kips/ft)		
	Fire in the exterior bay	Fire in the interior bay	Fire in both the exterior and interior bays
20°C	6.8136	6.8136	6.8136
100°C	6.6132	6.8136	6.6132
200°C	6.31761	6.8136	6.31761
300°C	5.7114	6.8136	5.7114
400°C	5.1102	5.9118	5.01501
500°C	4.165815	4.77453	4.29858
600°C	3.1062	3.1851075	3.1851075

Temperature	First hinge formation (kips/ft)		
	Fire in the exterior bay	Fire in the interior bay	Fire in both the exterior and interior bays
20°C	5.26	5.26	5.26
100°C	5.06	5.26	5.06
200°C	4.72	5.09	4.74
300°C	4.27	4.61	4.29
400°C	3.68	3.98	3.7
500°C	2.94	3.2	2.96
600°C	2.01	2.2	2.03

Temperature	β values		
	Fire in the exterior bay	Fire in the interior bay	Fire in both the exterior and interior bays
20°C	1.639987163	1.639987163	1.639987163
100°C	1.591752246	1.639987163	1.591752246
200°C	1.520605745	1.639987163	1.520605745
300°C	1.402430199	1.639987163	1.402430199
400°C	1.207078787	1.422930039	1.229990372
500°C	1.021977295	1.163667362	1.018962612
600°C	0.747641207	0.766633705	0.771758665

Appendix G: 2-story Model - Fire in the First Floor (Girder: W12x53; Column: W12x22 case)

Pinned-based frame

Temperature	Collapse Loads (kips/ft)		
	Fire in the exterior bay	Fire in the interior bay	Fire in both the exterior and interior bays
20°C	6.52302	6.52302	6.52302
100°C	6.52302	6.52302	6.52302
200°C	6.51801	6.51801	6.32262
300°C	6.31761	6.513	6.1623
400°C	5.6112	5.9118	5.6112
500°C	4.721925	4.721925	4.68809748
600°C	3.18511752	3.18511752	3.18511752

Temperature	First hinge formation (kips/ft)		
	Fire in the exterior bay	Fire in the interior bay	Fire in both the exterior and interior bays
20°C	5.49	5.49	5.49
100°C	5.37	5.49	5.37
200°C	5.02	5.48	5.03
300°C	4.55	4.95	4.55
400°C	3.91	4.27	3.91
500°C	3.13	3.41	3.13
600°C	2.14	2.33	2.14

Temperature	β values		
	Fire in the exterior bay	Fire in the interior bay	Fire in both the exterior and interior bays
20°C	1.570046534	1.570046534	1.570046534
100°C	1.570046534	1.570046534	1.570046534
200°C	1.568840661	1.568840661	1.521811617
300°C	1.520605745	1.567634788	1.483223684
400°C	1.350577664	1.422930039	1.350577664
500°C	1.136535221	1.136535221	1.128393168
600°C	0.766636117	0.766636117	0.766636117

Fixed-based frame

Temperature	Collapse Loads (kips/ft)		
	Fire in the exterior bay	Fire in the interior bay	Fire in both the exterior and interior bays
20°C	6.52302	6.52302	6.52302
100°C	6.52302	6.52302	6.52302
200°C	6.52302	6.52302	6.52302
300°C	6.32262	6.51801	6.31761
400°C	5.7114	5.9118	5.7114
500°C	4.6881075	4.6881075	4.6881075
600°C	3.1851075	3.1851075	3.1851075

Temperature	First hinge formation (kips/ft)		
	Fire in the exterior bay	Fire in the interior bay	Fire in both the exterior and interior bays
20°C	5.49	5.49	5.49
100°C	5.41	5.49	5.41
200°C	5.06	5.49	5.06
300°C	4.58	4.98	4.58
400°C	3.94	4.27	3.94
500°C	3.16	3.42	3.16
600°C	2.16	2.33	2.16

Temperature	β values		
	Fire in the exterior bay	Fire in the interior bay	Fire in both the exterior and interior bays
20°C	1.570046534	1.570046534	1.570046534
100°C	1.570046534	1.570046534	1.570046534
200°C	1.570046534	1.570046534	1.570046534
300°C	1.521811617	1.568840661	1.520605745
400°C	1.374695122	1.422930039	1.374695122
500°C	1.128395579	1.128395579	1.128395579
600°C	0.766633705	0.766633705	0.766633705

Appendix H: 2-story Model - Fire in the Second Floor (Girder: W12x53; Column: W12x22 case)

Pinned-based frame

Temperature	Collapse Loads (kips/ft)		
	Fire in the exterior bay	Fire in the interior bay	Fire in both the exterior and interior bays
20°C	6.52302	6.52302	6.52302
100°C	6.52302	6.52302	6.52302
200°C	6.31761	6.52302	6.31761
300°C	5.7114	6.51801	5.7114
400°C	5.03505	5.91681	5.0601
500°C	4.316115	4.721925	4.245975
600°C	3.18511752	3.18511752	3.18511752

Temperature	First hinge formation (kips/ft)		
	Fire in the exterior bay	Fire in the interior bay	Fire in both the exterior and interior bays
20°C	5.49	5.49	5.49
100°C	5.25	5.47	5.25
200°C	4.9	5.39	4.91
300°C	4.44	4.87	4.44
400°C	3.81	4.2	3.81
500°C	3.03	3.36	3.04
600°C	2.07	2.29	2.07

Temperature	β values		
	Fire in the exterior bay	Fire in the interior bay	Fire in both the exterior and interior bays
20°C	1.570046534	1.570046534	1.570046534
100°C	1.570046534	1.570046534	1.570046534
200°C	1.520605745	1.570046534	1.520605745
300°C	1.374695122	1.568840661	1.374695122
400°C	1.211902279	1.424135911	1.217931643
500°C	1.038859515	1.136535221	1.021977295
600°C	0.766636117	0.766636117	0.766636117

Fixed-based frame

Temperature	Collapse Loads (kips/ft)		
	Fire in the exterior bay	Fire in the interior bay	Fire in both the exterior and interior bays
20°C	6.52302	6.52302	6.52302
100°C	6.52302	6.52302	6.52302
200°C	6.31761	6.52302	6.31761
300°C	5.7114	6.5631	5.7114
400°C	5.12523	5.91681	5.12523
500°C	4.316115	4.721925	4.165815
600°C	3.1851075	3.1851075	3.1851075

Temperature	First hinge formation (kips/ft)		
	Fire in the exterior bay	Fire in the interior bay	Fire in both the exterior and interior bays
20°C	5.49	5.49	5.49
100°C	5.26	5.49	5.26
200°C	4.91	5.34	4.92
300°C	4.44	4.84	4.45
400°C	3.81	4.17	3.82
500°C	3.04	3.33	3.05
600°C	2.07	2.28	2.08

Temperature	β values		
	Fire in the exterior bay	Fire in the interior bay	Fire in both the exterior and interior bays
20°C	1.570046534	1.570046534	1.570046534
100°C	1.570046534	1.570046534	1.570046534
200°C	1.520605745	1.570046534	1.520605745
300°C	1.374695122	1.579693517	1.374695122
400°C	1.233607991	1.424135911	1.233607991
500°C	1.038859515	1.136535221	1.002683328
600°C	0.766633705	0.766633705	0.766633705

Appendix I: 25 foot Model - Member design

Girder Design

Length	25	
Tributary width	25	
Dead Load		
Slab	1.40625	
Beam =	0.088	
Total =	1.49425	
Live Load		
Office =	1.25	
Partition =	0.5	
Total =	1.75	
Mu max =	279.49	
Choose W12x53		
ϕ Mp =	292	

Column Design

Mu =	14.87	
Pu =	124.28	
Try	W12x22	
Ix =	156	
ry =	0.848	
Iy =	4.66	
Sx =	25.4	
ho =	11.9	
J =	0.293	
Cw =	164	
rts ^2 =	1.088382	
c =	1	
ϕ Mpx =	110	Table 3 -2
BF =	6.99	Table 3 -2
A =	6.48	
rts =	1.043255	

K =	1		
KL =	13		
Fe =	8.457466		
0.44Fy =	22		
Fcr =	43.85		
pc =	255.7332		
Pc =	255.7332		Table 4-1
Pr/Pc =	0.485975	> 0.2	Use AISC Eq H1-1a
Cm =	1		
Pe1 =	1834.734		
B1=	1.072659		
Mrx =	15.95044		
Lp =	2.995307		
Lb =	13		
Lr =	9.161209		
ϕ Mpx =	40.06719		
Pr/Pc +8/9(Mr/Mc)=	0.839835	< 1.0	OK

Appendix J: Example of ANSYS Code for Base Model at Normal Temperature

```
/BATCH
! /COM,ANSYS RELEASE 11.0SP1 UP20070830
/input,menust,tmp,",,,,,,,,,,,,,,,,1
! /GRA,POWER
! /GST,ON
! /PLO,INFO,3
! /GRO,CURL,ON
! /CPLANE,1
! /REPLOT,RESIZE
WPSTYLE,,,,,,,,0
/PREP7
!*
ET,1,BEAM24
!*
KEYOPT,1,1,0
KEYOPT,1,2,0
KEYOPT,1,3,1
KEYOPT,1,6,1
KEYOPT,1,10,0
! NOTE: GIRDER SIZE
R,1,0,0,0,10,0,.575,
RMORE,5,0,0,5,12.1,.345,
RMORE,0,12.1,0,10,12.1,.575,
RMORE,,,,,,,
```

RMORE,,,,,,,

RMORE,,,,,,,

RMORE,,,,,,,

RMORE,,,,,,,

RMORE,,,,,,,

RMORE,,,,,,,

RMORE,,,,,

! NOTE: COLUMN SIZE

R,2,0,0,0,4.03,0,.425,

RMORE,2.015,0,0,2.015,12.3,.260,

RMORE,0,12.3,0,4.03,12.3,.425,

RMORE,0,0,0,0,0,0,

RMORE,0,0,0,0,0,0,

RMORE,0,0,0,0,0,0,

RMORE,0,0,0,0,0,0,

RMORE,0,0,0,0,0,0,

RMORE,0,0,0,0,0,0,

RMORE,0,0,0,0,0,0,

RMORE,0,0,0,0,

! MATERIAL 1

MPTEMP,,,,,,,,

MPTEMP,1,0

MPDATA,EX,1,,29e6

MPDATA,PRXY,1,,0.3

TB,BISO,1,1,2,

TBTEMP,0

TBDATA,,50000,100,,,,

! NOTE: MATERIAL 2

MPTEMP,,,,,,,,

MPTEMP,1,0

MPDATA,EX,2,,29e6

MPDATA,PRXY,2,,0.3

TB,BISO,2,1,2,

TBTEMP,0

TBDATA,,50000,100,,,,

! NOTE: Key Point

K,1,0,0,0,

K,2,300,0,0,

K,3,600,0,0,

K,4,900,0,0,

K,5,0,156,0,

K,6,300,156,0,

K,7,600,156,0,

K,8,900,156,0,

K,9,600,300,0,

K,10,1500,75,0,

! NOTE: Draw Lines

LSTR, 1, 5

LSTR, 2, 6

LSTR, 5, 6

LSTR, 6, 7

LSTR, 3, 7

```
LSTR,      7,      8
LSTR,      4,      8
! Size Control
LESIZE,ALL, , ,10, ,1, , ,1,
FLST,5,3,4,ORDE,3
FITEM,5,3
FITEM,5,-4
FITEM,5,6
CM,_Y,LINE
LSEL, , , ,P51X
CM,_Y1,LINE
CMSEL,S,_Y
!*
!*
CMSEL,S,_Y1
LATT,1,1,1, , , ,
CMSEL,S,_Y
CMDELE,_Y
CMDELE,_Y1
!*
latt,1,1,1,,9
FLST,2,3,4,ORDE,3
FITEM,2,3
FITEM,2,-4
FITEM,2,6
LMESH,P51X
```

```
! LPLOT
FLST,5,4,4,ORDE,4
FITEM,5,1
FITEM,5,-2
FITEM,5,5
FITEM,5,7
CM,_Y,LINE
LSEL, , , ,P51X
CM,_Y1,LINE
CMSEL,S,_Y
!*
!*
CMSEL,S,_Y1
LATT,1,2,1, , , ,
CMSEL,S,_Y
CMDELE,_Y
CMDELE,_Y1
!*
latt,1,2,1,,10,
FLST,2,4,4,ORDE,4
FITEM,2,1
FITEM,2,-2
FITEM,2,5
FITEM,2,7
LMESH,P51X
FLST,2,4,3,ORDE,2
```

```
FITEM,2,1
FITEM,2,-4
!*
/GO
DK,P51X, , , ,0,UX,UY,UZ, , , ,
FLST,2,30,2,ORDE,2
FITEM,2,1
FITEM,2,-30
SFBEAM,P51X,1,PRES,1670, , , , , ,
FINISH
/SOL
NSUBST,20,100,10
OUTRES,ERASE
OUTRES,ALL,ALL
AUTOTS,1
LNSRCH,1
NEQIT,500
! /STATUS,SOLU
```

Appendix J: Example of ANSYS Code for Base Model with Fire in the First Span (600°C)

```
/BATCH
! /COM,ANSYS RELEASE 11.0SP1 UP20070830
/input,menust,tmp,",,,,,,,,,,,,,,,,1
! /GRA,POWER
! /GST,ON
! /PLO,INFO,3
! /GRO,CURL,ON
! /CPLANE,1
! /REPLOT,RESIZE
WPSTYLE,,,,,,,,0
/PREP7
!*
ET,1,BEAM24
!*
KEYOPT,1,1,0
KEYOPT,1,2,0
KEYOPT,1,3,1
KEYOPT,1,6,1
KEYOPT,1,10,0
! NOTE: GIRDER SIZE
R,1,0,0,0,10,0,.575,
RMORE,5,0,0,5,12.1,.345,
RMORE,0,12.1,0,10,12.1,.575,
RMORE,,,,,,,
```

RMORE,,,,,,,

RMORE,,,,,,,

RMORE,,,,,,,

RMORE,,,,,,,

RMORE,,,,,,,

RMORE,,,,,,,

RMORE,,,,,

! NOTE: COLUMN SIZE

R,2,0,0,0,4.03,0,.425,

RMORE,2.015,0,0,2.015,12.3,.260,

RMORE,0,12.3,0,4.03,12.3,.425,

RMORE,0,0,0,0,0,0,

RMORE,0,0,0,0,0,0,

RMORE,0,0,0,0,0,0,

RMORE,0,0,0,0,0,0,

RMORE,0,0,0,0,0,0,

RMORE,0,0,0,0,0,0,

RMORE,0,0,0,0,0,0,

RMORE,0,0,0,0,

! MATERIAL 1

MPTEMP,,,,,,,,

MPTEMP,1,0

MPDATA,EX,1,,29e6

MPDATA,PRXY,1,,0.3

TB,BISO,1,1,2,

TBTEMP,0

```
TBDATA,,50000,100,,,,
! NOTE: MATERIAL 2
MPTEMP,,,,,,,,
MPTEMP,1,0
MPDATA,EX,2,,14646780.89
MPDATA,PRXY,2,,0.3
TB,BISO,2,1,2,
TBTEMP,0
TBDATA,,18860.19826,100,,,,
! NOTE: Key Point
K,1,0,0,0,
K,2,300,0,0,
K,3,600,0,0,
K,4,900,0,0,
K,5,0,156,0,
K,6,300,156,0,
K,7,600,156,0,
K,8,900,156,0,
K,9,600,300,0,
K,10,1500,75,0,
! NOTE: Draw Lines
LSTR,      1,      5
LSTR,      2,      6
LSTR,      5,      6
LSTR,      6,      7
LSTR,      3,      7
```

```
LSTR,       7,       8
LSTR,       4,       8
! Size Control
LESIZE,ALL, , ,10, ,1, , ,1,
! NOTE: HEATED MEMBER
CM,_Y,LINE
LSEL, , , ,       3
CM,_Y1,LINE
CMSEL,S,_Y
!*
!*
CMSEL,S,_Y1
LATT,2,1,1, , , ,
CMSEL,S,_Y
CMDELE,_Y
CMDELE,_Y1
!*
latt,2,1,1,,9
LMESH,       3
! NOTE: NORMAL GIRDER MEMBER
FLST,5,2,4,ORDE,2
FITEM,5,4
FITEM,5,6
CM,_Y,LINE
LSEL, , , ,P51X
CM,_Y1,LINE
```

```
CMSEL,S,_Y
!*
!*
CMSEL,S,_Y1
LATT,1,1,1, , , ,
CMSEL,S,_Y
CMDELE,_Y
CMDELE,_Y1
!*
latt,1,1,1,,9,
FLST,2,2,4,ORDE,2
FITEM,2,4
FITEM,2,6
LMESH,P51X
! COLUMN MESH
FLST,5,4,4,ORDE,4
FITEM,5,1
FITEM,5,-2
FITEM,5,5
FITEM,5,7
CM,_Y,LINE
LSEL, , , ,P51X
CM,_Y1,LINE
CMSEL,S,_Y
!*
!*
```

```
CMSEL,S,_Y1
LATT,1,2,1, , , ,
CMSEL,S,_Y
CMDELE,_Y
CMDELE,_Y1
!*
latt,1,2,1,,10,
FLST,2,4,4,ORDE,4
FITEM,2,1
FITEM,2,-2
FITEM,2,5
FITEM,2,7
LMESH,P51X
! Boundary Condition
ANTYPE,0
FLST,2,4,3,ORDE,2
FITEM,2,1
FITEM,2,-4
!*
/GO
DK,P51X, , , ,0,UX,UY,UZ, , , ,
! APPLIED LOAD
FLST,2,30,2,ORDE,2
FITEM,2,1
FITEM,2,-30
SFBEAM,P51X,1,PRES,1670, , , , , ,
```

```
!SOlution Control
/SOL
NSUBST,20,100,10
OUTRES,ERASE
OUTRES,ALL,ALL
AUTOTS,1
LNSRCH,1
NEQIT,500
```

Appendix K: Example of Excel Spreadsheet for Base Model at Normal Temperature

Beam	W12x53	Colum	W12x40
Z =	77.9	Z=	57
Ft=	50	Ft =	50
Mp normal =	324.5833	Mp normal =	237.5

Total Collapse Load = 7.76 kips/ft

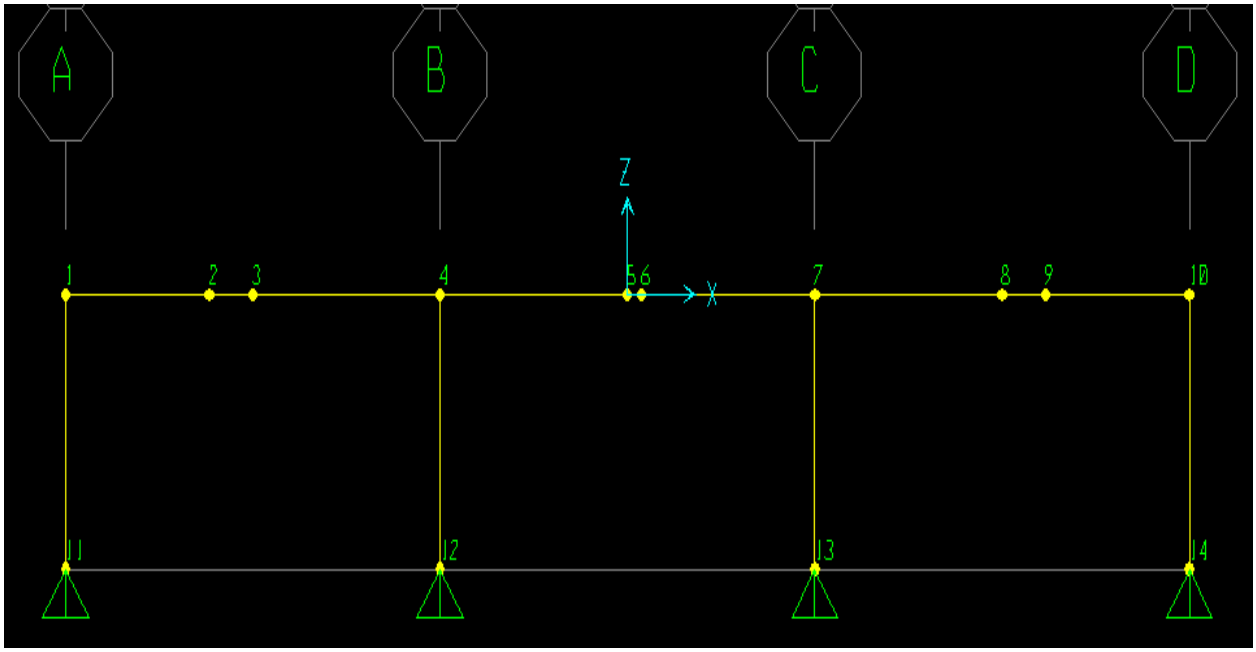

First Hinge 5.47 K/ft

TABLE: Element Joint Forces - Frames

Frame	Joint	M2		Target	
Text	Text	Kip-ft			
Beam					
1	1	-168.581	168.5812	156.00	
1	2	-176.109	176.1087	148.47	
1	2	176.1087	176.1087	148.47	
1	3	-180.898	180.8977	143.69	
1	3	180.8977	180.8977	143.69	
1	4	324.311	324.311	0.27	Formed
2	4	-295.631	295.6305	28.95	
2	5	-131.713	131.7133	192.87	
2	5	131.7133	131.7133	192.87	
2	6	-129.185	129.1848	195.40	
2	6	129.1848	129.1848	195.40	
2	7	295.6305	295.6305	28.95	
3	7	-324.311	324.311	0.27	Formed
3	8	-180.898	180.8977	143.69	
3	8	180.8977	180.8977	143.69	
3	9	-176.109	176.1087	148.47	
3	9	176.1087	176.1087	148.47	
3	10	168.5812	168.5812	156.00	
Column					
4	1	168.5812	168.5812	68.9188	
4	11	75.7707	75.7707	161.7293	
5	12	-13.6228	13.6228	223.8772	
5	4	-28.6805	28.6805	208.8195	
6	13	13.6228	13.6228	223.8772	
6	7	28.6805	28.6805	208.8195	
7	14	-75.7707	75.7707	161.7293	
7	10	-168.581	168.5812	68.9188	

Second Hinge 0.76 K/ft

TABLE: Element Joint Forces - Frames

Frame	Joint	M2		Target	
Text	Text	Kip-ft			
Beam					
1	1	-37.1524	37.1524	118.85	
1	2	-33.35	33.35	115.12	
1	2	33.35	33.35	115.12	
1	3	-40.7988	40.7988	102.89	
1	3	40.7988	40.7988	102.89	
1	4	0	0	0.27	
2	4	-28.4518	28.4518	0.50	Formed
2	5	-30.9232	30.9232	161.95	
2	5	30.9232	30.9232	161.95	
2	6	-30.5719	30.5719	164.83	
2	6	30.5719	30.5719	164.83	
2	7	28.4518	28.4518	0.50	Formed
3	7	0	0	0.27	
3	8	-40.7988	40.7988	102.89	
3	8	40.7988	40.7988	102.89	
3	9	-33.35	33.35	115.12	
3	9	33.35	33.35	115.12	
3	10	37.1524	37.1524	118.85	
Column			0		
4	1	37.1524	37.1524	31.77	
4	11	16.5834	16.5834	145.15	
5	12	12.8373	12.8373	211.04	
5	4	28.4518	28.4518	180.37	
6	13	-12.8373	12.8373	211.04	
6	7	-28.4518	28.4518	180.37	
7	14	-16.5834	16.5834	145.15	
7	10	-37.1524	37.1524	31.77	

Third Hinge 0.65 K/ft

TABLE: Element Joint Forces - Frames

Frame	Joint	M2		Target	
Text	Text	Kip-ft			
Beam					
1	1	-31.829	31.829	87.02	
1	2	-28.4899	28.4899	86.63	
1	2	28.4899	28.4899	86.63	
1	3	-34.8668	34.8668	68.02	
1	3	34.8668	34.8668	68.02	
1	4	0	0	0.27	
2	4	0	0	0.50	
2	5	-50.7812	50.7812	111.17	
2	5	50.7812	50.7812	111.17	
2	6	-50.4808	50.4808	114.35	
2	6	50.4808	50.4808	114.35	
2	7	0	0	0.50	
3	7	0	0	0.27	
3	8	-34.8668	34.8668	68.02	
3	8	34.8668	34.8668	68.02	
3	9	-28.4899	28.4899	86.63	
3	9	28.4899	28.4899	86.63	
3	10	31.829	31.829	87.02	
Column					
4	1	31.829	31.829	-0.06	Formed
4	11	14.288	14.288	130.86	
5	12	-0.1054	0.1054	210.93	
5	4	-7.4E-17	7.4E-17	180.37	
6	13	0.1054	0.1054	210.93	
6	7	-3.7E-17	3.7E-17	180.37	
7	14	-14.288	14.288	130.86	
7	10	-31.829	31.829	-0.06	Formed

Fourth Hinge 0.88 K/ft

TABLE: Element Joint Forces - Frames

Frame	Joint	M2		Target	
Text	Text	Kip-ft			
Beam					
1	1	2.37E-15	2.37E-15	87.02	
1	2	-65.0888	65.0888	21.55	
1	2	65.0888	65.0888	21.55	
1	3	-68.75	68.75	-0.73	Formed
1	3	68.75	68.75	-0.73	Formed
1	4	0	0	0.27	
2	4	0	0	0.50	
2	5	-68.75	68.75	42.42	
2	5	68.75	68.75	42.42	
2	6	-68.3432	68.3432	46.00	
2	6	68.3432	68.3432	46.00	
2	7	0	0	0.50	
3	7	0	0	0.27	
3	8	-68.75	68.75	-0.73	Formed
3	8	68.75	68.75	-0.73	Formed
3	9	-65.0888	65.0888	21.55	
3	9	65.0888	65.0888	21.55	
3	10	3.79E-14	3.79E-14	87.02	
Column					
4	1	0	0	-0.06	
4	11	-2.6E-14	2.59E-14	130.86	
5	12	-2.6E-14	2.62E-14	210.93	
5	4	0	0	180.37	
6	13	-2.6E-14	2.62E-14	210.93	
6	7	0	0	180.37	
7	14	-2.6E-14	2.59E-14	130.86	
7	10	0	0	-0.06	

Appendix L: Example of Excel Spreadsheet for Base Model with Fire in the Exterior Bay (600°C)

Beam	W12x53	Colum	W12x40
Z =	77.9	Z=	57
Ft=	18.8602	Ft =	50
		Mp	
Mp =	122.4341	normal =	237.5
Mp normal =	324.5833		

Total Collapse Load = 3.14 kips/ft

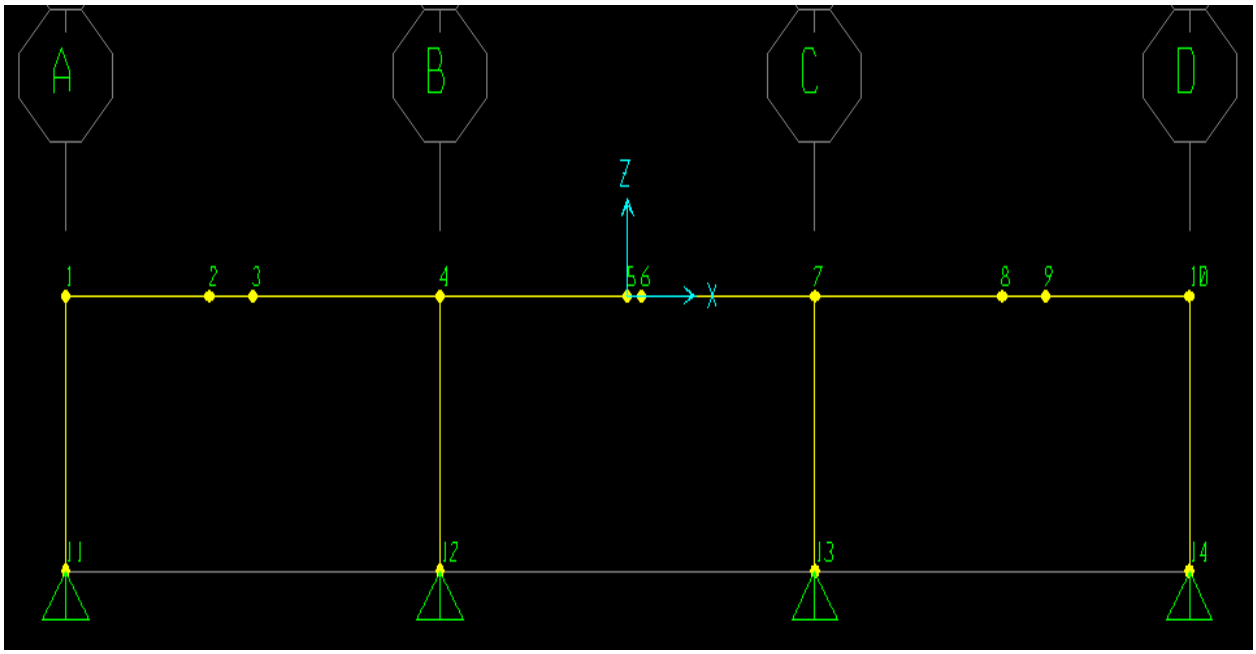

First Hinge 2.11 kips/ft

TABLE: Element Joint Forces - Frames

Frame	Joint	M2		Target	
Text	Text	Kip-ft			
Beam					
1	1	-78.9945	78.9945	43.44	
1	2	-60.2529	60.2529	62.18	
1	2	60.2529	60.2529	62.18	
1	3	-63.9862	63.9862	58.45	
1	3	63.9862	63.9862	58.45	
1	4	122.7206	122.7206	-0.29	Formed
2	4	-110.811	110.8111	213.77	
2	5	-51.3742	51.3742	273.21	
2	5	51.3742	51.3742	273.21	
2	6	-50.1944	50.1944	274.39	
2	6	50.1944	50.1944	274.39	
2	7	116.128	116.128	208.46	
3	7	-123.519	123.5191	201.06	
3	8	-69.495	69.495	255.09	
3	8	69.495	69.495	255.09	
3	9	-67.2173	67.2173	257.37	
3	9	67.2173	67.2173	257.37	
3	10	67.1783	67.1783	257.41	
Column					
4	1	78.9945	78.9945	158.5055	
4	11	32.5025	32.5025	204.9975	
5	12	-8.1971	8.1971	229.3029	
5	4	-11.9095	11.9095	225.5905	
6	13	1.0776	1.0776	236.4224	
6	7	7.3911	7.3911	230.1089	
7	14	-32.6809	32.6809	204.8191	
7	10	-67.1783	67.1783	170.3217	

Second Hinge 0.78 kips/ft

TABLE: Element Joint Forces - Frames

Frame	Joint	M2		Target	
Text	Text	Kip-ft			
Beam					
1	1	-43.523	43.523	-0.08	Formed
1	2	-30.909	30.909	31.27	
1	2	30.909	30.909	31.27	
1	3	-39.176	39.176	19.27	
1	3	39.176	39.176	19.27	
1	4	0	0	-0.29	
2	4	-16.6278	16.6278	197.14	
2	5	-25.5894	25.5894	247.62	
2	5	25.5894	25.5894	247.62	
2	6	-23.7888	23.7888	250.60	
2	6	23.7888	23.7888	250.60	
2	7	54.0685	54.0685	154.39	
3	7	-43.9511	43.9511	157.11	
3	8	-24.1552	24.1552	230.93	
3	8	24.1552	24.1552	230.93	
3	9	-22.5643	22.5643	234.80	
3	9	22.5643	22.5643	234.80	
3	10	29.6136	29.6136	227.79	
Column					
4	1	43.523	43.523	114.98	
4	11	11.9231	11.9231	193.07	
5	12	0.0853	0.0853	229.22	
5	4	16.6278	16.6278	208.96	
6	13	-11.8561	11.8561	224.57	
6	7	-10.1175	10.1175	219.99	
7	14	-20.572	20.572	184.25	
7	10	-29.6136	29.6136	140.71	

Third Hinge 0.25 kips/ft

TABLE: Element Joint Forces - Frames

Frame	Joint	M2		Target	
Text	Text	Kip-ft			
Beam					
1	1	0	0	-0.08	
1	2	-18.4911	18.4911	12.78	
1	2	18.4911	18.4911	12.78	
1	3	-19.5313	19.5313	-0.26	Formed
1	3	19.5313	19.5313	-0.26	Formed
1	4	0	0	-0.29	
2	4	-7.4333	7.4333	189.71	
2	5	-7.9632	7.9632	239.66	
2	5	7.9632	7.9632	239.66	
2	6	-7.5296	7.5296	243.07	
2	6	7.5296	7.5296	243.07	
2	7	15.7028	15.7028	138.68	
3	7	-15.696	15.696	141.42	
3	8	-7.9622	7.9622	222.97	
3	8	7.9622	7.9622	222.97	
3	9	-7.8745	7.8745	226.93	
3	9	7.8745	7.8745	226.93	
3	10	7.442	7.442	220.35	
Column					
4	1	9.25E-18	9.25E-18	114.98	
4	11	-0.0312	0.0312	193.04	
5	12	3.3793	3.3793	225.84	
5	4	7.4333	7.4333	201.53	
6	13	0.0148	0.0148	224.55	
6	7	-0.0068	0.0068	219.98	
7	14	-3.3474	3.3474	180.90	
7	10	-7.442	7.442	133.27	